Eirik Starheim Svendsen

Energy flow analysis of a poultry process plant

Master's thesis in Mechanical Engineering
Supervisor: Prof. Armin Hafner, EPT
June 2019

Master's thesis

NTNU
Norwegian University of Science and Technology
Faculty of Engineering
Department of Energy and Process Engineering

NTNU
Kunnskap for en bedre verden

Eirik Starheim Svendsen

Energy flow analysis of a poultry process plant

Master's thesis in Mechanical Engineering
Supervisor: Prof. Armin Hafner, EPT
June 2019

Norwegian University of Science and Technology
Faculty of Engineering
Department of Energy and Process Engineering

NTNU
Norwegian University of
Science and Technology

Preface

This report represents the final work of my Master's degree in Mechanical Engineering for the Department of Energy and Process Engineering at the Norwegian University of Science and Technology, and has been conducted during the spring of 2019. The thesis is concerned with conducting an energy analysis for an upcoming poultry process plant, and to investigate the potential and effects of integrating of cold thermal energy storages.

During the period I have had the pleasure to be supervised by Prof. Armin Hafner and Håkon Selvnes. They have supported me with guidance and advise, from which I have learned a lot, and I would like express my gratitude and thank them for their support.

A special thanks goes to my dear Katrine, who with her encouragement has never failed to lift my spirits, and with her patience supported me during what has been a very special time for the both of us.

Abstract

Industrial food-processing often includes a number of thermal processes to make food safe for human consumption and extend its shelf life. Large-scale plants in this industry must employ complex energy systems to handle the variety of loads, which often involves process equipment for chilling and freezing, cold storages and systems for heating, washing and drying. Norsk Kylling AS is in the process of building a large-scale poultry processing plant, and the aim of this thesis is to evaluate the plants refrigeration system in terms of energy consumption, peak power requirement and heat recovery. In addition, the potential and effect of integrating cold thermal storages (CTES) is to be evaluated.

A concept for integrating CTES was developed, and simulation models of the refrigeration system and CTES concept has been built in *Dymola.* A thermal demand profile with a duration of 24 hours was constructed, and simulations were carried out for both systems with this profile.

Results from the simulations showed that the refrigeration system had an energy consumption of 20 800 kWh for the period and peak power was 2,21 MW. Heat was recovered in two different utilities and used for hot water pre-heating, and the system was able to produce a total of 74 500 l water at 70 °C and 95 600 l water at 50 °C. The power consumption profile revealed that the system was running at partial capacity for a majority of the time, indicating potential for CTES.

Results for the CTES concept showed a significant reduction in peak power, which was observed to be 1,07 MW – a reduction of 52%. To accomplish this reduction, the energy consumption increased with 2000 kWh, but it was assessed that the economic consequence of this is insignificant when accounting for reduction in electrical demand charges. Further benefits were found in increased hot water production; 120 600 l of 70 °C water and unchanged for the 50 °C water.

Sammendrag

Industriell prosessering av mat innebærer ofte en del forskjellige termiske prosesser som er nødvendige for å gjøre maten trygg for oss mennesker. For bedrifter som produserer og foredler mat betyr dette at de må ha komplekse energissentraler som sørger for at disse prosessene blir ivaretatt. For store anlegg kan typiske forbrukere av termisk energi være prosessutstyr til kjøling og frysing, kjøle- og fryserom, samt systemer for oppvarming av vann, vasking og uttørking. Norsk Kylling AS skal bygge en ny fabrikk for foredling og prosessering av kylling, og denne oppgavens formål har vært å evaluere virkningsgraden til fabrikkens energisentral. Sentrale parametere i så måte har vært strømforbruk, topplast og varmegjenvinning, samt utforske potensialet for å integrere energilagring på de kalde kretsene.

For å gjennomføre analysen ble det bygget en modell av energisentralen i simuleringsverktøyet *Dymola*, samt en foreslått modifikasjon av energisentralen som inkluderte energilagring. Videre ble det laget en termisk lastprofil som gjenspeilet fabrikkens termiske behov gjennom et døgn, og simuleringer av begge modellene ble gjort med denne profilen som utgangspunkt.

Simuleringsresultatene viste at energianlegget hadde et strømforbruk på 20 800 kWh i døgnet, mens registrert topplast var 2,21 MW. Varme ble gjenvunnet i to separate kretser og brukt til å varme opp vaskevann, og resultatene viste at anlegget var i stand til å varme opp 74 500 og 95 600 l vann på henholdsvis 70 og 50 °C i løpet av et døgn. Den elektriske lastprofilen viste videre at anlegget kjørte med redusert kapasitet mesteparten av døgnet, og indikerte dermed en god mulighet for energilagring.

Resultatene for det modifiserte energianlegget viste at en stor reduksjon i topplasten er oppnåelig, med en registrert toppverdi på 1,07 MW – en reduksjon på 52%. For å greie denne reduksjonen økte strømforbruket med 2000 kWh sammenlignet med det konvensjonelle anlegget. Det ble vurdert, ut i fra et økonomisk perspektiv, at denne relativt små økningen er ubetydelig sammenlignet med gevinsten topplast-reduksjonen fører med seg. Produksjonen av varmtvann økte også i dette tilfellet, med en akkumulert mengde på 120 600 l vann på 70 °C. Mengden vann på 50 °C forble uendret.

Table of Contents

List of Figures

List of Tables

Nomenclature

Abbreviations

CCC	Closed Vapour Compression Cycle
CFC	Chlorofluorocarbon
CTES	Cold Thermal Energy Storage
CWS	Chilled Water Storage
DX	Direct Expansion (..evaporator)
GWP	Global Warming Potential
HCFC	Hydrochlorofluorocarbon
HFC	Hydrofluorocarbon
HFO	Hydrofluoro-olefin
HVAC	Heating, Ventilation and Air-Conditioning
HX	Heat Exchanger
LT	Low temperature
MT	Medium Temperature
ODP	Ozone Depletion Potential
PCM	Phase Change Material
PG	Propylene Glycol
PI	Proportional-integral (..controller)
TES	Thermal Energy Storage
UTES	Underground Thermal Energy Storage
VRC	Volumetric Refrigeration Capacity

Symbols

c_p	Specific heat	[kJ/kgK]
E	Energy	[kWh]
EER	Energy efficiency ratio	[-]
m	Mass	[kg]
$\dot{m}_R$	Mass flow of refrigerant	[kg/s]
η_{Ca}	Carnot efficiency	[-]
η_e	Effective isentropic efficiency	[-]
η_{is}	Isentropic efficiency	[-]
η_v	Volumetric efficiency	[-]
ρ	Density	[kg/m3]
$\dot{P}$	Compressor shaft work	[kW]
$Q_{storage}$	Storage capacity	[kWh]
$\dot{Q}_0$	Evaporation heat	[kW]
$\dot{Q}_c$	Condensation heat	[kW]
V	Volume	[m3]
$\dot{W}$	Compression work	[kW]
$\dot{W}_{is}$	Isentropic compression work	[kW]
Δh_{pc}	Phase change enthalpy	[kJ/kg]
ΔT	Temperature difference	[K]

1 Introduction

Norsk Kylling AS is currently in the process of building a large-scale poultry processing plant, and has ambitions of setting a new standard for efficient use of energy and sustainability within its sector. Characterizing for this plant and others which operate in the food industry, is a high need for thermal energy at different temperature levels due to the many different cold and hot processes. The thermal loads are relatively low outside production hours, mainly associated with maintaining room temperature in cold storages, but increases significantly during production when process equipment is switched on. This results in distinctive peaks in the daily thermal demand pattern, and it can be challenging for a refrigeration system to perform with high efficiency during periods of both high and low demands. The aim of this thesis is to evaluate the energy central of the upcoming poultry processing plant, and report on system performance parameters related to energy consumption, heat recovery and peak power requirement. In line with Norsk Kylling AS stated ambitions, the potential for integration of cold thermal energy storages will also be explored.

On a broader scale, improving energy efficiency in industrial processes is a key measure for reducing energy consumption and greenhouse gas emissions, and thus important in order to face the challenge of global warming. The industrial sector has a large share of both primary energy consumption and greenhouse gas emissions; respectively 30% and 20% in Norway based on numbers from 2016 [1][2]. A study published by Enova [3] reported that the potential energy savings in the food industry is 30%, which amounts to 1,3 TWh/year. Thermal energy storage is an interesting supplemental feature which can contribute to increase energy efficiency, and can be particularly apt with the variable demands typical for the food industry.

1.1 Objectives

The following tasks and objectives are to be covered by this master thesis:

- Review of relevant literature; industrial refrigeration systems, industrial HVAC, thermal demands of processing plants, thermal energy storage
- Develop simplified model(s) representing the energy system of the processing plant, including cold energy storage
- Perform dynamic simulations with varying thermal loads
- Analyse the results in terms of system performance, energy consumption and thermal energy storage potential
- Summary report
- Draft version of a scientific paper
- Proposals for further work

1.2 Problem description

The following is the thematic description for the thesis as it is formulated in the Masters Agreement:

Industrial food processing plants and supermarket chains prefer to apply natural working fluids such as CO2, ammonia and hydrocarbons as working fluids for centralized refrigeration systems whenever possible due to the environmental concerns of applying the HFC and HFO refrigerants. REMA 1000, the owner of Norsk Kylling, is in the process of building a large-scale poultry processing plant in Orkanger (Central Norway). The energy system in these types of plants are complex, involving cooling and freezing process equipment, cold storage rooms, systems for heating, washing, drying and HVAC. In addition, there is ambitions to integrate innovative solutions to store cold and hot thermal energy to reduce the peaks in electricity consumption. The building and the equipment of the process plant has different heating and cooling demands over the course of a day, week, month and year. The master thesis will focus on developing a simplified process flow chart and dynamic model of the plant in the object-oriented modelling language Modelica. The work involves mapping the energy demands in the various subsystems of the plant and perform simulations of the plant model with varying thermal loads. The results should be analysed and the potential for storing cold energy during off-peak periods is to be investigated.

2 Theory and literature review

This chapter will provide an overview of relevant literature for the topics covered in this thesis, including basic theory on refrigeration and thermal energy storage. The review of industrial refrigeration covers different system solutions where key features are exemplified, while thermal loads give a general overview over thermal demands in food processing industry and equipment used for covering them.

2.1 Refrigeration principles

Refrigeration can be defined as the process of removing heat from a space or product to reach a lower temperature than its surroundings. Historically, natural ice was used as a means to accomplish this task. By harvesting ice during the winter period and storing it in such a manner that it did not completely melt, it could be used later during warmer periods to chill food [4]. In fact, the Parliament House of Hungary is air-conditioned by harvested ice to this day [5].

Today there are more modern and efficient ways to refrigerate, and this report will focus on the closed vapour compression cycle (CCC). The CCC utilizes a working fluid that extracts heat ($\dot{Q}_0$) from a cold source via an evaporator, compresses it to higher pressure and temperature, and rejects heat ($\dot{Q}_C$) to a hot sink via a condenser. The fluid is then expanded down to low pressure and temperature, enters the evaporator and the cycle continues. For this cycle to run there must be a power input ($\dot{W}$) to the compressor.

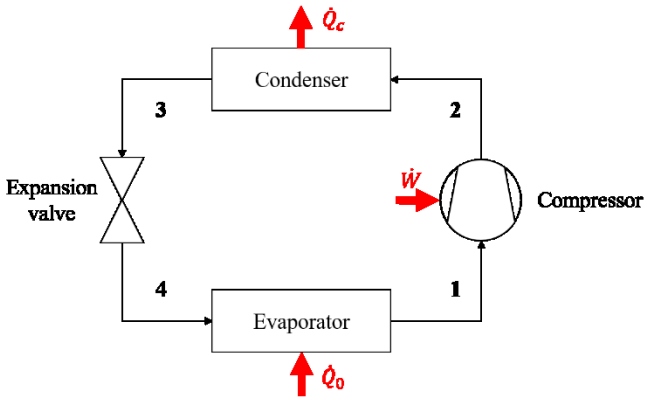

Figure 1: *Simple CCC system*

Two diagrams are often used to better understand the cycles involved in this reverse heat machine, namely the Ts- and pH-diagram (Temperature-entropy and pressure-enthalpy). These diagrams are unique for each refrigerant. In Figure 2, these diagrams are shown with the CCC

cycle in bold red with state points in accordance to Figure 1. The different processes and their mathematical descriptions are:

- **1-2:** Isentropic compression. The theoretical work done by the compressor can be described as $\dot{W}_{is} = \dot{m}_R(h_{2s} - h_1)$, and given the isentropic efficiency η_{is} of the compressor the real work can be calculated as

$$\dot{W} = \dot{W}_{is}/\eta_{is}\ [kW] \tag{2.1}$$

- **2-3:** Isobaric heat rejection in a condenser. The heat rejected in the condenser is the sum of the compressor work and heat extracted in the evaporator, or the enthalpy difference over the condenser times the refrigerant mass flow rate.

$$\dot{Q}_c = \dot{Q}_0 + \dot{W} = \dot{m}_R \cdot (h_2 - h_3)\ [kW] \tag{2.2}$$

- **3-4:** Isenthalpic expansion. When throttling the refrigerant the enthalpy stays the same, that is $h_4 = h_3$
- **4-1:** Isobaric heat extraction in the evaporator. The amount of heat that the evaporator picks up is equal the refrigerant mass flow rate times the enthalpy difference over the evaporator.

$$\dot{Q}_0 = \dot{m}_R \cdot (h_1 - h_4)\ [kW] \tag{2.3}$$

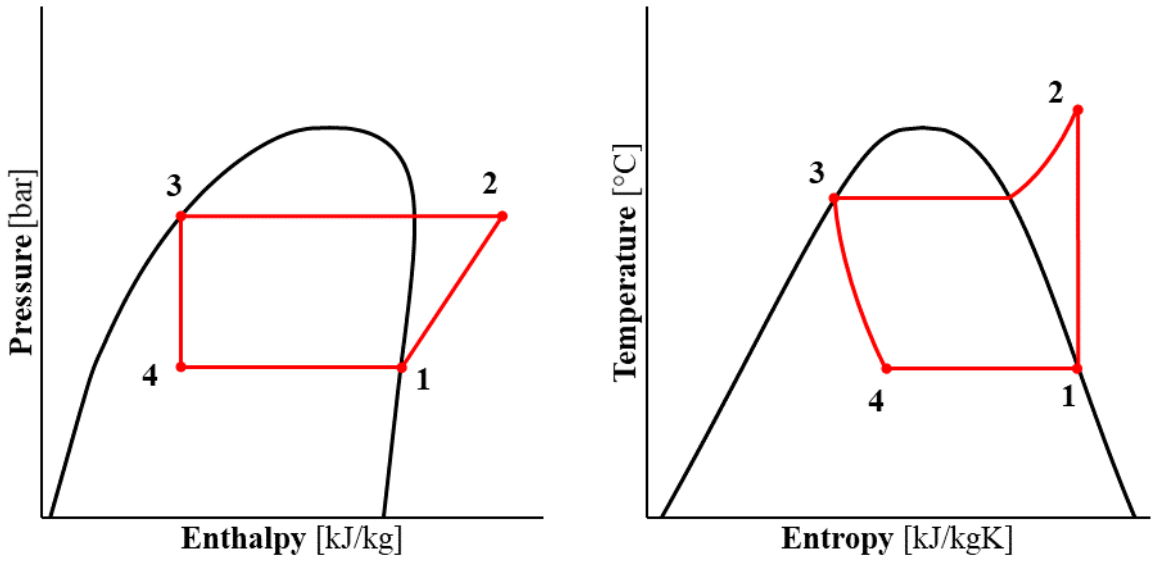

Figure 2: *pH-diagram and Ts-diagram for the simple CCC*

To express the performance of such a system it is common to use coefficient of performance (COP), also termed power factor. The COP is a dimensionless ratio of useful thermal energy output over power input to the system. From this definition, we see that COP can take different forms depending on whether we evaluate the extracted heat, rejected - or both - as useful thermal energy. Commonly used terms are COP_{REF} for refrigeration, COP_{HP} for heat pump and COP_{COMB} for the combined COP.

$$COP_{REF} = \dot{Q}_0/\dot{W} \ [-] \tag{2.4}$$

$$COP_{HP} = \dot{Q}_c/\dot{W} \ [-] \tag{2.5}$$

$$COP_{COMB} = \frac{\dot{Q}_0 + \dot{Q}_c}{\dot{W}} \ [-] \tag{2.6}$$

Furthermore, for given source (T_L) and sink (T_H) temperatures, the theoretical maximum value is limited by the ideal Carnot cycle (or reverse Carnot cycle), which is termed COP_{Ca}. Due to unavoidable and irreversible losses in a real system, the real COP cannot equal or be greater than the ideal COP. Hence the ratio of real COP over ideal COP gives the Carnot efficiency, η_{Ca}, where typical values for refrigeration systems lies between 0,4-0,6 [4].

$$COP_{Ca} = \frac{T_L}{T_H - T_L} \ [-] \tag{2.7}$$

$$\eta_{Ca} = \frac{COP}{COP_{Ca}} \ [-] \tag{2.8}$$

2.2 Refrigerants

In the early stages of mechanical refrigeration, availability and efficiency was the main criteria for selecting working fluids. The first commercial refrigerant was ethyl ether (R610), suggested by Jacob Perkins in 1834 [6]. In the search for suitable refrigerants, natural substances such as ammonia (R717), carbon dioxide (R744), ethyl chloride (R160), air (R729), sulphur dioxide (R764) etc. were introduced the following years. Due to the flammability and toxicity of many of these refrigerants, the industry aimed to develop safer and more efficient synthetic refrigerants. As a result, chlorofluorocarbons (CFCs) were introduced in the 1930s, followed by hydrochlorofluorocarbons (HCFCs) in the 1950s. They effectively dominated the market due to their excellent ability as refrigerants and was thought to be harmless to the environment.

The latter statement however proved to be wrong. In the 1970s, scientists learned that these fluids had a substantial detrimental effect on the ozone layer. The Montreal protocol of 1987

aimed to regulate the production and use of chemicals harmful to the ozone layer [7]. The treaty led to phase out of CFCs by 1996 and scheduled phase out of HCFCs by 2030. In the wake of this, hydrofluorocarbons (HFCs) with no effect on the ozone layer was introduced. However, these chemicals have high impact on greenhouse warming and the Kyoto protocol of 1997 was established to regulate usage of such fluids. Further regulation of the HFCs came with the EUs F-Gas regulation of 2006 and Kigali amendment of 2016, which aims for 80% reduction in consumption by 2045. In addition, some countries have implemented taxes on HFC acquisition, including Norway [8].

The latest addition to the classes of refrigeration is hydrofluoro-olefins (HFOs). This class is characterized by low global warming potential (GWP) and ozone depletion potential (ODP), low toxicity, but are mildly flammable. There are some concerns related to the formation of trifluoroacetic acid (TFA), which total effect on environment is still under investigation [9]. At the same time, natural refrigerants are having a renaissance with an increasing interest on developing technology suited to utilize these. Natural refrigerants include ammonia, CO_2, water, air and hydrocarbons such as propane and butane. A survey conducted among companies in the Portuguese food industry (n=148) reported in 2017 that the most common refrigerant in use was R404A, followed by the HCFC R22 [10]. The average GWP for the study is 2640 and with the implementation of the aforementioned regulations, it is clear that a transition towards natural and/or low-GWP refrigerants is impending.

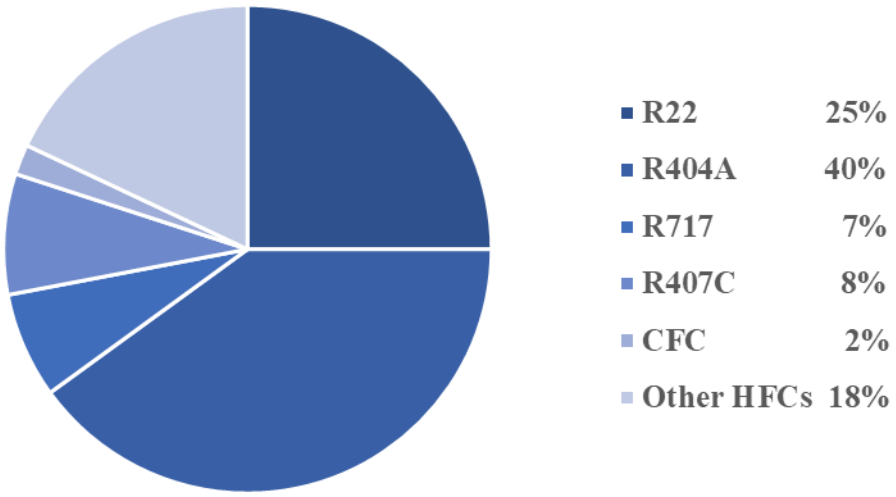

Figure 3: *Refrigerants used in the Portuguese food industry [10]*

2.2.1 Ammonia

Ammonia is well established as an excellent refrigerant for industrial refrigeration and has been in use throughout the evolution of refrigerants. This is due to the thermodynamic and physical properties, such as high latent heat of evaporation, low molecular weight, high thermal conductivity in both vapour and liquid state, low boiling point at atmospheric pressure and relatively low change in pressure per unit temperature change. The practical implications of these properties are smaller components (compressor, pipes, heat exchangers) which in turn means lower initial cost. However, a disadvantage that counter this effect is ammonias inability to work with copper or copper alloys due to its corrosive effect, leading to more expensive material choices such as steel or aluminium. Having a safety rating B2L means ammonia is highly toxic and mildly flammable, but the longevity of ammonia systems has led to well established routines and measures to handle these issues. The noticeable odour serves as an early warning for personnel in case of leakage, and the fact that ammonia gas is lighter than air makes it easily ventilated to the atmosphere. With an ODP and GWP of 0, it is environmentally friendly. Due to its high critical temperature it has also been utilized in heat pumps, with multi-stage systems on the market able to produce hot water up to 90 °C [11].

2.2.2 CO_2

CO_2 differs from many other refrigerants in several aspects. After its re-introduction as a refrigerant in the late 1980s, technology has been developed to utilize its properties. Due to the low critical temperature, CO_2 systems are often used transcritical, meaning there is no condensing of the fluid but heat rejection occurs at a gliding temperature in the supercritical region. In itself this is not a desired feature, but with proper heat recovery strategies it has proven competitive in many areas [4]. In particular, the supermarket sector in Northern Europe has adapted these kind of systems, and according to [12] the ongoing development in system architecture makes this solution viable in warm-climate regions. In low-temperature industrial refrigeration, CO_2 has traditionally found its place as the working fluid in the bottom stage of cascade systems and as secondary fluid in indirect systems. CO_2 as a working fluid is inexpensive, readily available, non-toxic and non-flammable (safety class A1). It is very dense in gas form and has a quite steep pressure saturation curve, which has some practical implications. For the compressor this means the size can be much smaller since the volumetric refrigeration capacity (VRC) will be higher. Lower pressure ratio means less compressor work and compressors designed for CO_2 therefore tends to have better isentropic efficiency. Pipe

walls have to be thicker to withstand the high pressure, but also smaller in diameter which overall lessens the total pipe weight. The steep pressure saturation curve also makes CO_2 more tolerable for pressure losses, and this also applies for heat exchanger design; the penalty for pressure loss isn't as severe as for other refrigerants. On the other side, the importance of a carefully selected suction temperature is of more importance with regards to the pressure ratio and hence compressor work. Because of this CO_2 system with flooded evaporators tend to have better COP than for direct expansion (DX) evaporators. Due to the high pressure levels and possible formation of dry ice, there are also some safety measures that must be implemented into a CO_2 system. All these special considerations that must be made for component selection and system design will normally lead to higher level of complexity and initial cost for CO_2 systems, but proper design and fulfilment of expected increase technology usage will be a driver for lowered cost in the future and can be regained through lower operation expenses.

		NH_3	**CO_2**	**R22**	**R404A**
Molecular weight	g/mol	17,03	44,01	86,47	97,60
Normal boiling point	°C	-33,3	-56,6[1]	-40,8	-45,5
Heat of evaporation[2]	kJ/kg	1345	293	224	186
VRC[2]	kWh/m3	0,48	3,57	0,56	0,66
Thermal conductivity[2]					
..liquid	W/mK	0,6382	0,1407	0,1061	0,0830
..gas	W/mK	0,0214	0,0143	0,0079	0,0106
Critical point	°C/bar	132,3/113,3	31,0/73,8	96,1/49,9	72,0/37,3
GWP[3]	[-	0	1	1870	3922
ODP[4]	-	0	0	0,055	0

[1] Evaluated at triple point pressure (5,18 bar) due to the high triple point of CO_2 [2] Evaluated at -25 °C
[3] 100 year values, mass basis [4] Relative to R11

Table 1: *Selected properties of NH_3 and CO_2*

2.3 Industrial refrigeration

Industrial refrigeration is characterized by its specialized nature and temperature range of operation. Systems are often custom-built in order to meet the refrigeration loads and tasks, as opposed to the more standardized nature of HVAC. In the food industry, there are many applications for industrial refrigeration since we need to thermally process and store food in a

manner that makes it safe for human consumption. The thermal processes can be freezing, freeze-drying, cold and frozen storage, and hot processes such as pasteurizing of milk. The evaporation temperature range in industrial refrigeration can be between 15 °C to -60 °C [13]. Often the temperature lift between source and sink can be quite high, and there can be a need to cover demands at several temperature levels, which has an impact on system design. A general approach is to divide compression and/or expansion in several stages to minimize energy losses, and two possible configurations will be further explored.

2.3.1 NH_3/CO_2 cascade refrigeration

A cascade system consists of two (or more) CCC systems connected through a common heat exchanger. This allows for selection of different refrigerants in each cycle to better utilize the fluid properties and reduces the amount of thermodynamic losses compared to a single stage system. For this case, NH_3 is the refrigerant in the high temperature cycle (HTC) and CO_2 in the low temperature cycle (LTC). The cascade heat exchanger acts then as an evaporator for the NH_3 and a condenser for the CO_2.

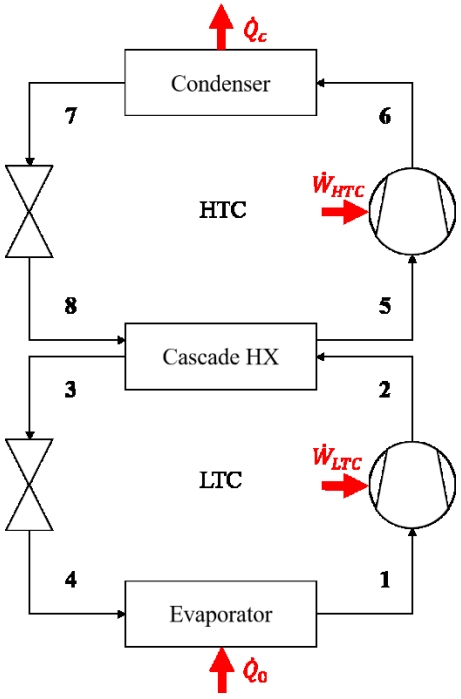

Figure 4: *Principle sketch of a cascade system*

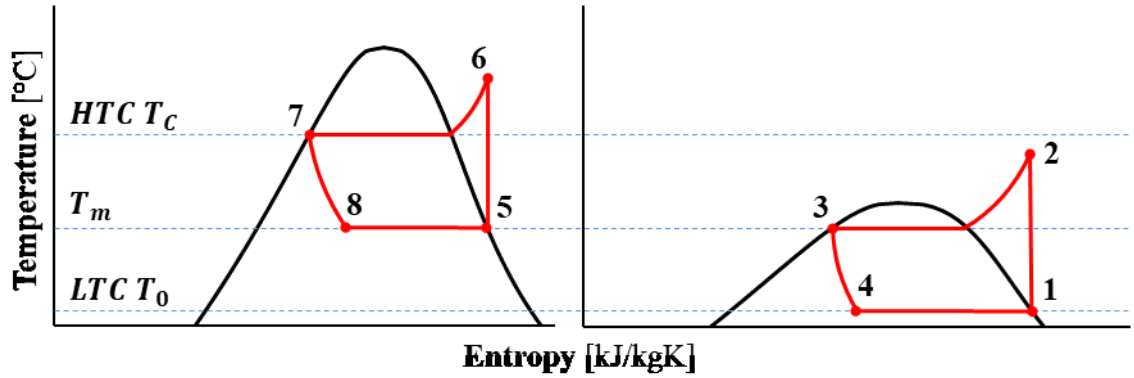

Figure 5: *Ts-diagrams for HTC fluid (left) and LTC fluid (right)*

The overall performance of a cascade system is related to the temperature levels in the cascade heat exchanger. COP of the individual cycles depends on their temperature lift, meaning a decrease in the HTC temperature lift would increase HTC COP, but also decrease the LTC COP. A parametric study ([14]) reveal that there exists an optimal overall COP of the system dependent on selection of cascade heat exchanger temperatures. Considering a system with condensation temperature of 35 °C, evaporation temperature of -35 °C, fixed isentropic compressor efficiencies and a 5 K temperature difference in the cascade heat exchanger, the results from the study are reproduced in Figure 6.

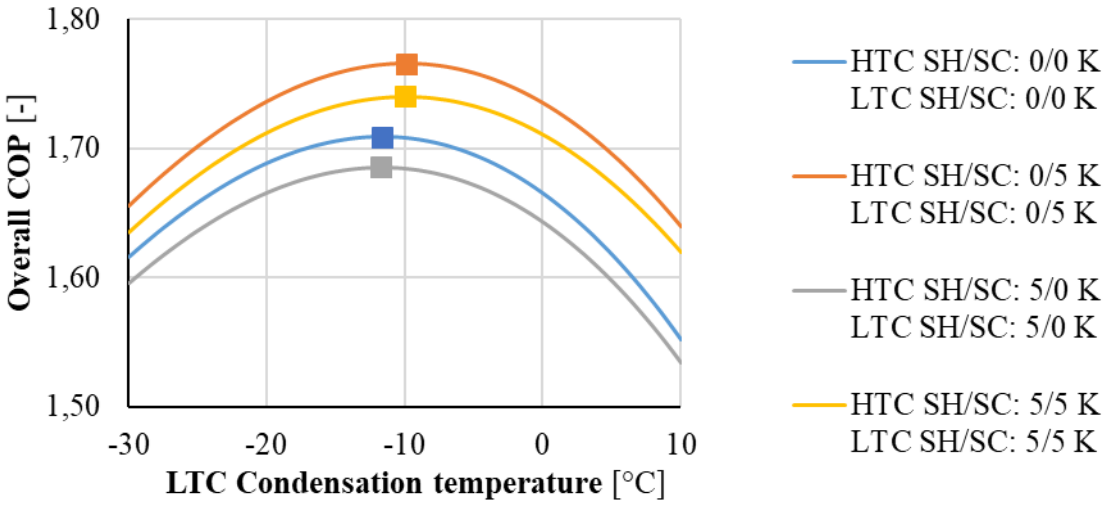

Figure 6: *Overall COP of a NH3/CO2 cascade system as a function of LTC condensation temperature. Reproduced from [14]*

Four cases with different superheating and subcooling settings are illustrated. The results reveal an optimal COP for each case. Also note that subcooling has a positive effect on overall performance, while superheating has a negative effect. The numerical values are only valid for

the particular case, and optimal LTC condensation temperature would change with different boundary conditions.

Practical implications of using a NH_3/CO_2 cascade system is the reduced amount of NH_3 charge. This is positive with regards to the safety restrictions attached to NH_3. Specific volume of NH_3 rapidly increases at low temperatures, which consequently means compressor sizes also rapidly increase. Also, using NH_3 at low temperatures, i.e. below -33,3 °C implies sub-atmospheric pressures in pipes and components. Because of this it is rational to have a bottom stage with another fluid, and CO_2 with its described properties makes for a good choice.

2.3.2 Multistage refrigeration

High temperature lifts in refrigeration can be achieved by dividing the compression and expansion in several stages, hence the term multistage refrigeration. While multistage design might be a necessity due to high pressure ratios following the high temperature lift, it also provides opportunities to improve the thermodynamic processes. Flash gas removal is one opportunity accompanying two stage expansion. Separating vapour and liquid after the first expansion stage means reduced work for the low stage compressor, increased refrigeration capacity and increased refrigeration effect of the evaporator. Two stage compression leads to reduced total compressor work and lowers the discharge temperature from the compressors. Based on thermodynamics, the optimal intermediate pressure level can be chosen on the basis of both compression stages having equal compression ratios [4].

$$P_m = \sqrt{P_c \cdot P_0}\,[-] \tag{2.10}$$

However, for systems required to match several evaporation temperature levels, intermediate pressure level will be a result of those temperatures. The penalty which occurs at off-optimum level (increased compression work) depends on how large the offset is and type of refrigerant. In most cases the penalty is rather low, meaning the systems performance relationship to optimal intermediate pressure is non-critical. Two different systems designed for meeting two refrigeration load temperatures will described to exemplify different features.

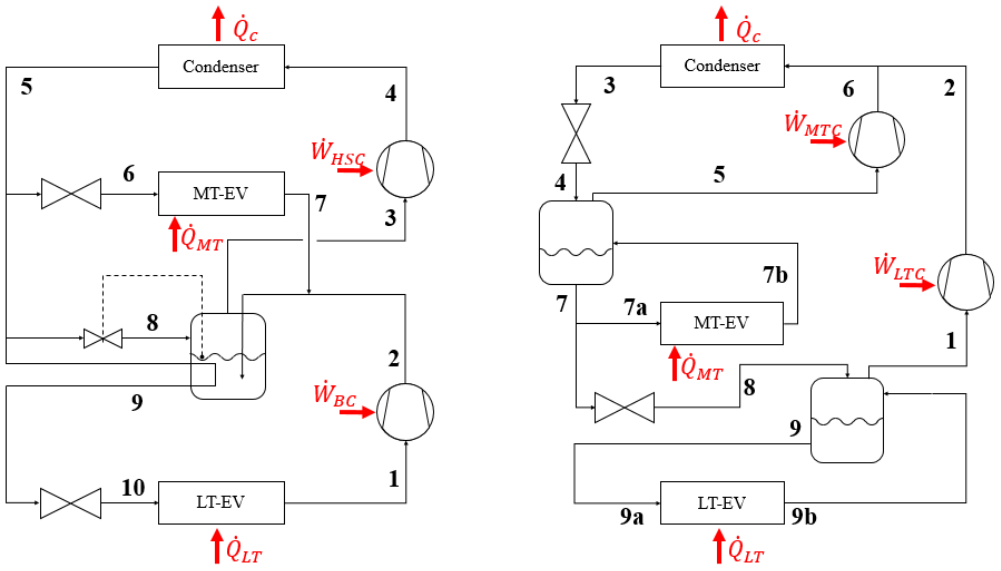

Figure 7: *Two examples of multistage refrigeration systems (system A and system B)*

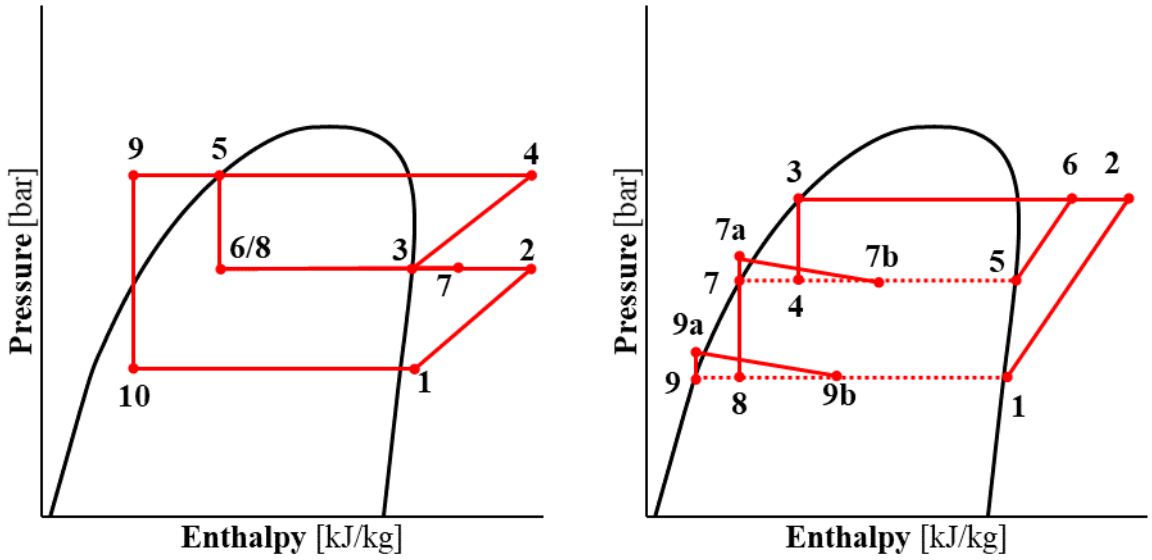

Figure 8: *pH-diagrams for system A and system B*

System A includes two compression and expansion stages. The high stage compressor (HSC) draws saturated vapour from a separator vessel, which is then compressed and condensed. After the condenser, a part of the liquid is expanded down to meet the medium temperature evaporator (MT-EV), a part is expanded into the separator vessel to maintain liquid level and a part is subcooled internally through the vessel. If the MT-EV is a direct expansion evaporator, the hot vapour can be routed directly back to the HSC, or as pictured, routed to the vessel in order to

de-superheat before compression. Flooded type evaporators must be connected to the vessel in order to prevent liquid suction in the HSC. The low temperature evaporator (LT-EV) will experience a greater fraction of liquid due to the subcooling effect, and hence have better refrigeration effect. The low stage compressor compresses the vapour up to intermediate pressure and is then de-superheated before entering the high stage.

System B includes two expansion stages and one compression stage with a medium temperature compressor (MTC) for removal of flash gas. The low temperature compressor (LTC) draws saturated vapour from the low pressure separator vessel and compresses it directly to high stage where it mixes with vapour from the MTC before entering the condenser. This is energy efficient since we avoid unnecessary expansion and compression from a lower pressure level. The high pressure separator vessel contains a two-phase mix, of which the MTC draws the vapour and liquid is being fed to the MT-EV and for further expansion. The low pressure vessel feeds liquid to the LT-EV. This system utilizes flooded evaporators, which can be driven by gravity or forced circulation (pumps). Flooded evaporators have excellent heat transfer properties compared to the direct expansion type and no area is required for superheating of the refrigerant, but the charge amount is larger [13]. This gives the possibility for elevated evaporation temperatures, which is particularly important for CO_2 due to its steep pressure-temperature relationship; for each Kelvin we can elevate, the suction pressure also elevates and thus less work for the compressor.

2.4 Thermal energy storage

As the name suggests, TES is saving of thermal energy for later use, and is a supplemental feature that can be integrated in cold and hot industrial processes. One of the main reasons to implement such a feature is to offset the mismatch between supply and demand (in time), but there are also other reasons in terms of energy efficiency, technical flexibility and economic benefits. With respect to the food-processing industry, perhaps the most significant benefit of this technology is that it can reduce electrical demand and energy charges by shifting a portion of the cooling production from high-cost to low-cost hours. In TES terminology this means that we charge a storage during low-cost hours, and discharge it during high-cost hours. Storage size is dimensioned according to operational strategy, where the two main strategies are either full-storage or partial-storage. As an example of the latter, a case adapted from [15] is seen in Figure 9. What can be seen is the thermal load profile for an Italian exhibition centre which during opening hours has a peak in cooling demand. Without TES, the chiller system would

have to cover the total cooling demand, and thus the energy consumption of the chillers would have a similar trend as the thermal load profile.

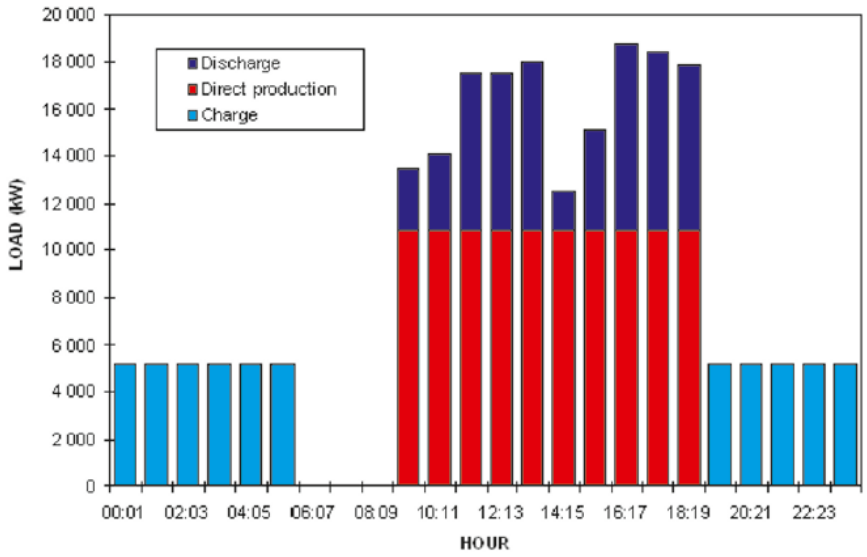

***Figure 9**: Thermal load profile illustrating charge, discharge and direct production processes of TES. Adapted from* [15]

To avoid this peak in energy consumption during day time, the centre has installed TES storages which assist with cooling day time (dark blue discharge bars). In effect this caps the direct production by the chillers and thus the energy consumption. During night-time when there is no cooling demand, the chillers are used to charge the storages.

Charging and discharging refers to two of the basic processes involved with TES storages, with storing being the third. Storage design and choice of storage medium are important parameters which influences size, capacity and at which rates heat transfer occur. With respect to heat transfer, [15] distinguishes between three basic design options:

- Exchanging heat at the surface of the storage
- Exchanging heat on large surfaces within the storage
- Exchanging heat by exchanging the storage medium

The latter two designs are the most relevant for industrial applications due to higher heat transfer rates and better control over the heat transfer process. With respect to choice of storage medium, it is typical to distinguish between sensible and latent mediums.

2.4.1 Sensible TES

Sensible storage is accomplished by transferring thermal energy to a liquid or solid in which the temperature changes, hence the name sensible. A typical liquid storage medium is water, and probably one of the most common examples of TES methods is the domestic hot water storage tank. The amount of energy that can be stored in a medium can be defined as:

$$Q_{storage} = \frac{m \cdot c_p \cdot \Delta T}{3600\ s} = \frac{\rho \cdot V \cdot c_p \cdot \Delta T}{3600\ s}\ [kWh] \tag{2.11}$$

By inspecting Equation 2.11 we see that the specific heat and mass are important factors that influence the amount of stored energy. For this reason, water with its relatively high specific heat of $\sim 4200\ \frac{J}{kgK}$ is widely used as a medium. Other advantages of using water is that it is inexpensive and widely available, it can be used as both the storage medium and heat transfer medium and allows for simultaneous charging and discharging of the storage tank. Having the storage medium acting as heat transfer medium means there is no need for additional heat exchangers and therefore less overall temperature lift in the system [16]. A drawback for cold TES (CTES) using water tanks is of course the freezing temperature of water that limits the range of applications. Another drawback is the large storage tank volume required [5]. A common application is integrating chilled water tanks with the air-condition system. This provides the opportunity to produce cooling (charge the tanks) at night when cooling loads and electricity rates are low, and discharge them during the day when cooling loads increases. Dependent on sizing of the tanks, the TES can provide either all cooling loads or part-load. For water tanks to be effective, they should be thermally insulated to avoid heat loss/gain and the tank should be thermally stratified [5].

Another common application is underground TES (UTES), which provides the opportunity for long-term storage (seasonal) of thermal energy in the ground, groundwater or caverns. The ground temperature below a depth of 10-15 m approximately equals the annual average air temperature, meaning that it is higher than ambient air temperature during the winter and vice versa in the summer [17]. By inserting long vertical heat exchangers in boreholes at depths from 20 to 300 meters, heat can be extracted during the winter and used as a heat sink during the summer (recharging the ground), thus act as a storage system. Low temperature UTES ranges from 0-40 °C, while the current upper limit for high temperature is around 90 °C due to hydrochemical, biological and geotechnical challenges [17]. Geological conditions decide the

type of UTES system, and has an important influence on storage efficiency and investment cost, which is typically high.

2.4.2 Latent TES

Latent heat storage uses a phase changing material (PCM) as storage medium. When transferring heat to such a medium we utilize phase change in the medium, typically the solid-liquid transition. Phase change occurs at constant temperature, and with the wide range of material choices, it provides a wide range of applications. The amount of energy that can be stored as latent heat in a material is described as:

$$Q_{storage} = m \cdot \Delta h_{pc} \tag{2.12}$$

In Equation (2.12), Δh_{pc} is the phase change enthalpy for the given substance. A common example is the use of water, or ice. It has a phase change temperature of 0 °C and a phase change enthalpy of 333 kJ/kg. A great advantage with latent storage over sensible storage is the reduced storage volume. For a ΔT of 20K, liquid water can hold 23 kWh/m^3, while ice can hold 86 kWh/m^3, almost 4 times as much. For temperature requirements below 0 °C, eutectic mixtures of water and salt are typically used [15]. There is a wide variety in the design of a latent heat storage system, with regards to geometry of PCM storage and how heat transfer from/to storage occurs.

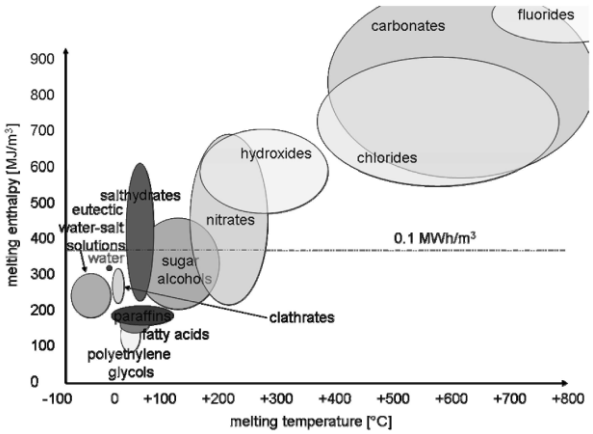

Figure 10: *Different PCM classes with typical range of phase change temperature and phase change enthalpy. Figure obtained from [17]*

2.5 Thermal loads in the food industry

Many thermal processes are involved to make food safe for human consumption and extend its shelf life. Sterilization of food, that is to reduce the amount of microorganisms dangerous for

humans and contributes to food spoilage, is achieved by applying heat to the product for a certain amount of time (e.g. pasteurization of milk). Water removal is achieved through evaporation for liquid foods such as tomato paste, or by dryer units for solid food. Many food products are often chilled or frozen at the end of processing, a state that is maintained throughout the distribution chain until it ends up at the consumer.

Which processes are involved depend on the food being processed, and many different methods can be applied for each process. Hence, the sequence of processing may be different for different plants processing the same food. Figure 11, which is a simplified adaption from [18], describes the primary processes of a poultry plant. The thermal processes here are scalding, chilling, freezing and chiller/freezer storages. Scalding is done to loosen the feathers before the de-feathering process, and is achieved by either immersing the bird in hot water (50-60 °C) or by steam. After evisceration and washing, chilling takes place to minimize growth of microorganisms and for easier handling when portioning. Final product is then packaged and stored in a chiller storage, or frozen and stored, ready for distribution. Norwegian law dictates that the core temperature of poultry should be kept below 4 °C after preliminary chilling and throughout distribution chain (FOR-2008-12-22-1624, appendix III, section I, chapter VIII, item 4b). For frozen products, temperature requirement is -18 °C, but allows for a 3 K temperature deviation during distribution (FOR-2008-12-19-1618, chapter II, § 5).

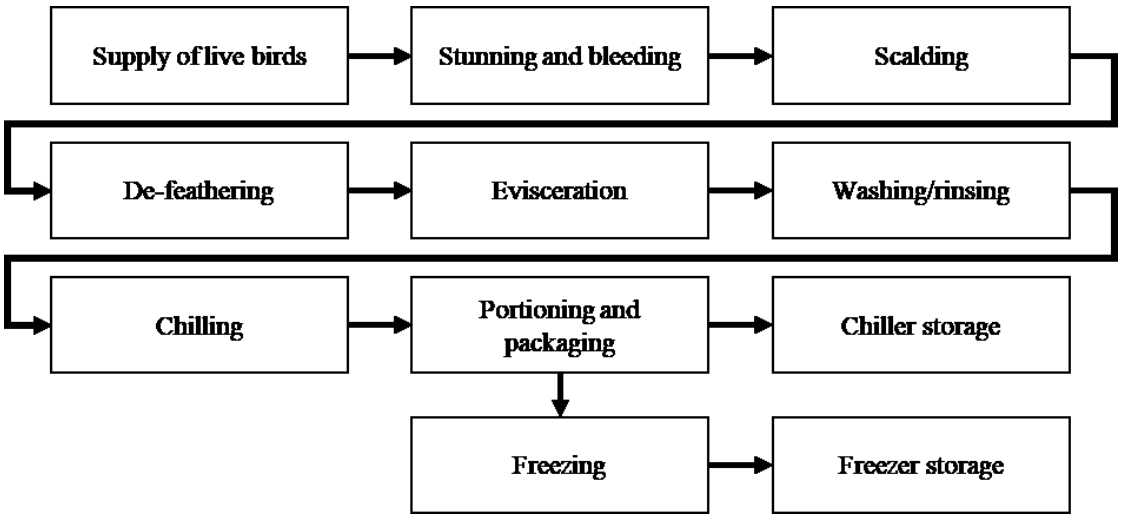

Figure 11: *Simplified flow diagram showing the primary sequence of poultry processing*

What is common for these processes are that they occur during production, which gives the thermal load-time profile for a food processing plant a very characteristic form, almost like a

bell curve with the peak during production period. Thermal loads outside this period are mostly associated with upkeep of cold storage, if any.

2.5.1 Principle processes of chilling and freezing food

Thermal handling of food requires knowledge about the thermal properties of food, which differs greatly between the different types of food. This great variation makes it difficult to tabulate properties over a wide range of conditions, so methods for predicting thermal properties have been developed based on composition of food. The primary components in food are water, protein, fat, carbohydrate, fiber and ash. With the knowledge of food composition and use of empirical formulas found in different literature such as ASHRAE Handbook - Refrigeration [19], we can predict relevant properties such as specific heat, density, enthalpy, initial freezing point and thermal conductivity, which are essential when performing calculations involving heat transfer. Figure 12 depicts the curves of some selected properties, calculated with formulas from [19]. The characteristic form of the curve is independent of type of food. The vertical, black stapled line indicates the initial freezing temperature, and the graphs clearly illustrate the change in behaviour when crossing this line. The more or less linear behaviour of properties ceases when food is brought below initial freezing temperature, and the non-linear behaviour which occurs is reflecting the complex processes which are involved with freezing of food. The rapid change which occurs right below initial freezing temperature is mostly influenced by the predominant component in most foods, water. Most food has an initial freezing temperature below that of water because the water is mixed with dissolved substances from the food, like salt and sugar.

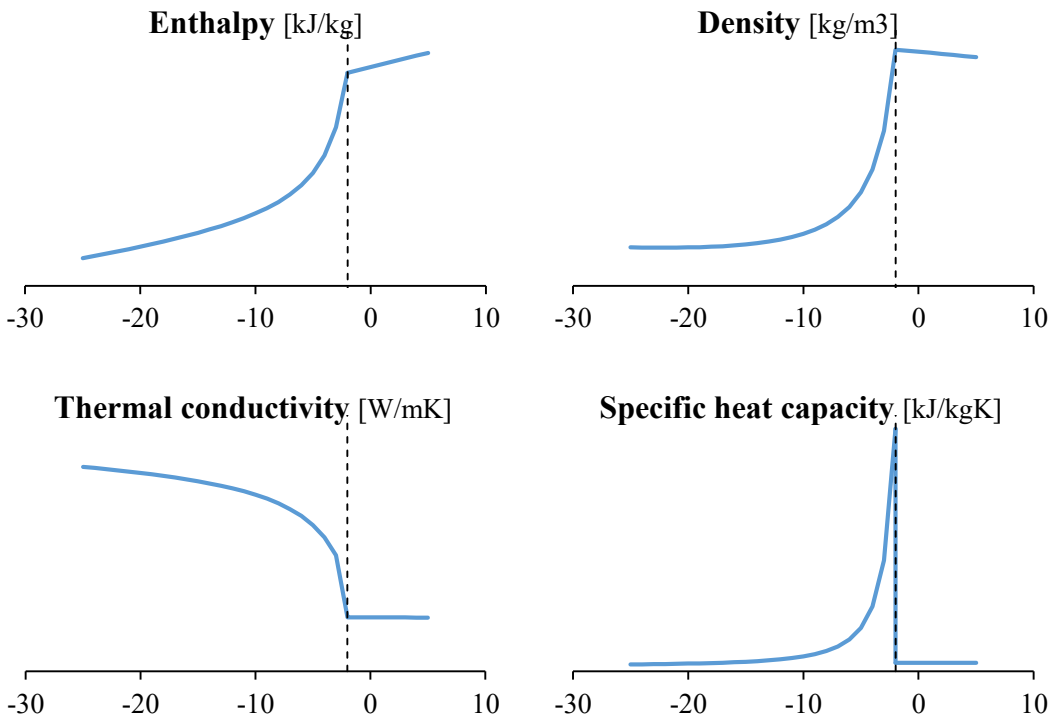

Figure 12: *Characteristic curves of selected thermal properties, relative values independent of food. All abscissas are temperature [°C]*

This leads to depression of the freezing point, and this depression continues as more and more water has formed ice due to the remaining water solution becoming more concentrated. When most of the water in the food has frozen, the rate of change in properties decrease.

By looking at the enthalpy curve, it can be clearly seen that freezing food is a much more energy intense process compared to chilling. Using poultry data and formulas from [19], the amount of energy that needs to be removed from poultry (chicken) when decreasing temperature from 30 °C to -18 °C is three times more than a decrease down to 4 °C.

Temperature [°C]	**Energy removal** [kJ/kg]
30 → 4	88
30 → -18	306

Table 2: *Required energy removal compared for freezing and chilling of poultry*

Knowledge of these thermal properties are important when performing load calculations for storages and equipment. With regards to chilling and freezing times, physical properties such as size and shape of food product are also important parameters. While chilling time is not dictated by Norwegian law, it is an important parameter with regards to the production rate of the process plant. For freezing, time plays a larger role in terms of quality of the final product.

An important aspect when freezing food is to attain desirable crystallization structure, which means the formation of many, small ice crystals as opposed to fewer and larger. Formation of large ice crystals tends to dehydrate and damage the shape of cells within the food, which leads to increased drip losses upon thawing and undesired softening of the food [20]. Time spent in the critical zone is what determines the growth of ice crystals. Critical zone is an interval around the initial freezing point of the food, from slightly before the first ice crystal forms till end of freezing plateau.

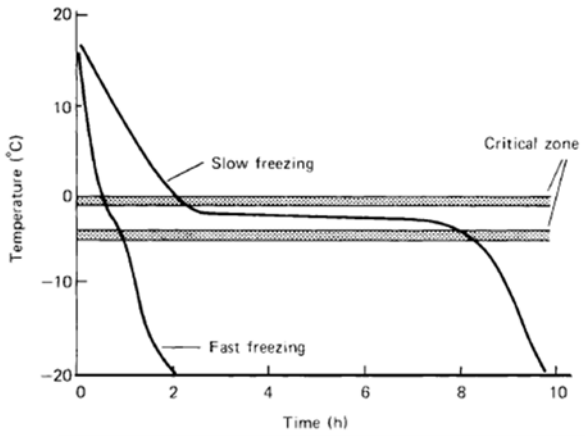

Figure 13: *Freezing of food. Adapted from* [20]

As can be seen in Figure 13 a rapid freezing process is able to achieve this desirable structure, and thus reduce unwanted loss of quality. However, skin damage can occur if the freezing happens too rapidly, due to internal stresses that are built up within the food. Thus is the optimum freezing time somewhere in between these two phenomena's.

2.5.2 Methods for chilling

Chilling of poultry is typically done by chilled water-immersion, air chillers, spray chillers or a combination of these methods, and there exists different designs for each option. Immersion chilling can be done in a counter-flow screw chiller, where the poultry is moved forward by an auger through chilled water in a cylindrical vessel. Such chillers exist in different diameters, and length can often be set to match production rate requirement through modular design. Heat transfer can be enhanced by manipulating the water flow, and typical dwelling time is between 30-90 minutes depending on poultry size [18]. Immersion chilling can to some extent be combined with the washing process, but a drawback is that the poultry must be allowed to drain to remove excess water after chilling.

According to [18], air chillers are more common in European plants. Typical design can be a chilling tunnel where cold air circulates over the poultry, which can be stacked on trays or hanging on an overhead conveyor system, allowing for continuously chilling. Another design is to have the product on multi-layered conveyor belts moving through a compact-form vessel in which cold air circulates. Control over air temperature, flow pattern and humidity gives good control over chilling rate and poultry quality. A benefit by using such equipment as opposed to immersion chilling is reduced moisture uptake in the poultry. Additional benefits are described in a study comparing air- and immersion chilling of marinated broiler breast filets, which concluded that air-chilling has advantages with regards to shelf life, tenderness, ability to take up marination (because of drier product) and colour [21].

Spray chilling is a hybrid between immersion and air chilling, where the poultry is placed in a refrigerated air system while being sprayed with water. Usually the spraying occurs at intervals and not continuously, and the principle is to increase the heat transfer rate due to evaporation, while at the same time reduce the overall weight loss [22].

2.5.3 Methods for freezing

Freezing methods can be categorized in different manners. With regards to basic method of heat extraction, they can be categorized as blast freezing (convection), contact freezing (conduction), cryogenic freezing (convection and/or conduction) and cryomechanical freezing (convection and/or conduction) [19]. Another manner is to divide them into slow freezers, quick freezers, rapid freezers and ultra-rapid freezers, where slow/quick/rapid and ultra-rapid refers to the rate of movement of the ice-front [20]. A home freezer would be an example of a slow freezer, where still air at around -20 °C extracts heat from the product in it. Due to the crystallization phenomena discussed earlier, such freezers are not meant to freeze food, but rather keep already frozen food at a frozen state. For poultry it is common to utilize quick freezers, such as different designs of air-blasting freezers where the product is individually frozen (IQF – individual quick freezing). For small, thin products this can be achieved in an impingement freezer, where air nozzles are placed perpendicular to the product which moves through the freezer on a conveyor belt. Air flows out of the nozzles at high velocity, like depicted in Figure 14, disturbing the boundary layer surrounding the product and thus increases the heat transfer rate and has a freezing time between 1-10 minutes.

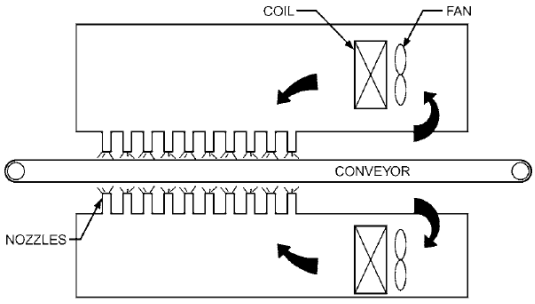

Figure 14: *Principle sketch of an impingement freezer. Adapted from* [19]

Another common method is the air blast freezer. As the name suggests, cold air is blasted at high velocities in the freezer. The product may either be stacked stationary on trolleys, or moving through on belt conveyors or overhanging conveyors. A spiral belt freezer, or gyro freezer, is an example of such a type. As depicted in Figure 15, product moves in at bottom left, moving on a conveyor belt which is formed in a spiral fashion, before exiting at top right.

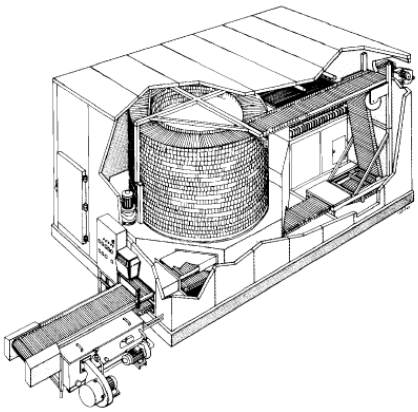

Figure 15: *Gyro freezer. Adapted from [20]*

The fastest methods for freezing are of the cryogenic type. Spraying the product with either liquid CO_2 or liquid nitrogen at very low temperatures, heat is extracted from the product while the refrigerant vaporizes. In order to utilize most of the refrigerant, the vapour is recirculated and used to pre-cool the product, while the remaining liquid is recirculated back to the liquid stream. The freezing rate for such freezers are very high, and this type of equipment has a relatively low capital cost. This is however offset by the high cost of refrigerant, meaning that pure cryogenic freezers are uncommon for food process plants with continuous production. According to [20] the refrigerant consumption rates are around 100-300 kg liquid nitrogen per 100 kg frozen product, and 120-375 kg liquid CO_2 per 100 kg frozen product.

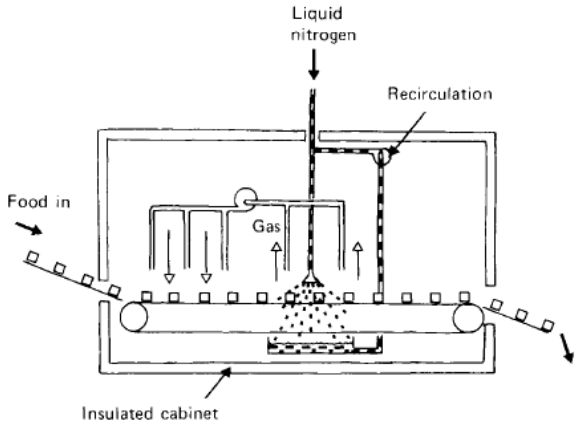

***Figure 16**: Principle sketch of cryogenic freezer utilizing liquid nitrogen. Adapted from* [20]

2.5.4 Storages and production areas

A large contributor to the overall load for the energy central is associated with the storing of chilled and frozen product, and also keeping production areas cold enough to ensure that the poultry core temperature does not rise above the 4 °C limit. The objective of the energy central is to keep the room temperature in these areas at a desired level. Failure to properly calculate these kinds of loads can inhibit the energy centrals ability to do so, and an increase in room temperature will ultimately lead to spoilage of product or decrease of storage capacity.

The storage load is influenced by a number of factors. Heat transmission through walls, ceiling and roof is usually one of the largest contributors, and is a consequence of the temperature difference over the storage envelope. Chapter 24 of [19] suggests that the transmission load, at steady state, can be calculated as in Equation (2.13).

$$Q_t = UA\Delta t \tag{2.13}$$

In Equation (2.13) A is the outside section area, U is the overall heat transfer coefficient and Δt is the temperature difference between the ambient and desired room temperature. Proper calculation of the U-value depends on thickness and construction of the section, and highly on type of insulation. For sections illuminated by the sun, the temperature difference should account for this effect. Given the daily and seasonal variations in outdoor temperature, this difference should be selected so that the capacity of the central is able to cope with the warmest

conditions. Heating cables are often used in floor sections to prevent frost heaving, and the added heat gain due to this should also be accounted for.

Shifting of air, due to ventilation and opening-closing of doors, means that warm and moist air enters the storage and this air has to be cooled down to storage temperature. Cooling of said air includes not only the sensible energy removal, but also condensing (and freezing for freezer storages) of the moisture. This heat gain can be inhibited through some different means, like the usage of air curtains, vestibules, plastic strips and compartmentalization of loading docks.

Product load is dependent on amount of product and temperature levels. Any difference between room and product entry temperature means removal of sensible heat from the product. This is typical for frozen storages: product temperature of poultry is -18 °C after freezing, and room temperature for a frozen storage can typically be around -25 °C. Product packaging, pallets or trolleys they are stacked on etc. also must be accounted for in the same manner.

All equipment and internal operations taking place in the refrigerated area creates a load. This includes working people, lights, fans, trucks etc. Type of storage greatly influence the size of this factor. There will most likely be a higher degree of internal operations taking place in a short-term distribution storage than for a long-term storage. Defrosting of evaporators must be done to ensure proper refrigeration, which also adds to the total load. Methods to estimate these different kinds of loads can be found in [19].

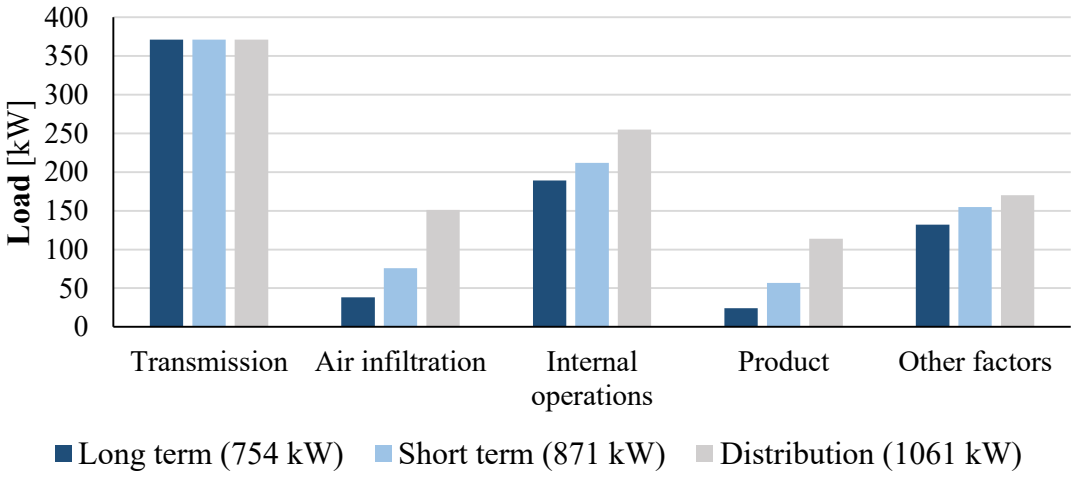

Figure 17: *Refrigeration loads in different storages. Based on numbers from* [4].

To illustrate the variation of refrigeration loads dependent on type of storage, Figure 17 has been made based on a numerical example from [4]. The size is the same for all three storages

(single floor 10 000 m^2 frozen storage), thus the transmission loads are equal. However, there is an increase in the other loads due to the increased amount of operations and activity in each type of storage.

2.5.5 Industrial HVAC

While human comfort is the objective of a residential HVAC system, the industrial HVAC system is directed towards the processes. For a food plant this means maintaining an appropriate environment in which food is processed to facilitate for safe and high quality product. Control over room air temperature, humidity level and air ventilation is what constitutes an appropriate environment. Norwegian law (FOR-2008-12-22-1624, appendix III, section I, chapter VIII, item 4b) dictates that the room air temperature should be 12 °C or below when further processing chilled poultry. This is to help maintain the poultry core temperature below 4 °C, which is important for inhibiting bacteria growth. Proper ventilation is important to minimize the potential of airborne bacteria and contaminants, and for releasing undesired odours and built-up gases. Control of humidity is important with regards to both food safety and preventing corrosion on process equipment. This is especially important after periods of cleaning and sanitation, where the air will contain a high degree of moisture.

3 Design and operation of the energy central

The energy central plays a critical part of the poultry process plant as it designed to cover all thermal demands necessary for production and storing of goods. At the heart of the central is the refrigeration system, which will be described in this chapter. A simplified process and instrumentation diagram (P&ID) is presented in Figure 18, accompanied with description of primary functions and working principles.

3.1 System description

Primary function of the refrigeration system is to cover all internal refrigeration demands, which are divided in three temperature levels; freezing (LT), chilling (MT) and cooling of air (AC). In addition, hot water pre-heating is planned for by recovering heat from parts of the system. The final hot water production, and also steam production, is covered by other means and is not further described.

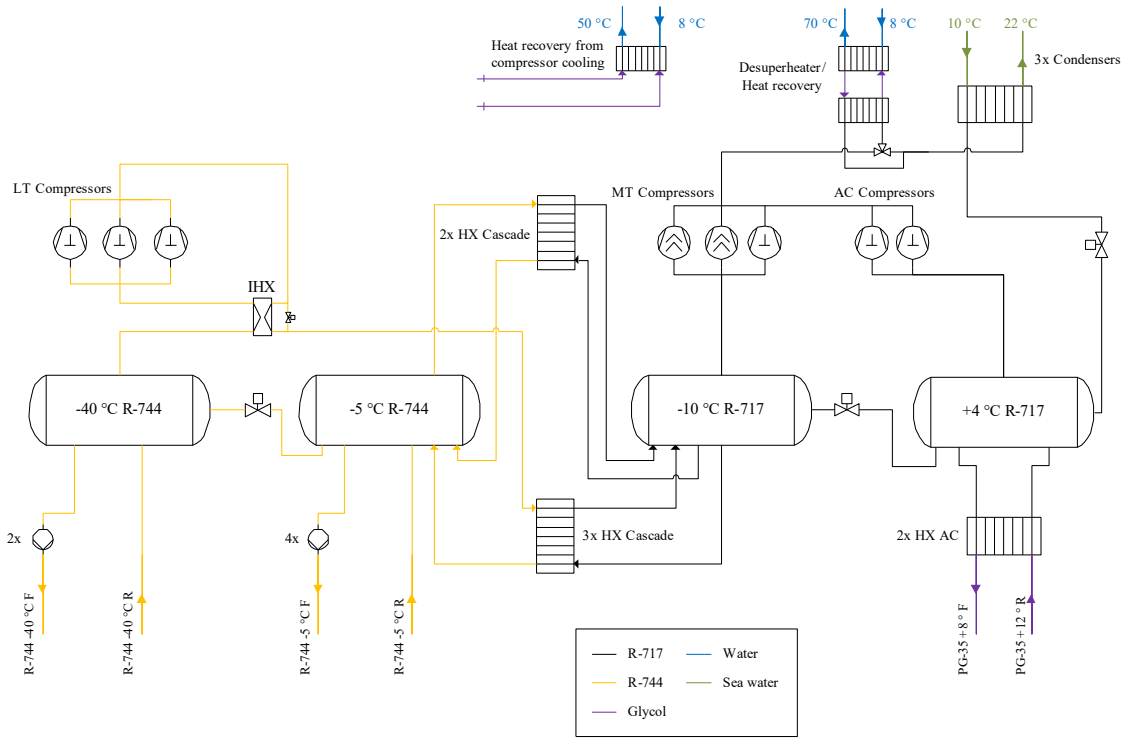

Figure 18: *Simplified P&ID for the refrigeration system*

A cascade solution is selected for the system, with a bottom cycle utilizing CO_2 as working fluid to cover refrigeration demands at low and medium temperature level. Consumers for these circuits are process equipment for chilling and freezing, and maintaining room temperature in the cold storages, production and dispatch areas.

Condensation heat from the bottom cycle is transferred to the upper cycle via two groups of cascade heat exchangers, employing NH_3 as working fluid. In addition to further lift and reject condensation heat, this cycle covers the AC demands through cooling a glycol circuit in a group of heat exchangers. Dehumidifying of production areas follows after sanitary cleaning, involving cooling of intake air. This cooling is served by the AC circuit, thus a significant peak demand occurs during this process.

Hot water pre-heating is achieved in two utilities at different temperature levels. A de-superheater (DSH) recovers heat from the MT and AC compressor discharge lines and is able to produce 70 °C water, while heat from the compressor motor cooling circuit (MC) can produce 50 °C water.

Energy circuit	**Capacity** [kW]	**Refrigeration demand**
LT (-40 °C)	1250	Freezing process equipment and storages
MT (-5 °C)	3250	Chilling process equipment, storages and production areas
AC (+4 °C)	2600	Air cooling with particular demand during washdown and dehumidifying
DSH	430	Pre-heats water from 8 to 70 °C
MC	620	Pre-heats water from 8 to 50 °C

Table 3: *Description of energy circuits in the refrigeration system*

3.2 Cycle descriptions

Bottom cycle

The bottom cycle consists of the low temperature and medium temperature circuit. Each circuit has a separator and a set of refrigerant pumps which delivers cold liquid to consumers. CO_2 is a non-toxic refrigerant which is suitable for food refrigeration applications and therefore the need for a secondary coolant and additional circuit is deferred. Properties of CO_2 also allows for small pipelines and is relatively easy to pump, resulting in little pump work for the refrigerant pumps. The pumps are configured to maintain a circulation ratio of 3, which allows for easier distribution to the different consumers, and also facilitates for good heat transfer. Returning refrigerant is then in a two-phase mix of liquid and vapour.

Vapour from the LT separator is drawn by a group of three piston compressors (LT compressor group) which compresses it to a condensation pressure of 30,5 bar. An internal heat exchanger (IHX) is employed to prevent liquid slugging of the compressors, and a modulating by-pass valve controls the amount of superheat to the compressors common suction line. The compressor discharge stream is condensed in a group of three heat exchangers, transferring heat to the upper cycle, before returning to the MT separator.

Fluid in the MT separator holds the same pressure level of 30,5 bar. Vapour from this tank is condensed in another group of cascade heat exchangers, where circulation occurs naturally. An expansion valve between the separators ensures that there is enough liquid in both tanks to satisfy the refrigeration demands.

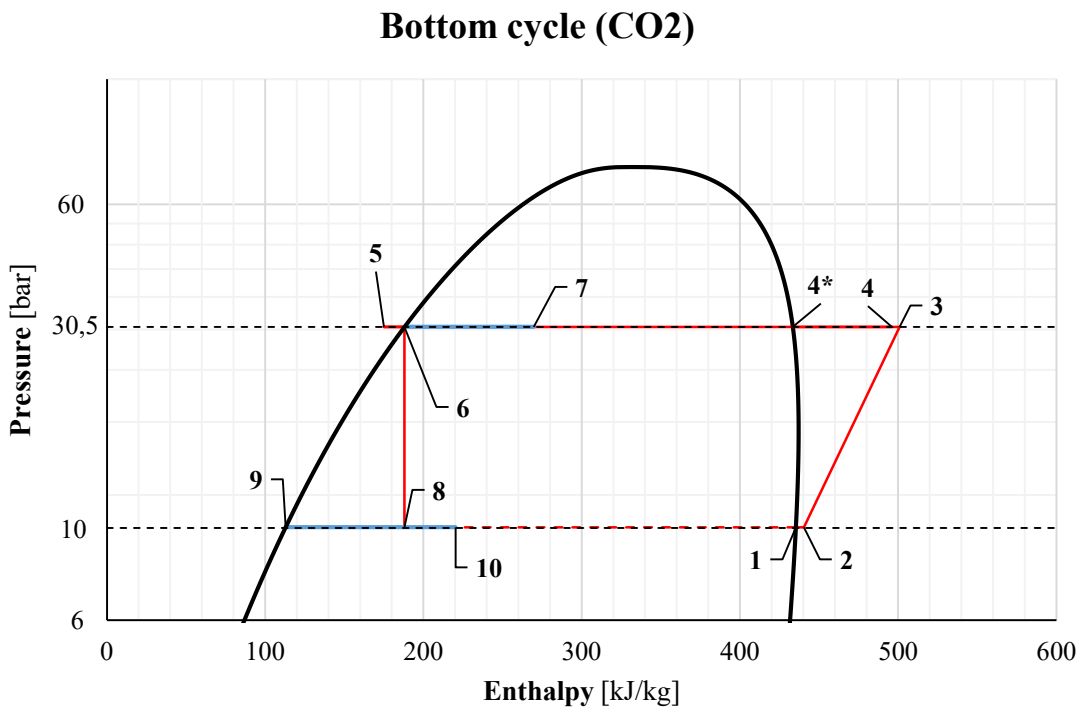

Figure 19: *pH-diagram for bottom cycle*

State points	Process
1-2	Superheating of suction line by IHX pre-compression
2-3	Compression by LT group (condensation level 30,5 bar/-5 °C)
3-4	Mixture of stream from IHX and IHX by-pass
4-5	Condensation of compressor discharge streams, included subcooling
4*-5	Condensation of vapour drawn from -5 °C separator, included subcooling
6-7	Evaporation in chiller consumers ($\dot{Q}_{chilling}$)
6-8	Expansion to freezing pressure level (10 bar/-40 °C)
9-10	Evaporation in freezing consumers ($\dot{Q}_{freezing}$)

Table 4: *Processes in bottom cycle*

Upper cycle

The upper cycle extracts the condensation heat from both groups of cascade heat exchangers by supplying cold liquid NH_3 to the exchangers. The supply is driven by gravity, and this type of system is referred to as a gravity flooded heat exchanger. This allows for an efficient heat transfer process and defers the need for a pump to supply liquid to the exchangers, but has some practical implications with regards to how equipment is placed in the machine room and demands proper design of the heat exchanger. Proper circulation through the heat exchangers depends on establishing a sufficient large liquid leg between the low pressure NH_3 separator and the heat exchangers, but is also affected by the rate of heat transfer. Typically, such heat exchangers have a co-current flow profile to better initiate boiling of cold side refrigerant, but due to high temperature difference between the LT compressor discharge and NH_3 streams, counter-current flow profile have been chosen to avoid circulation instabilities [23]. This process is illustrated in a pH-diagram for the upper cycle (Figure 20) as the points 13-14-15. The MT compressor group, consisting of two screw compressors and one piston compressor, is responsible to lift this condensation heat further for rejection. This group can be considered the "work horse" of the system, having the largest share of compressor cooling capacity.

Refrigeration demand by the AC system is also covered by the upper cycle. A group of two heat exchangers are fed liquid NH_3 by gravity in the same manner as for the cascade heat exchangers, the only difference being that this group is configured with a co-current flow profile. A glycol circuit serves the AC consumers and is cooled against the NH_3 in the AC heat exchangers, which is dimensioned for a heat duty of 2600 kW at supply/return temperatures of 8 °C and 12 °C. The evaporated NH_3 is handled by an own set of compressors, which prevents unnecessary expansion and recompression, and thus less total compression work for the system.

Condensation heat from the refrigeration system is rejected through a group of three sea water condensers dimensioned for a total capacity of 8500 kW. Compared to dry air coolers, this solution provides the possibility for more stable operation conditions due to the lesser deviation in sea water temperature, both day & night and seasonal. The sea water must however be extracted from a certain depth and delivered to the exchangers, which means infrastructure in form of sea water pipes, pumps and filters must be constructed. The condensed liquid is throttled down first to AC level (4, 97 bar/+4 °C) and fed to the medium pressure NH_3 separator, and an additional expansion valve between the separators controls the charge level of both tanks.

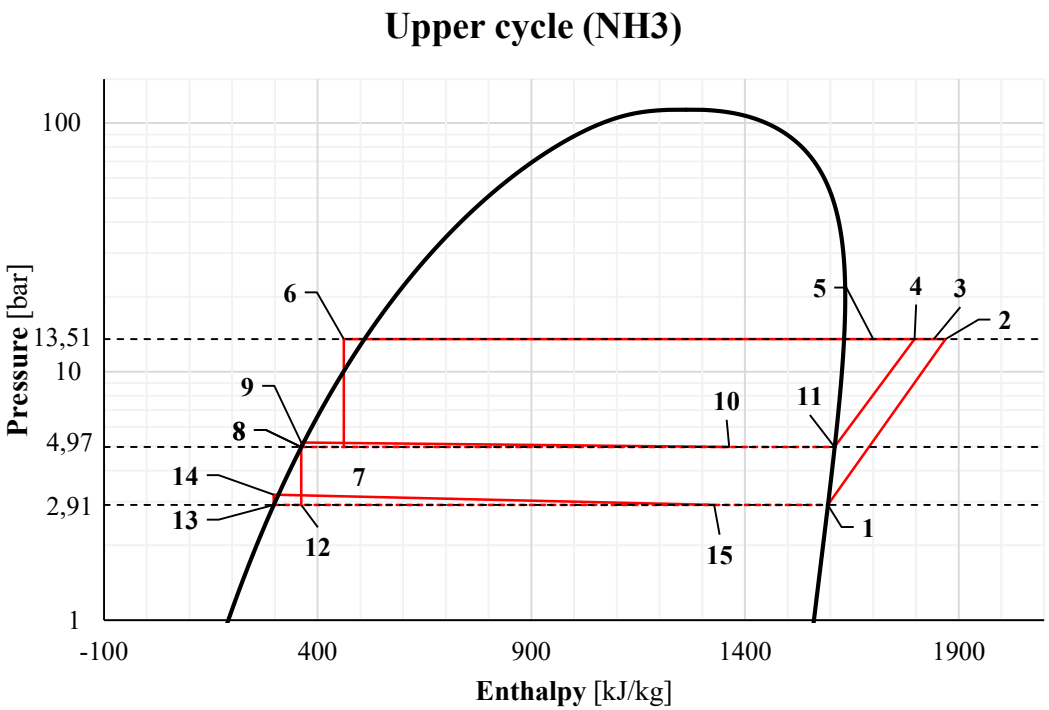

Figure 20: *pH-diagram for upper cycle*

State points	Process
1-2	Compression by MT compressor group
2-4-3	Mixing of discharge streams from both compressor groups
3-5	DSH/Heat recovery, pre-heating of washing water
5-6	Condensation included subcooling
6-7	Expansion to AC pressure level (4,97 bar/+4 °C)
8-9-10	Evaporation in AC heat exchangers ($\dot{Q}_{AC}$)
11-4	Compression by AC compressor group
8-12	Expansion to cascade pressure level (2,91 bar/-10 °C)
13-14-15	Evaporation in cascade heat exchangers

Table 5*: Processes in upper cycle*

Heat recovery

Heat recovery is used for hot water pre-heating and is accomplished by using two different heat sources. To cool the compressors, a glycol cooling circuit is utilized. Head heat from piston compressors are rejected through cooling jackets, while the screw compressors are equipped with their individual oil heat exchanger. Heat from the cooling circuit is rejected in three possible ways, either through a sea water cooler, dry air cooler, or as depicted in Figure 18; used as a source for heat recovery. The cooling circuit delivers glycol at 40 °C to the compressors, and assuming a return temperature of 55 °C and 5 K difference in the heat exchanger, it is possible to produce pre-heated water at 50 °C.

The other source is the superheat in the discharge vapour from the NH_3 compressors. Two heat exchangers with an intermediate glycol circuit is connected upstream of the condensers, and is dimensioned for a duty of 430 kW.

3.3 Operation of system

Operational modes, with respect to the different consumers, are listed in the table below.

Cold storages	Production areas	Freezer equipment
- Stop	- Stop	- Operational
- Auto	- Auto	- Defrosting
- Constant	o Production	- Off
	o Washdown	
	o Dehumidify	
	o Night/Weekend	
	- Constant	

***Table 6**: Operational modes of the energy central*

Stop and off-mode indicates that the different consumers are off, meaning refrigerant valves are closed and evaporator fans are off. Auto-mode means that refrigerant feed and speed of evaporator fans should be controlled as a function of measured room temperature against desired room temperature. This mode should also allow for defrosting of evaporators, up to 5 times a day, which is accomplished by hot gas piping. Evaporator fans should be turned off during defrost to reduce fluctuation in room temperature. If the auto-mode is not able to reach

desired room temperature within a given time frame, a constant mode (forced cooling) should be available in which the refrigerant feed valves are fully open and evaporator fans are running at maximum speed, in order to speed up the process.

Auto-mode for production areas should regulate in self according to a week plan, with sub-modes available. Production-mode means regulation of refrigerant feed and fans according to room temperatures. The same goes for washdown-mode, but at an increased desired room temperature. After washdown is complete, the energy system needs to handle the increased moisture by means of a dehumidify-mode. This mode indicates that the system should ventilate affected sections and bring in new air which is cooled and heated alternately with 100% capacity. After production hours, and during weekend, night/weekend mode indicates that the system is turned off.

Freezer equipment should be possible to switch on or off, plus allow for defrosting. Start-up and shut-down sequences should gradually increase/decrease capacity in accordance to a predetermined program, but the possibility to speed up this sequences should also be present.

4 Concept for CTES integration

To properly evaluate the potential for CTES integration, a concept has been developed and is presented in this chapter along with working principles. There are different methods and strategies for integration, so this chapter starts with a section where the motivation and purpose of the concept is explained, along with boundaries and constraints which have led to the final design.

4.1 Integration goal and design constraints

The refrigeration demand for plants operating in the food-processing industry correlates with the production rate, resulting in distinct peaks during production hours. This means that a peak in power consumption can be expected during the same time. Integration goal of the CTES system is then to reduce this peak by shifting a portion of the cooling production to outside production hours. In economic terms, the motivation for this is:

- A reduction in monthly electrical demand charges can be expected as these typically are based on the highest measured peak in power consumption for that month
- Assuming a price differentiation in energy rates between day and night, savings on the electricity bill can be expected when shifting energy usage from day to night

Besides the economical motivation, this system provides the opportunity to operate the refrigeration system at more stable conditions, i.e. reducing part load operation of the compressors. In case of a power failure, storages can also function as backup if charged.

In order to explore the full potential of possible benefits, storages will be integrated on each of the three cooling circuits (LT, MT and AC). To charge the storages, new circuits will be introduced to maintain flexibility of the system. A design constraint for this matter will be to utilize the existing equipment from the original refrigeration system, thus a re-arrangement of compressors is necessary.

Expecting high levels of refrigeration demand during production, sizing of the storages will be in accordance with the partial-storage strategy. This means that the storages will assist during peak demand hours rather than covering the total demand, which would likely result in very large storage volumes. A starting point for storage sizing will be to cover approximately half of cooling energy needed for each circuit during peak hours.

Two modes of operation will be present with regards to the storages, charging and discharging. It is desirable to have control over the charging and discharging rates to avoid peaks in power

consumption during charging, and to avoid too quick discharging of the storages. This implies that a controller configuration must be implemented to attain this control. Guideline for capping of rates will be to evenly distribute the storage capacity over the available time for charging and discharging.

4.2 System design

In line with the described purpose and constraints, a concept has been developed and is presented in Figure 21 as a simplified process and instrumentation diagram. For illustration purposes the combined loads for each temperature level is represented with a grey heat exchanger. Comparing the concept with the original refrigeration system, the most distinct changes can be seen by the introduced charger circuits and re-arrangement of compressors. A number of three-way valves and controllers (not pictured) are also included in order to achieve the described control over discharging and charging operation, and switching between these modes.

Removing compressors from the LT, MT and AC circuit and repurposing them as charger compressors obviously reduces the cooling capacity of said circuits. Furthermore, cooling capacity of the charger compressors must also match the required demand during charging. An iterative approach was conducted to comply with these constraints, and final compressor arrangement with cooling capacities is listed in the table below. Calculations are based on unchanged compressor efficiency, and a full description is available in Appendix A.2.

Circuit	**Evaporation level**	**Cooling capacity** [kW]
LT	10 bar/-40 °C (CO_2)	667
LT-C	6,82 bar/-50 °C (CO_2)	608
MT	2,91 bar/-10 °C (NH_3)	2802
MT-C	19,7 bar/-20 °C (CO_2)	1352
AC	4,97 bar/4 °C (NH_3)	1110
AC-C	3,41 bar/-6 °C (NH_3)	1148

Table 7: *Cooling capacity for the different circuits of the refrigeration/CTES-concept*

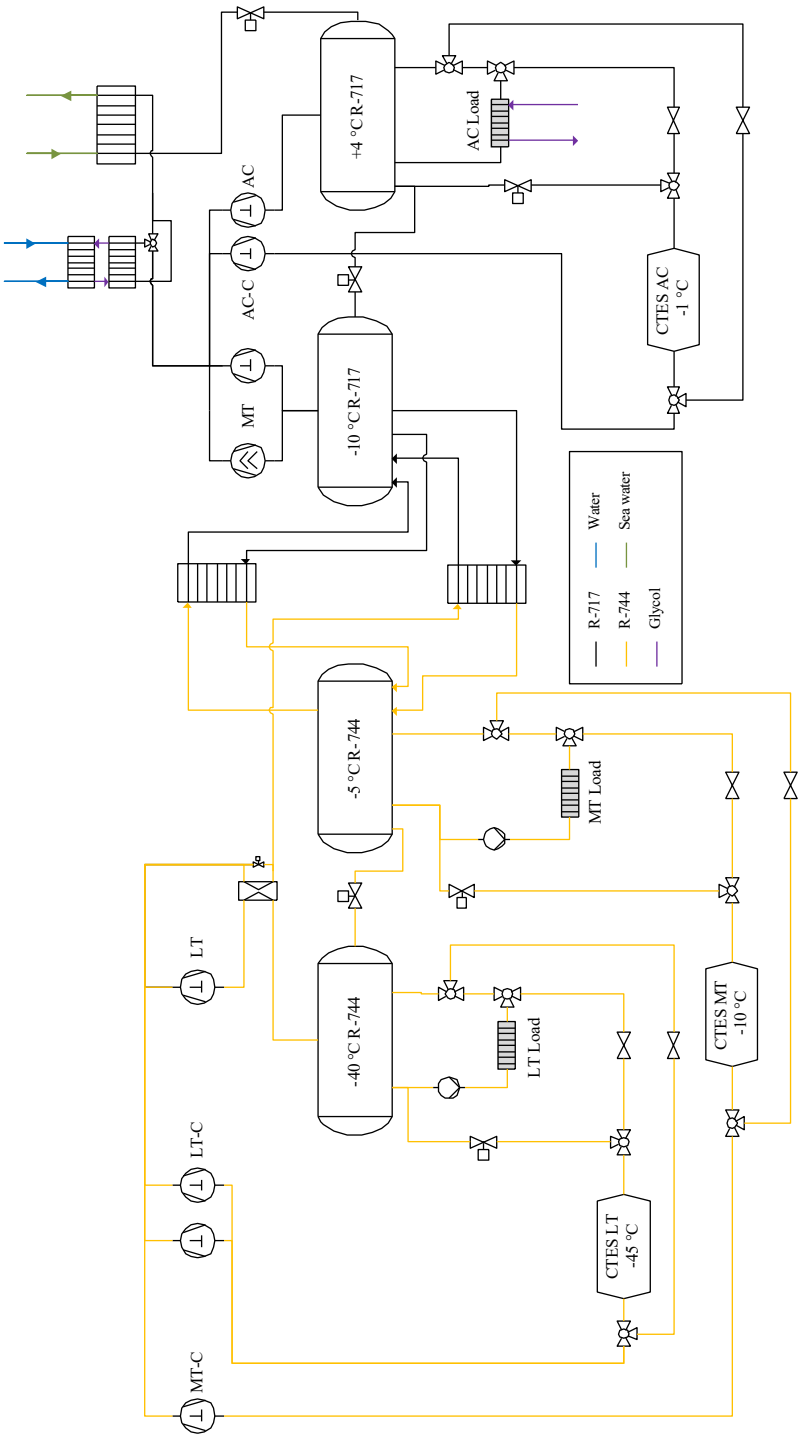

Figure 21: *Simplified process and instrumentation diagram for the CTES concept*

Energy storages are designed as physical volumes containing a phase change material with a number of internal channels in which refrigerant flows while charging and discharging. A temperature difference of 5 K between the materials phase change temperature and refrigerant is assumed to facilitate for proper heat transfer during both charging and discharging. This implies that phase change temperatures for the LT, MT and AC storage should be approximately -45 °C, -10 °C and -1 °C.

Data	Value	Unit
CTES AC		
Phase change material	PlusICE E-2[1]	-
Phase change temperature	-2	°C
Phase change enthalpy	325	kJ/kg
Thermal conductivity (liq. / sol.)	0,58 / 2,00	W/mK
Density (liq. / sol.)	1070 / 970	kg/m^3
CTES MT		
Phase change material	Water-salt solution[3]	-
Phase change temperature	-10,7	°C
Phase change enthalpy	283	kJ/kg
Thermal conductivity (liq. / sol.)	0,56 / 2,2	kJ/kgK
Density (liq. / sol.)	1126 / 1105	kg/m^3
CTES LT		
Phase change material	Puretemp -37[4]	-
Phase change temperature[5]	-45	°C
Phase change enthalpy	145	kJ/kg
Thermal conductivity (liq. / sol.)	0,15 / 0,25	kJ/kgK
Density (liq. / sol.)	880 / 970	kg/m^3

[1] Retrieved from [24] [3] Retrieved from [15] [4] Retrieved from [25] [5] Manipulated phase change temperature

***Table 8**: Phase change materials with selected properties*

These values have been used to search for suitable phase change materials from the commercial market, and the chosen materials with some selected properties are listed in Table 8. Materials with phase change temperature in the range of what is needed for the low temperature circuit was difficult to come by and the author was only able to find materials in the range of either - 50 °C or -37 °C. Therefore, the selected material for the low temperature circuit is based upon technical data for the listed PCM, with adjusted phase change temperature, and an assumption is made that a suitable material is accessible with properties not straying far from selected PCM.

4.3 Working principle

Working principle for the CTES concept is illustrated in Figure 22 using the low temperature energy storage (CTES LT) as an example. By operating a number of valves, the flow direction can be controlled, indicated with yellow lines in the figure. To charge the system, the valves are configured like in (a) where an expansion valve controls the liquid feed. Controlling the feed flow rate can be done by ensuring that the CO_2 is fully evaporated and superheated to a degree, like a DX evaporator. The PCM will solidify as the CO_2 evaporates in the CTES channels. The superheated CO_2 vapour is then drawn to the charger compressor which maintains pressure level in the charging circuit, and compresses the vapour to condensation pressure. The refrigeration system handles the refrigeration demand in the same period, i.e. the LT circuit is operated as normal simultaneously.

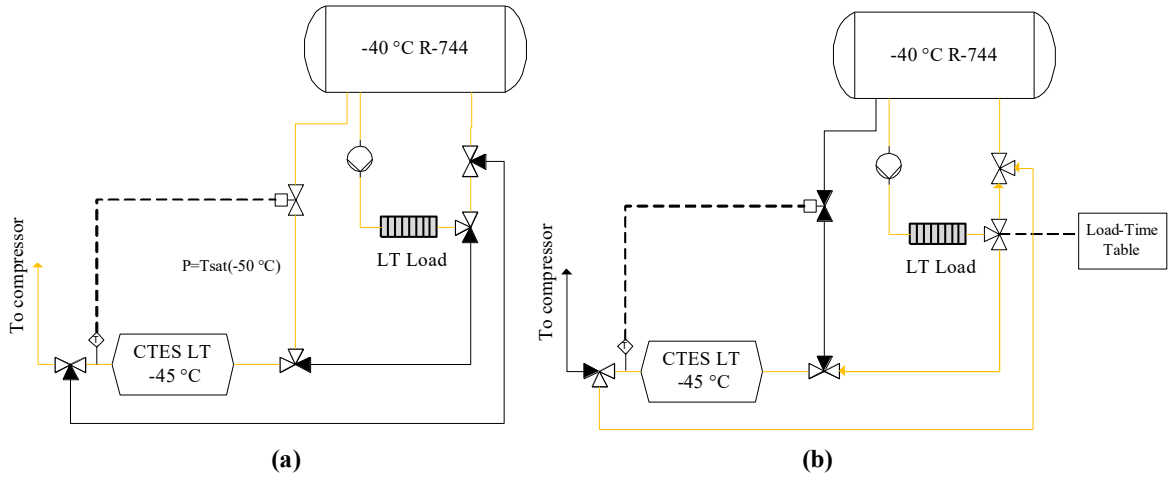

Figure 22: *Detailed view of the CTES system as integrated on the LT circuit.*

(a) Charging (b) Discharging

Discharging of the system is illustrated in (b). The charging circuit is now switched off, i.e. valves are shut and charger compressor is off. Refrigerant pumps deliver liquid CO_2 to the consumers in the same manner as before. However, the return stream is now divided in a three-way valve, in which a fraction of the flow is routed through the CTES where it condenses by melting the PCM before its returned to the separator. The flow distribution can be controlled by a load-time table where desired discharge rate from the CTES can be programmed. This configuration is to counter the typical characteristic of a latent storage with internal heat transfer medium channels where the discharge rate is decreasing as more and more PCM is melted. In effect, the CTES has now reduced the vapour fraction of the return stream which leads to less work needed for the refrigeration system.

5 Method

This chapter aims to describe the tools and methods used to enable an analysis of the energy central. Simulations models which have been built are described in detail, along with any preliminary work and reasoning for chosen solutions. A case scenario with thermal demands is described early on, acting as boundary condition for the analysis. Subsequently follows a detailed description of the simulation models which have been built, along with any preliminary work and reasoning for chosen solutions.

5.1 Tools

To create models and simulate the energy flow, *Dymola* was used in conjunction with refrigerant and component libraries from TLK-Thermo GmbH. Based on the Modelica language, this software provides the user necessary tools to model advanced energy systems and run transient simulations. The component library, *TIL 3.5.0*, supplies many common pre-modelled objects such as compressors, heat exchangers etc., where the user has a high level of control over input parameters. In addition, the refrigerant library *TIL-Media* is equipped with many common refrigerants and secondary fluids.

This chapter includes snippets of the models from the Dymola environment. The snippets show various components connected together with different coloured lines which representation are given in the table below. Most of the symbols are intuitive or otherwise denoted

Colour	**Representation**
Green	R-717
Brown	R-744
Blue	Water/Sea Water
Purple	PG35
Dark blue (thin)	Signals
Dark red	Heat port signal

***Table 9**: Line representation in the models*

5.2 Case scenario

To evaluate performance of the energy central, a thermal demand profile has to be determined to be used as input to the simulation model. Due to limited information about the thermal demands of the plant, a profile has been constructed. It was assumed that the thermal demands

correlated with production rate of the plant, with a gradual initiation and completion of production. Furthermore, peak demands correspond with maximum capacity of each energy circuit so that system performance could be captured under this condition.

A timescale of 24 hours was chosen, assuming production hours between 08:00 and 15:00, followed by washdown and dehumidifying of the plant.

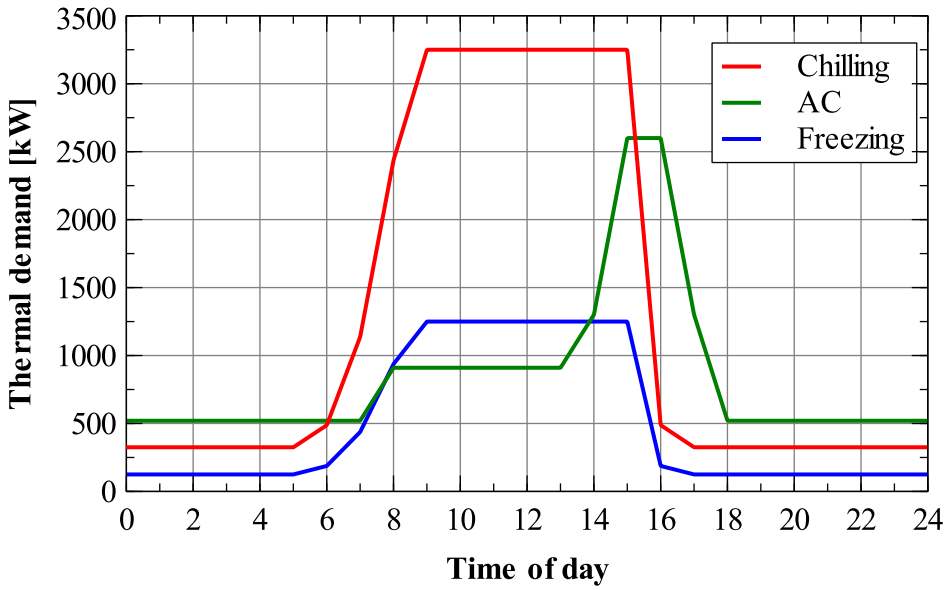

Figure 23: *Thermal demand profile for a 24 hour period*

Outside production hours, the demand corresponds to serving the cold storages and a minimum level of air cooling is assumed. To prepare for production, chilling and freezing process equipment is started before the first poultry enters the factory and thermal demand increases over a 4-hour window as the production capacity increases to maximum. The AC demand also increases prior to production, and is kept at a constant level throughout production hours. At end of production, chilling and freezing equipment is switched off in a gradual manner, while at the same time the demand for air cooling increases as washdown and dehumidifying processes takes place. With regards to hot water pre-heating, no demand has been assumed, but is regarded a consequence of the refrigeration demands. The simulations will then indicate how much water can be pre-heated given this thermal demand profile.

For the CTES concept, this profile gives necessary inputs to size the energy storages and set times for charging and discharging. Aiming for a large effect of integrating the storages, discharge times are set to 06:00-16:00 for the LT and MT storage, while the AC storage will

assist in the timeslot 13:00-18:00. Set to assist with approximately 50% of the refrigeration demand during these times, gives the following rated capacity for each storage:

	Discharging time	**Charging time**	**Capacity** [kWh]
CTES LT	06:00 – 16:00	16:00 – 06:00	5000
CTES MT	06:00 – 16:00	16:00 – 06:00	12 775
CTES AC	13:00 – 18:00	18:00 – 13:00	3800

Table 10: *Capacities and discharging times for storages*

5.3 Simulation models

To create simulation models accounting for every aspect of the energy systems is time-consuming and adds complexity which effects simulation time and reliability. A number of simplifications have been made in the simulation models, some arising from limitations in tools used, others from trying to balance the trade-off between accuracy and efficiency. Maintaining system functionality so that relevant parameters to the energy analysis can be reported on, has been the driving motivation for choices made during modelling. This subchapter details the different sections of the simulation models, highlighting reasoning and effect of the simplifications made.

Two models have been developed with number of components approaching 300. An effort to ensure simulation performance must be upheld during the development of such a large and complex system, and an important factor in that regard is choosing the right solver. Based on recommendation from [26], the Radau IIa solver with an integration tolerance of 1E-6 was chosen, which is suited for thermo-fluid flow systems. In order to avoid faulty results stemming from numerical iterations during initiation of each simulation, a period of 20 000 seconds with constant input loads were allowed preceding scenario load values. Data were recorded and stored with 1500 data points per simulation.

The primary purpose of the simulation models is to generate results relevant for the energy analysis with sufficient accuracy. One large simplification is the choice of not modelling tubes between the different components. This means that no pressure drop or heat loss are accounted for between components. All heat exchangers, with the exception of the AC and cascade heat

exchangers, are modelled without accounting for pressure drop. Furthermore, constant heat transfer coefficients have been selected dependent on fluid:

- R-717 $2500 \frac{W}{m^2 K}$
- R-744 $2500 \frac{W}{m^2 K}$
- Water $1000 \frac{W}{m^2 K}$
- Sea water $1000 \frac{W}{m^2 K}$
- PG35 $1000 \frac{W}{m^2 K}$

5.3.1 Refrigeration system

Compressors

Compressors are modelled as "efficiency compressors", a model available from the TIL library allowing the user to program speed, displacement volume and efficiencies. Speed of all compressors are set to 50 Hz, and PI-controllers adjust the relative displacement volume in order to maintain suction pressure.

Some preliminary work was done in order to model the compressors. Efficiencies have been calculated from catalogue data for each compressor model as they were described in the tender document. Volumetric efficiency is calculated in the following manner:

$$\eta_v = \frac{\dot{Q}_{ci} \cdot v_s}{\dot{V}_s \cdot \Delta h_{ref}} \tag{5.1}$$

Where $\dot{Q}_{ci}$ is the indicated compressor cooling capacity (from data), v_s is the specific volume at suction, $\dot{V}_s$ is the stroke volume of the compressor (from data) and Δh_{ref} is the specific enthalpy difference between evaporator outlet and condenser discharge.

Isentropic efficiency is calculated as:

$$\eta_{is} = \left(\frac{\dot{V}_s \cdot \eta_v}{v_s} \cdot (h_{ds} - h_s) \right) / \dot{P}_i \tag{5.2}$$

Where h_{ds} is the specific discharge enthalpy from the compressor assuming isentropic compression, h_s is the specific enthalpy at suction and $\dot{P}_i$ is the indicated power consumption as supplied from manufacturer.

Effective isentropic efficiency, η_e, is a term which accounts for all heat losses from the compressor, which Dymola uses to calculate the total power consumption. The difference between $\dot{P}_{shaft}$ and $\dot{P}_{fluid}$ is then labelled $\dot{Q}_{loss}$, and in order to determine these efficiencies the fraction $\dot{Q}_{loss}/\dot{P}_{shaft}$ was set to 10% for piston compressors and 30% for screw compressors.

Compressor	**Type**	$\dot{V}_s\ [m^3/h]$	$\dot{Q}_{ci}\ [kW]$	η_v	η_{is}	η_e
LT 1	Piston	452	667	0,850	0,807	0,727
LT 2	Piston	222	337	0,874	0,831	0,748
LT 3	Piston	222	337	0,874	0,831	0,748
MT 1	Screw	3370	2440	0,990	0,879	0,615
MT 2	Screw	2676	1940	0,990	0,877	0,614
MT 3	Piston	679	362	0,740	0,866	0,780
AC 1	Piston	1018	1110	0,897	0,743	0,669
AC 2	Piston	1357	1480	0,898	0,747	0,672

Table 11: *Compressor efficiencies*

The calculated efficiencies can be seen in the table above, and are constant. This assumption is fair with respect to the fact that all pressure ratios are constant, but it fails to capture the decrease in effective efficiency at part load operation. Full set of data with boundary conditions can be seen in Appendix A.1.

Compressor cooling circuit

Cooling circuit for the compressors picks up heat from head of the piston compressors, but mainly from oil coolers attached to the screw compressors. A common supply of glycol at 40 °C is distributed to each compressor and oil cooler, while cooling of the glycol can be done either by heat rejection to sea water, dry air cooler or pre-heating washing water. In line with the intention of investigating the latter option, model of this circuit has been simplified to a single glycol circuit transferring all compressor heat losses to water in a plate heat exchanger.

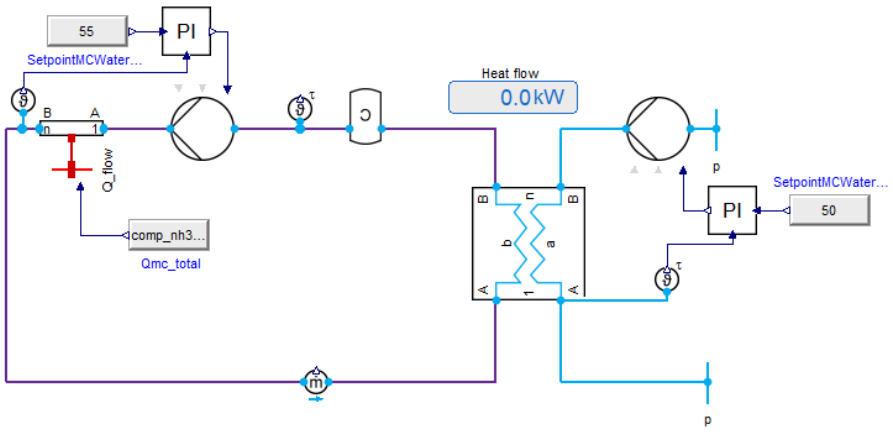

Figure 24: *Heat recovery from compressor cooling circuit*

Heat from the compressors/oil coolers, which in the model is equivalent to $\dot{Q}_{loss}$ from the compressors, is transferred to the glycol via a tube element. A glycol pump is set to adjust flow rate to maintain a 55 °C inlet temperature to the glycol-water HX, where water inlet temperature is 8 °C. Outlet water temperature is set to 50 °C, assuming a 5 K temperature difference in the heat exchanger, and a water pump adjusts the flow rate to maintain this temperature.

Flooded plate heat exchangers

Albeit the libraries used includes several of the most common components that are used in refrigeration systems, no such model exists for a flooded plate heat exchanger. A combination of components and settings were introduced to resemble the characteristics of process; pressure increase prior heat exchanger inlet due to liquid leg, overfeeding to ensure a two-phase refrigerant exit and pressure drop in the heat exchanger.

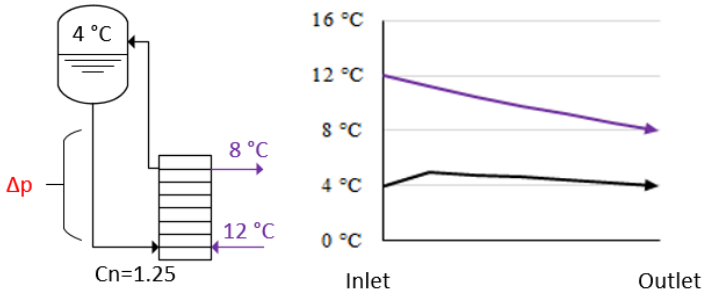

Figure 25*: Working principle for gravity flooded heat exchanger and temperature profile*

Figure 25 illustrates the process as it should be for the AC circuit, but the principle is the same for the cascade heat exchangers. Circulation number is the ratio between liquid feed and evaporation level, calculated as

$$C_n = \frac{1}{x_{out}} \tag{5.3}$$

Even though the circulation number for gravity fed heat exchangers is dependent on heat transfer load and pressure drop across evaporator, a constant value of 1.25 was selected. Note the effect of subcooling in the temperature profile, which means a part of the heat exchanger area must be used to heat the subcooled liquid before evaporation can begin.

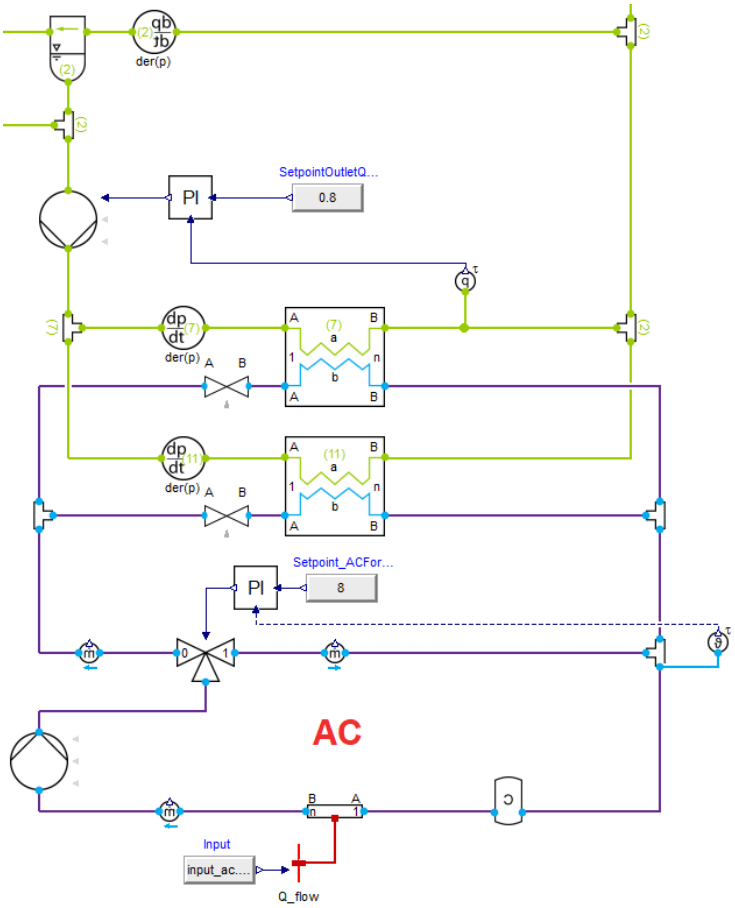

Figure 26: *Modelling of AC circuit with flooded heat exchangers. Snippet from Dymola*

In the simulation model a pump feeds the evaporator as depicted in Figure 26. The pump is controlled by a PI-controller, set to maintain the circulation ratio by controlling outlet quality from the heat exchangers (80%). Work input to the pump is not accounted for in the energy

calculations. The heat exchangers are configured with pressure drop characteristics dependent on mass flow rate, which in conjunction with the pump is able to simulate the pressure increase in front of the evaporators. A small deviation from real world operation is that the pressure increase due to a liquid leg should be constant, while in the model it fluctuates between 0,05 and 0,2 bar. This however has small impact on the overall energy analysis.

AC Circuit

The AC circuit is designed to deliver glycol at a temperature of 8 °C to cover all AC demands with a return temperature of 12 °C at full load. A tube element is representing the load, and the load input is retrieved from a spreadsheet describing the load scenario. Heat is transferred via two identical plate heat exchangers which are dimensioned to a combined capacity of 2600 kW with the boundary conditions as pictured in Figure 25. To ensure correct temperature delivery for the AC consumers, a three-way valve modulates the mass flow distributed to the heat exchangers. If the glycol return temperature is below 12 °C, the supply temperature will approach 4 °C due to the dimensions of the heat exchangers. The three-way valve distributes the total mass flow rate of 180 kg/s in such a manner that the HX outlet stream and return stream mixes to 8 °C. This can be seen in Figure 26.

Desuperheating and condensation

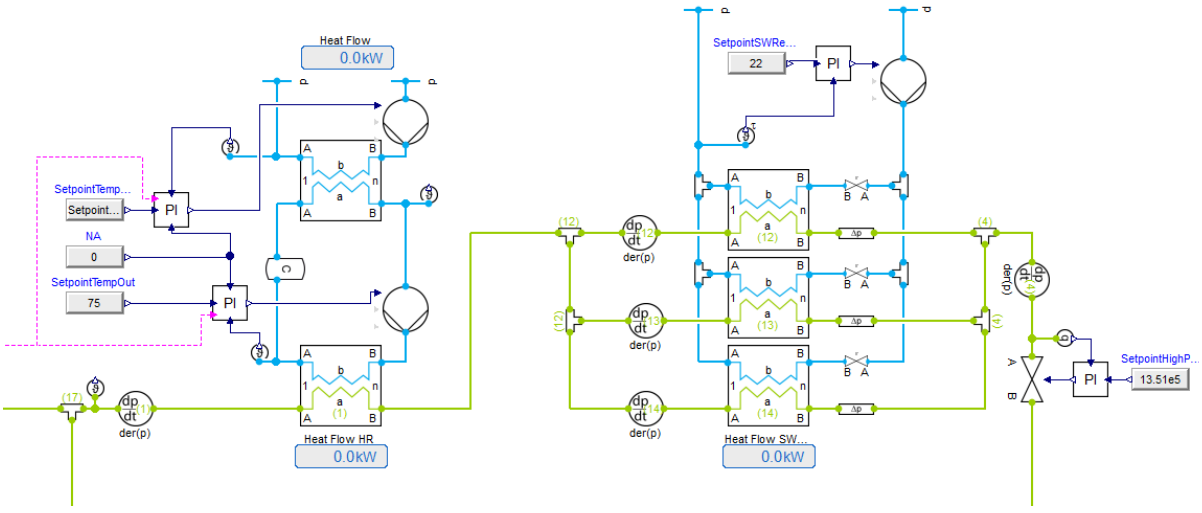

Figure 27: *DSH and condenser units for the upper cycle*

Condensation level in the upper cycle is 13,51 bar ($T_{cond} = 35\ °C$) which is maintained by an expansion valve and PI-controller. Before rejection of condensation heat, some heat recovery

takes place in the de-superheater unit. Deviating from the design, the DSH unit is connected in series as opposed to parallel, which is done in order to improve simulation performance. The DSH system is operated with two PI controllers in conjunction with pumps, and are possible to turn completely off if heat recovery is not to take place. This on/off-possibility is assumed to create no deviation regarding energy flow patterns with the real world system, and the input signals can be viewed in Figure 27 as the dotted pink lines.

An intermediate glycol loop carries superheat from the NH_3 vapour to the water. At full load the system is dimensioned for a capacity of 430 kW, pre-heating the water from 8 °C to 70 °C. In order to ensure proper heating of the water, a pump regulates the water flow in conjunction with a PI-controller. This means that the accumulation of pre-heated water is dependent on the load of the system.

Condensation is carried out in three identical plate heat exchangers with a total capacity of 8500 kW. The refrigerant is cooled with a stream of sea water entering at 10 °C, and a sea water pump controls that the exit temperature is 22 °C. At full capacity this means that the maximum flow of sea water is approximately 612 m^3/hr. The condensers are also dimensioned to subcool the refrigerant with 10 K. Due to the dimensioned size of the condensers and choice of control system, the discharge temperature of refrigerant approaches the inlet temperature of sea water at part load operation. This does not increase refrigeration capacity however, as the liquid quickly heats as it enters the separation tank at the AC level.

Heat transfer between cycles

Condensation heat from the bottom cycle is to be lifted to the upper cycle via two sets of cascade heat exchangers. As described earlier both groups are gravity fed from the NH_3 side, while from the CO_2 side only one group are gravity fed. In order to simulate this behaviour, a compressor was modelled to draw saturated vapour from the -5 °C CO_2 tank and feed the HX group. The compressor is controlled by an PI-controller and maintains the pressure level (30,5 bar/-5 °C), as can be seen in Figure 28. Power input to the compressor is neglected in the energy calculations.

For both groups the heat exchangers were lumped together in one unit for simulation performance issues. Dimensioning was done in accordance with each groups total capacity and design temperature levels. For the rightmost HX group (Figure 28), discharge vapour from the LT compressors enter at approximately 50 °C, condenses and is subcooled to almost -10 °C. Same amount of subcooling occurs in the other groups, and their discharge streams mixes in an

ideal junction before returning to the separator. Capacity of each group is 4000 kW (left) and 1650 kW (right).

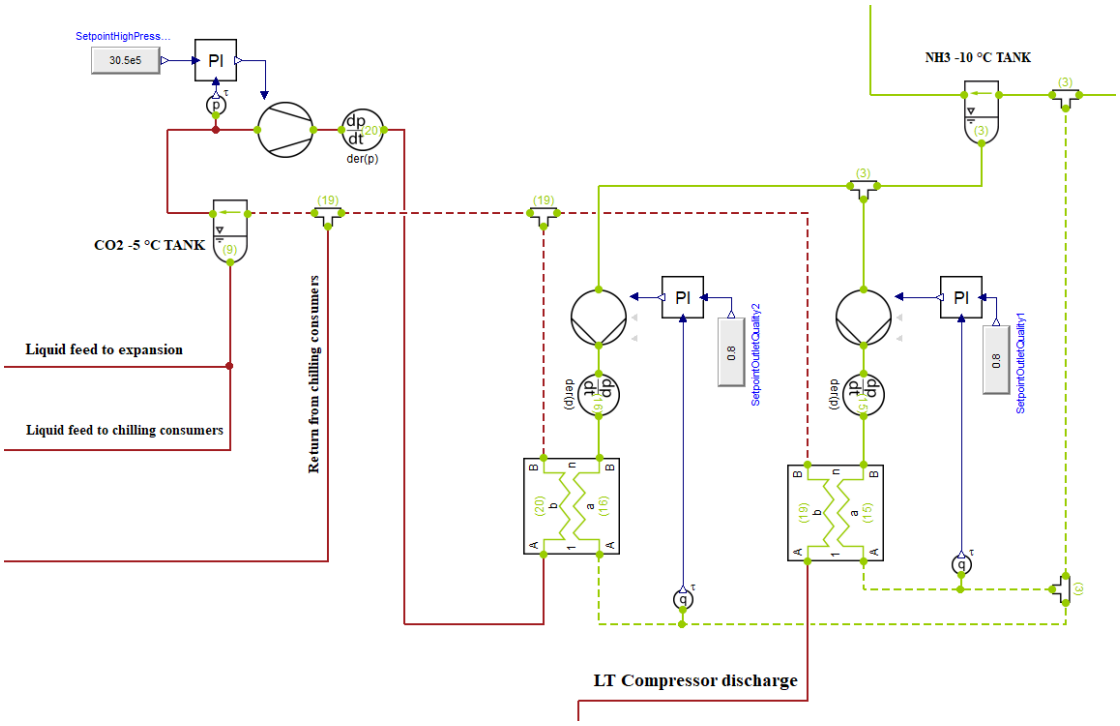

***Figure 28**: Heat transfer between bottom and upper cycle. Snippet from Dymola*

Feeding liquid NH_3 occurs by gravity, and the process is modelled in the same manner as for the AC heat exchanger.

Low and medium temperature circuit

All loads from chilling storages and equipment have been lumped together in the model, as well as freezing storages and equipment loads. The lumped demands are represented by tube elements which retrieves input values from a spreadsheet in the same fashion as for the AC load, and can be seen in Figure 29. Liquid pumps are also lumped together, feeding each consumer at a constant flow rate. The flow rates have been determined to ensure a circulation ratio of 3 at maximum capacity, as according to design. This means that return stream from consumers always are two-phase with a maximum vapour quality of 33%. Work input to the pumps are neglected in the energy consumption calculations due to their relative small share of the total energy consumption of the system.

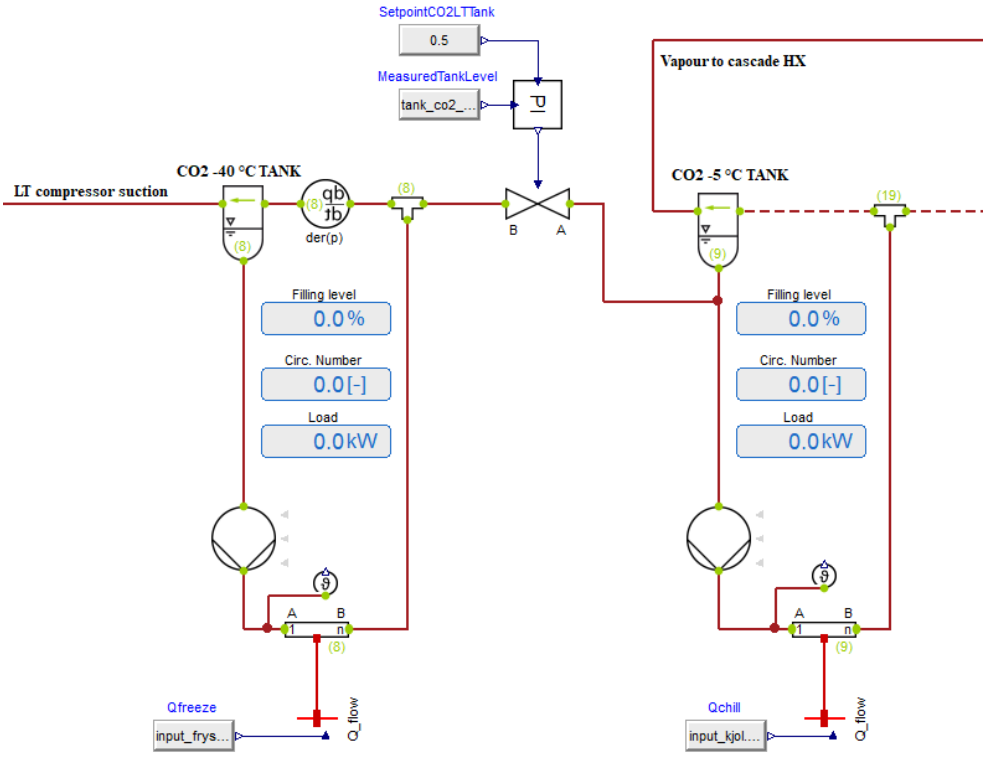

Figure 29: *Modelling of low and medium temperature circuits. Snippet from Dymola*

5.3.2 CTES concept model

Modelling the CTES concept has been conducted as a modification of the already described simulation model for the original refrigeration system. Thus, many of the described features are alike and will not be repeated in this section. The energy storages were not directly integrated into the modified model, but rather modelled as separate stand-alone models. Results stemming from simulations carried out from the stand-alone models were then used as input to the top-level model. This is a simplification which removes some of the dynamics between the storages and rest of the refrigeration system, but it was deemed necessary due to performance issues.

Stand-alone models utilize the add-on library *SLEHX* from TLK-Thermo GmbH. This library contains models of thermal storages with internal tubes, with or without fins, going through a rectangular volume filled with phase change material. Available parameterization of the model includes physical dimensions of the storage & tubes, and the user can define their own phase change material to be used. The phase change materials listed in Table 8 were added and used for the models.

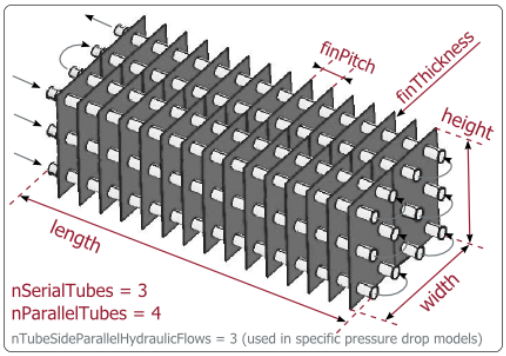

Figure 30: *Representation of energy storage in SLEHX*

The stand-alone models were used as tools for designing of the storages, meaning that a series of simulations were carried out to determine the storage size, heat exchanger area and mass of phase change material needed to perform with the rated capacities described in Chapter 5.2. Heat gain between the ambient and storages were neglected in the model, and the storages were modelled as lumped units opposed to a more authentic modular design. The resulting dimensions must therefore be treated as indicators on required storage size rather than optimized values.

Stand-alone models were built separately for the charging and discharging process. Setup for the discharge model was made to resemble the intended operation of discharging as described in Chapter 4.3, and can be viewed in Figure 31.

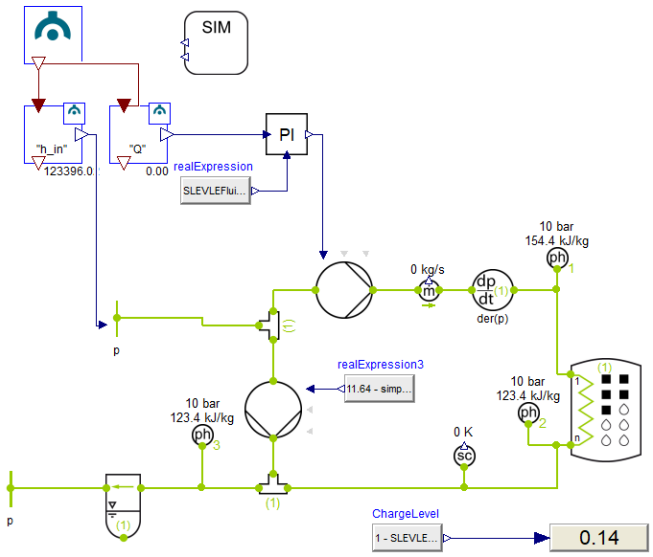

Figure 31: *Model for discharging of energy storage. Snippet from Dymola*

The top left boundary resembles the common return line from consumers. Based on refrigeration demand, the specific enthalpy for at this point has been calculated and used as input to the discharge model. Resembling the three-way valve, a junction with individual pumps have been modelled to distribute the return flow according to a capacity schedule. The total mass flow of the two pumps are constant and equal to that of the consumer return line. The storage and by-pass stream then mixes and returns to the separator.

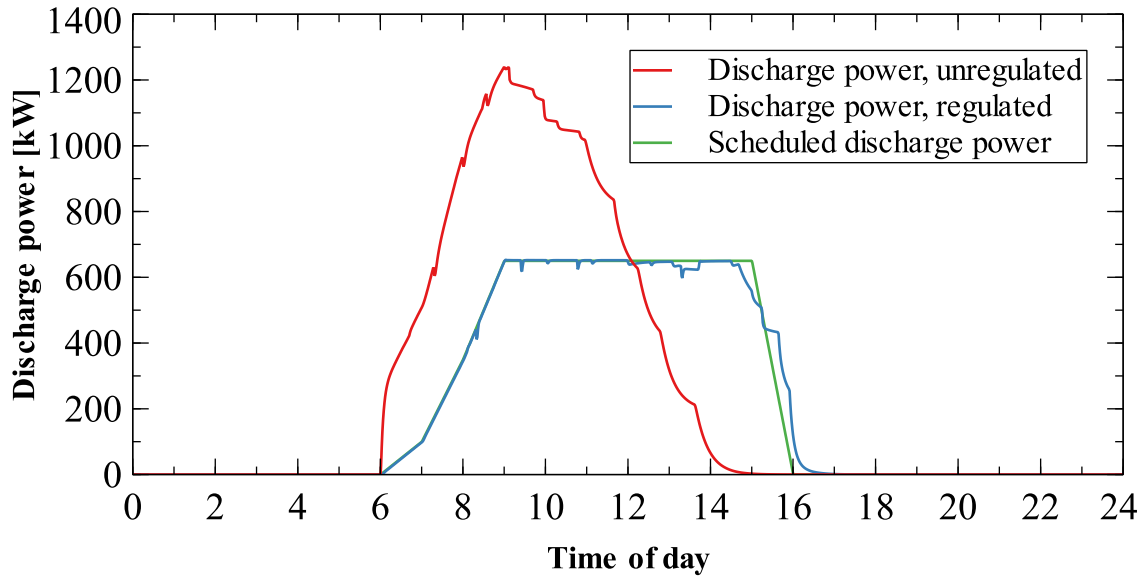

Figure 32: *Discharge rate results from CTES LT. Snippet from Dymola*

As an example, the results from dimensioning of the low temperature storage is pictured in Figure 32. The green dotted line represents the capacity schedule which the three-way valve is supposed to adjust accordingly to for distribution of flow, while the blue line shows the actual discharge rate. To illustrate the desire for this regulation, the red line shows the discharge rate from a simulation were this regulation is neglected, i.e. all refrigerant is routed through the storage. What can be seen is that the discharge rate very quickly rises towards a maximum, which is a consequence of large heat exchange area and large fraction of solid PCM. As the PCM melts, the thermal resistance increases leading to a drop in heat transfer rate, before succumbing to zero as all PCM is melted and the liquid is in thermal equilibrium with the refrigerant.

The charge model has been developed simultaneously with the discharge model, in which the storage component shares the same properties as in the discharge model. As pictured in Figure 33, an expansion valve is controlling its flow area by measuring the degree of superheat on the storage outlet. The charger compressor regulates pressure in the circuit, and is brought to a complete stop outside charging periods.

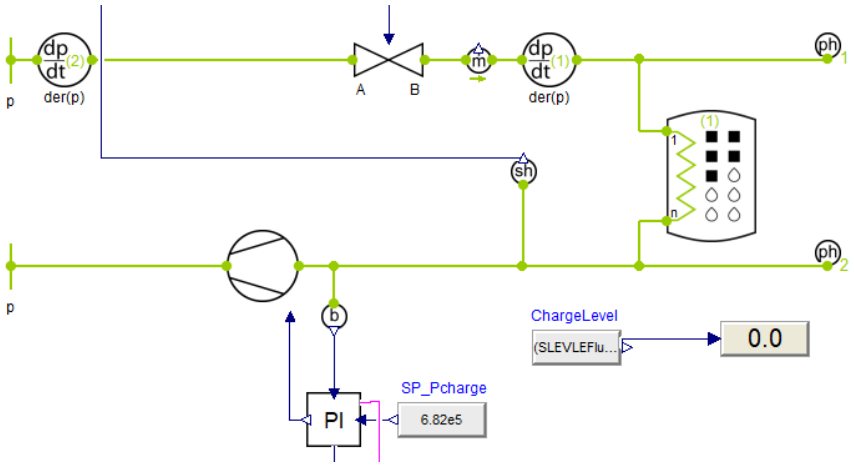

***Figure 33**: Charge model. Snippet from Dymola*

Carrying out simulations for all energy storages led to curves for discharge and charging power which then could be used as input to the top-level model. Some oscillation was observed for all cases, both for the charging and discharging curves. This is assumed to be caused by improper settings of the PI-controllers used in the standalone models. This assumption combined with simulation performance reasons led to the input curves being filtered. The resulting discharge and charge rate curves can be seen in Appendix B.1 along with final dimensions for each storage. Note that the capacity for each storage is larger than the rated capacity. This is typical according to [5], who draws a distinction between *rated* and *nominal* capacity. When a storage is nearly completely melted, the discharge rate is lowered towards useless levels, an effect which can be avoided by not completely melting the storage.

To connect these input values to the top-level model, tube elements with heat ports were added to represent the charging and discharging loads. This is seen in Figure 34 for the LT circuit, and is modelled in the same manner for the MT and AC circuit. When charging is initiated (grey box, left), an expansion valve opens and starts regulating according to outlet superheat. Results from the charge simulations are tabulated into a spreadsheet and used as input to the tube element, emulating the charging process. The superheated outlet stream then continues to the charger compressor which maintains correct pressure level in the charging circuit. When charging is complete, expansion valve closes completely and compressor is switched off.

Discharging of the storage is emulated in the same manner (grey box, right), with a tube element linked to the tabulated results from previous simulations. During charging, its function is rendered useless as the input value is zero, and thus has no unintended impact on the simulation.

The three-way distribution valve is not necessary in this model, as its purpose is to regulate the discharge rate which is accounted for in the input values.

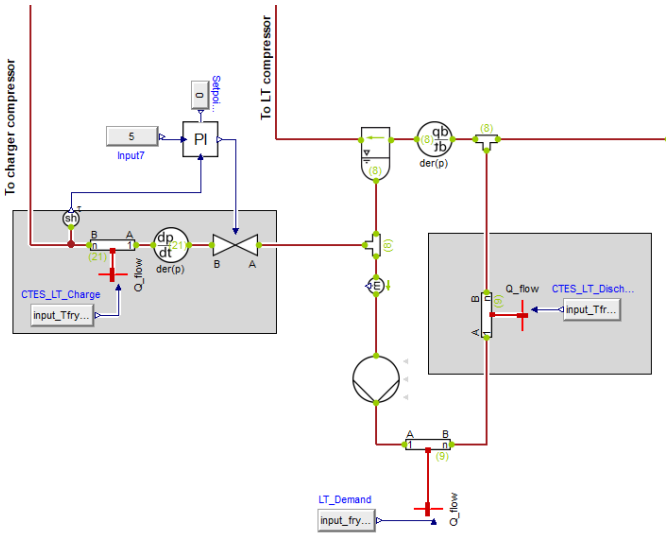

Figure 34: *Tube elements representing charging and discharging process in simulation model of CTES concept. Snippet from Dymola*

6 Results

This chapter will present results from the various simulations which indicates the performance of the energy central. The main intention of this chapter is to highlight the difference in performance with and without CTES integration, in terms of power and energy consumption. It is important to note that only power consumption by the compressors are considered in the results, as they are the largest consumers for the system. Heat recovery, or hot water pre-heating, will also be reported on as it is an important function of the refrigeration system.

6.1 Refrigeration system

Simulation of the refrigeration system has been carried out for the 24-hour thermal demand profile earlier established. Figure 35 shows the power consumption for each compressor group and total consumption.

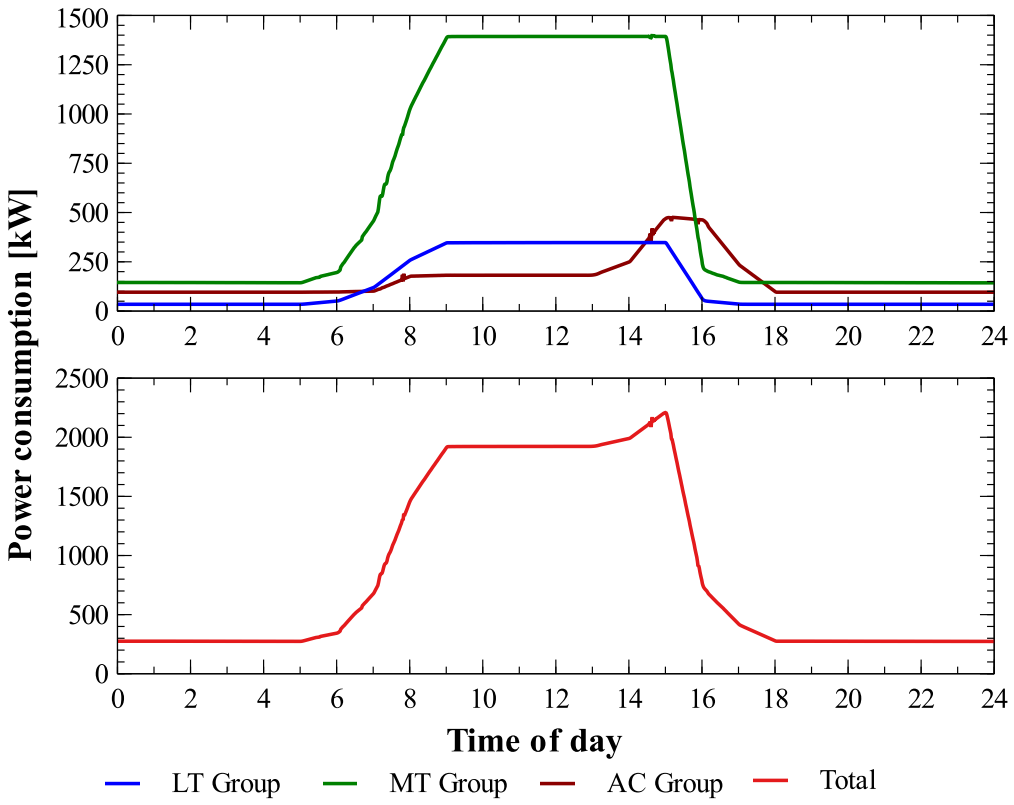

***Figure 35**: Power consumption for the base case design*

The characteristic of the curves reveals the relationship between the different compressor groups and thermal demands. Peak power consumption happens in the shift between production and dehumidifying process, where all thermal demands are maximum for an instant. The MT compressor group holds the largest share of total power consumption, and by observing the

large capacity range it operates in, it indicates that proper controls should be in place to avoid simultaneous part-load operation of the compressors in that group.

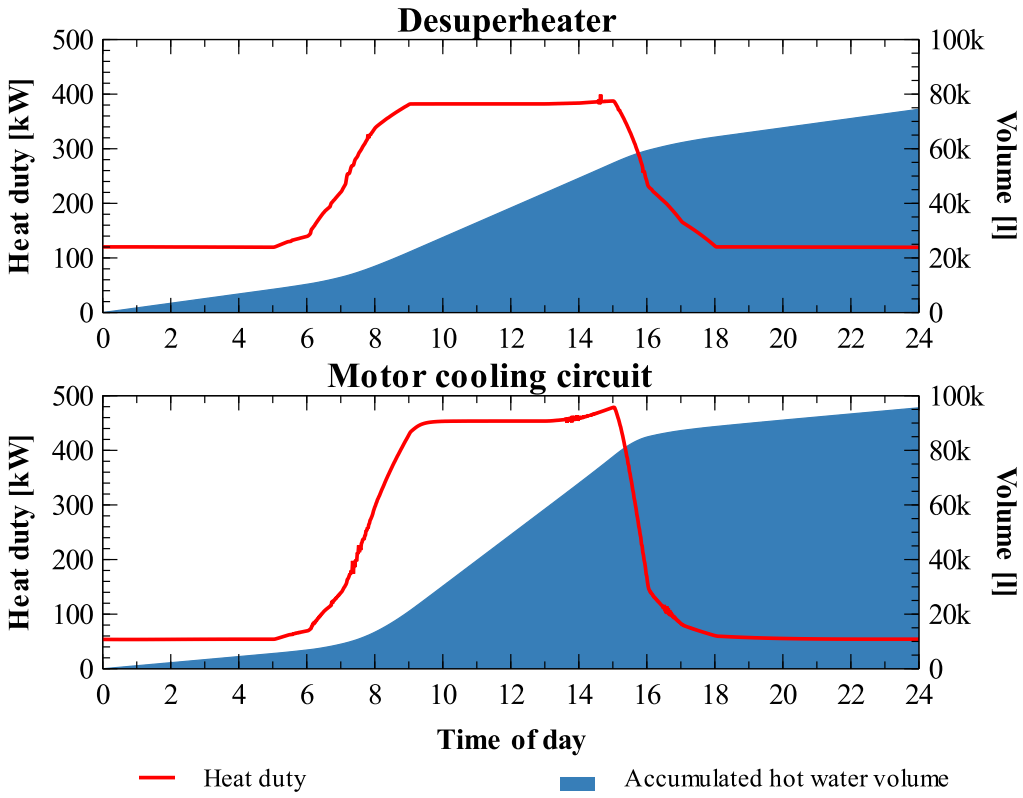

***Figure 36**: Heat duty and hot water accumulation in heat recovery utilities for the base case simulation*

The figure above shows the heat duty and accumulation of pre-heated water through the period. Water accumulation is not accounting for withdrawal from water storages, so the results only expresses the system production ability. Total accumulated volume amounts to 170 000 l, but at different qualities; 70 °C for the de-superheater and 50 °C for the motor cooling circuit.

The next figure illustrates the amount of heat recovered in the de-superheater, and the available superheat, assuming it can be calculated as:

$$\dot{Q}_{SH} = \dot{m} \cdot (h_{in} - h_{f=(P_c,T_c+5)})$$

Where mass flow $\dot{m}$ and specific enthalpy h_{in} is retrieved from the NH_3 compressors common discharge, and specific enthalpy h_f is evaluated at condensation pressure and 5 K above condensation temperature.

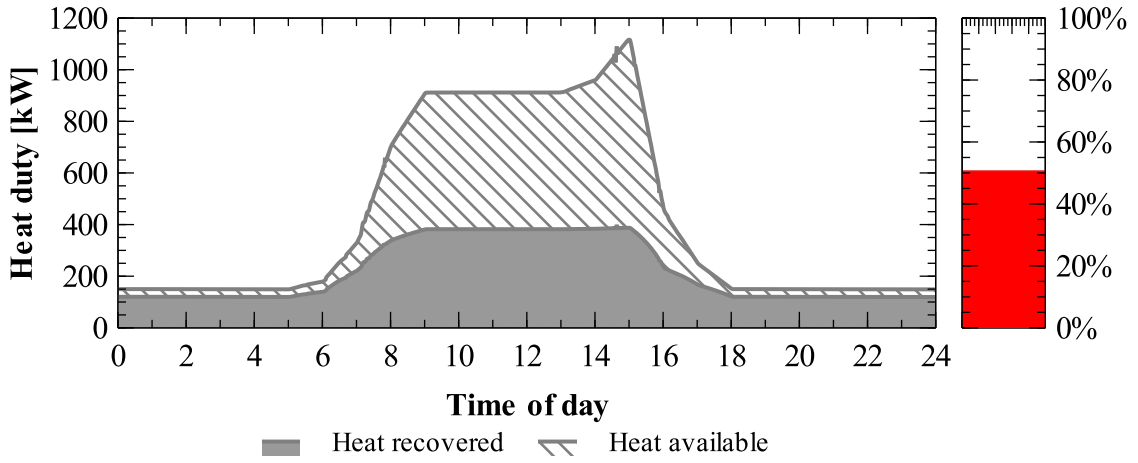

Figure 37: *Heat recovered in the de-superheater. Result from base case simulation.*

The fraction of heat recovery amounts to 51% for the period, whereof most of the "losses" occurs during production hours due to limited size of the de-superheater. In absolute values, the recovered energy amounts to 5247 kWh of 10 359 kWh available for the period.

Coefficient of performance for the system is presented in two ways, with COP_{ref} being calculated as the sum of the instantaneous refrigeration duties divided by the instantaneous power consumption of the compressors, and COP_{comb} which also accounts for heat recovery duty.

$$COP_{ref} = \frac{\dot{Q}_{LT} + \dot{Q}_{MT} + \dot{Q}_{AC}\ [kW]}{Total\ power\ consumption\ [kW]}$$

$$COP_{comb} = \frac{\dot{Q}_{LT} + \dot{Q}_{MT} + \dot{Q}_{AC} + \dot{Q}_{DSH} + \dot{Q}_{MC}\ [kW]}{Total\ power\ consumption\ [kW]}$$

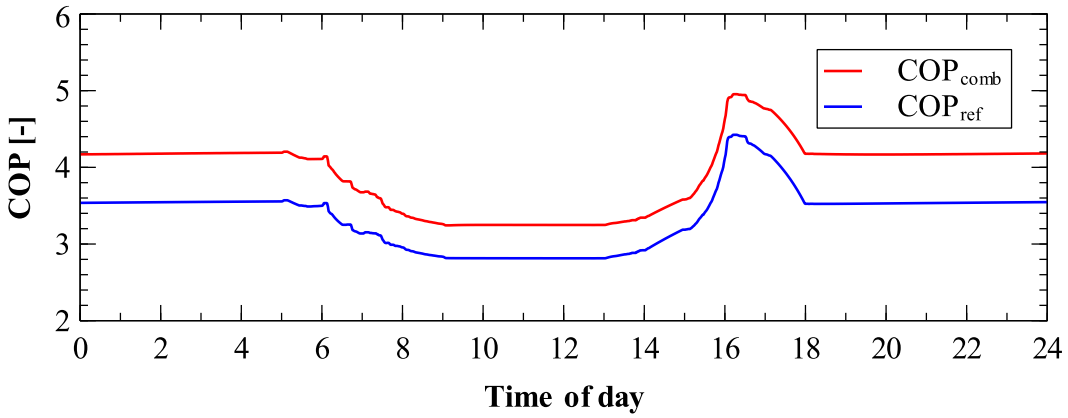

Figure 38: *Variation in COP for the refrigeration system during the period*

In both cases a general trend can be observed with more or less constant COP at low demand hours, which decreases as production is initiated, followed by a rapid rise towards peak performance in the shift between production stoppage and washdown/dehumidifying. This trend can be understood by the relationship between power consumption and thermal demands at different levels; it is more taxing to produce refrigeration at LT and MT levels than for the AC level, which is reflected in the peak performance which occurs when the latter demand is dominant.

A summarization of the main findings from the simulation is listed in the table below. Energy efficiency indicators, EER_{ref} and EER_{comb}, are calculated as the ratio between refrigeration energy produced and total compressor work for the 24-hour period, where the latter includes recovered heat.

Parameter	**Value**	**Unit**
Peak load	2 209	kW
Energy consumption, 24 hr	20 767	kWh
Heat recovered, DSH	5 247	kWh
Heat recovered, MC	4 608	kWh
Hot water production, 70 °C	74 500	liter
Hot water production, 50 °C	95 600	liter
EER_{ref}	3,09	-
EER_{comb}	3,57	-

Table 12*: Summarization of main findings from base case simulation*

6.2 CTES concept

Simulation of the CTES concept was performed using the same thermal demand profile as for the previous case, but has additional loads associated with charging of energy storages. However, the storages assist with cooling during production hours, which should reduce the workload of the system. The first figure shows the share of refrigeration duty which is covered by discharging of storages for each circuit, and the total share covered for the total demand.

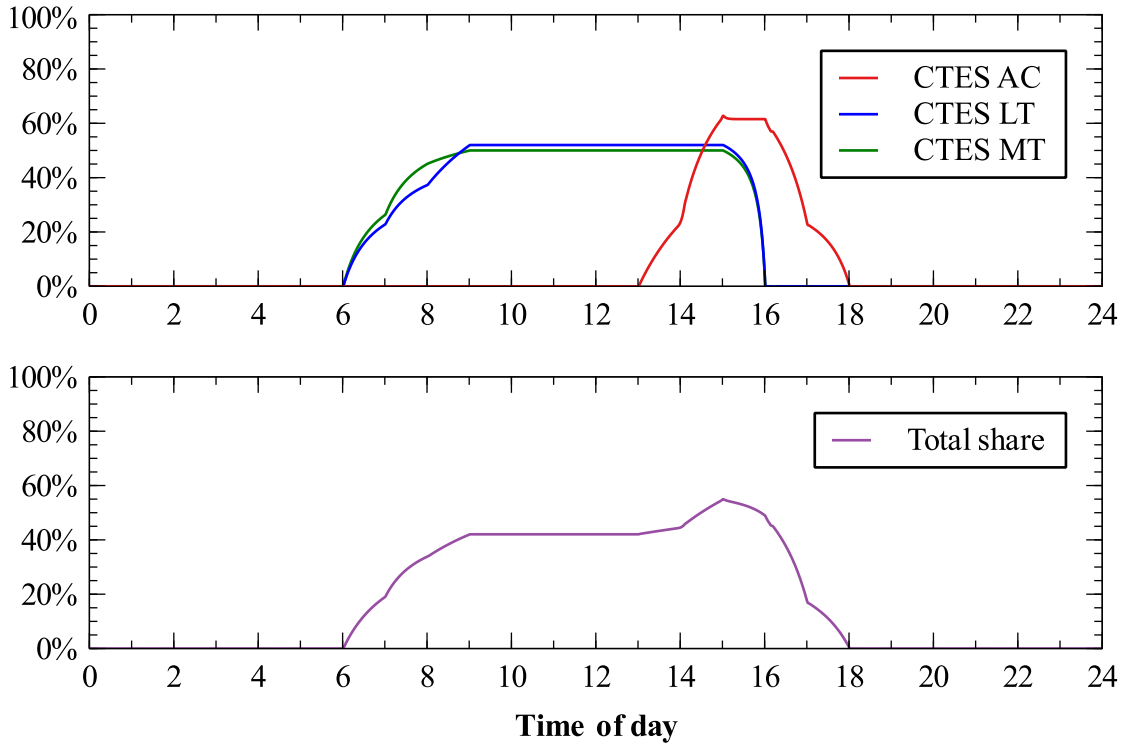

***Figure 39**: Top: Curves showing the share of refrigeration duty covered by the different energy storages with respect to each demand. Bottom: Total share with respect to total refrigeration duty.*

The upper graph shows how the storages discharge energy as intended, supplying approximately half of the refrigeration duty during production hours for the LT and MT circuit, and around 60% for the AC circuit. Note how regulation of discharge rate allows for a smooth transition towards the capped maximum rate, which in numbers read 1625, 650 and 1600 kW for the MT, LT and AC circuit. As seen in the intermediate results from simulation of stand-alone models in Chapter 5.3.2, a higher discharge rate is possible as it is a function of the storage design, but will limit the discharge period. The lower graph shows the total share of refrigeration duty covered by all storages with respect to the total refrigeration demand.

Power consumption of compressors are shown in the figure below.

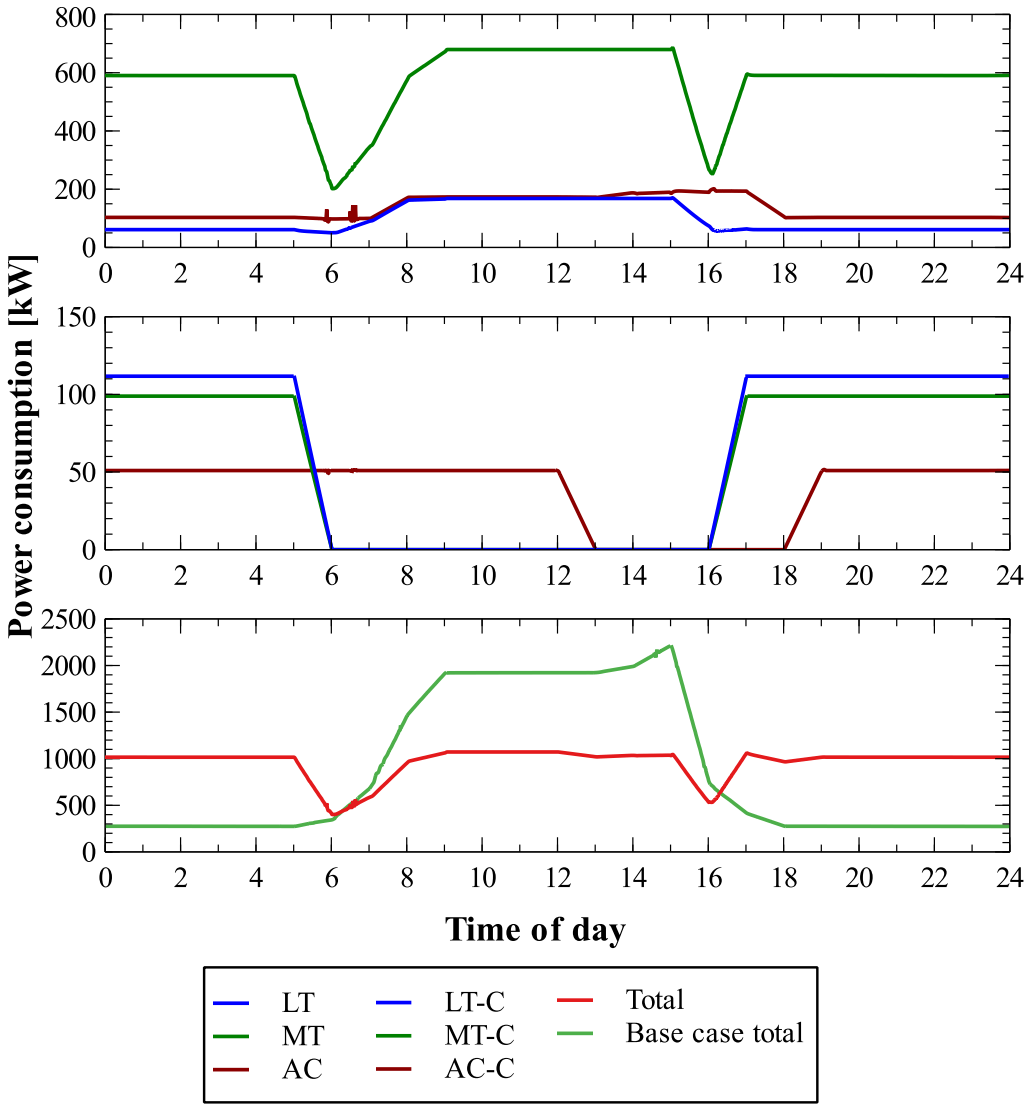

Figure 40: *Compressor power consumption in the combined CTES/refrigeration system*

Pattern of the total power consumption throughout the 24-hour period shows a very different trend compared to the base case, as shown in the bottom graph with red and green dotted lines. Power consumption outside production hours has increased from around 300 kW to 1000 kW, due to charging of storages. Besides power input to the charger compressors, it can be seen that the MT compressor group holds the largest share of this increase. This is because charging of the low and medium temperature storages results in condensation heat which is transferred through the cascade heat exchangers and further lifted by the MT compressor group.

During discharge of storages, a significant reduction in peak power can be observed. Peak value is registered at 1,07 MW, which is a reduction of over 50% from the base case. With regards to

total energy consumption throughout the period, this has increased to approximately 23 000 kWh. This can be explained by the fact that charging the storages is more energy expensive than directly covering the refrigeration demand, because of the reduced evaporation temperature in the charger circuits.

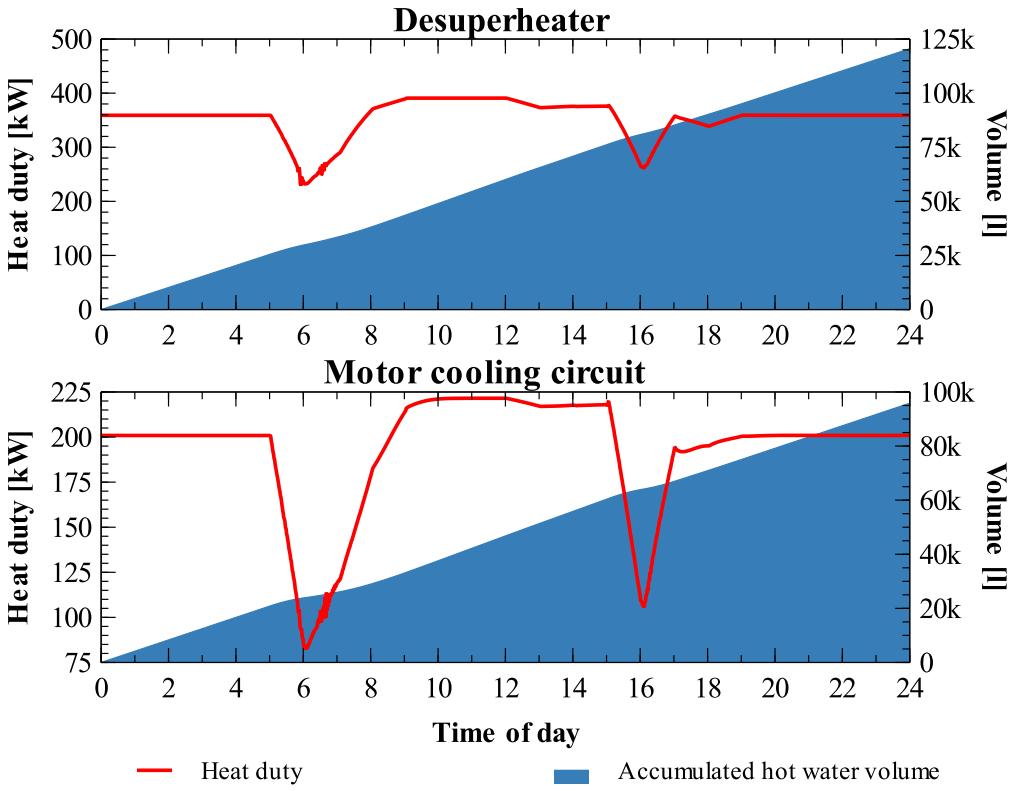

Figure 41: *Hot water production for the combined CTES/refrigeration system*

The changed behaviour of compressor power consumption has an impact on the hot water pre-heating, which results can be seen in the figure above. Elevated power consumption during low-demand hours means that the de-superheater is able to recover more heat during the whole period. This is reflected in the ratio of recovered heat and available heat; 8500 kWh heat recovered of 10 900 kWh, or a ratio of 78%, is a rather large improvement from the base case. This means that this system has the ability to produce 120 000 liter of 70 °C water during the period. No significant change has occurred in production of 50 °C water, besides a more stable heat recovery throughout the period.

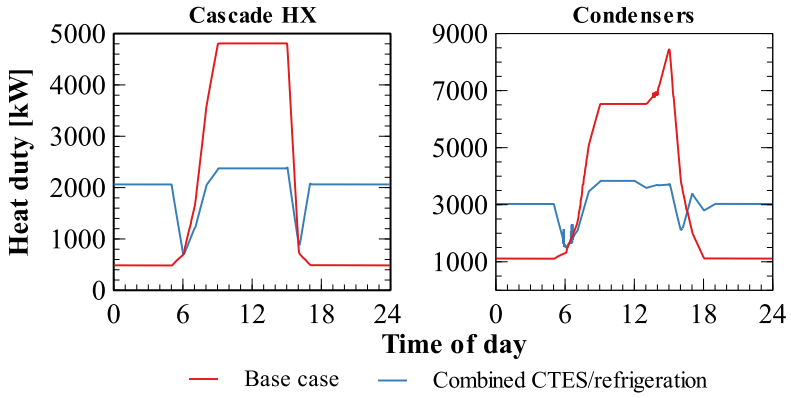

Figure 42: *Comparison of heat duties in the cascade heat exchangers and condensers between the base case and the combined CTES/refrigeration system*

A comparison between heat duties in the cascade heat exchangers and condensers should also be considered. Peak duty is decreased with approximately 50% in both cases, which means heat exchanger sizes can be reduced. Furthermore, for the condensers, this reduction can realize energy savings on the auxiliary equipment used to pump sea water. For the base case simulation, a peak of sea water flow just above 600 m^3/hr was logged, while flow rate for the combined system peaked at 275 m^3/hr. Another possibility is to keep the size of the condensers, which can facilitate for smaller temperature pinches and thus the ability to reduce condensation pressure.

6.3 Additional investigation of CTES integration

To further investigate the effect of energy storages, additional studies were conducted, considering the storages separately. In total, a series of 6 cases were simulated with the following characteristics:

Case	Description
T1	Only CTES MT present
T2	Only CTES LT present
T3	Only CTES AC present
T4	CTES MT and CTES LT present
T5	CTES MT and CTES AC present
T6	CTES LT and CTES AC present

Table 13*: Description of additional CTES studies conducted*

Capacities of the individual storages remain the same as before, and system design is unaltered.

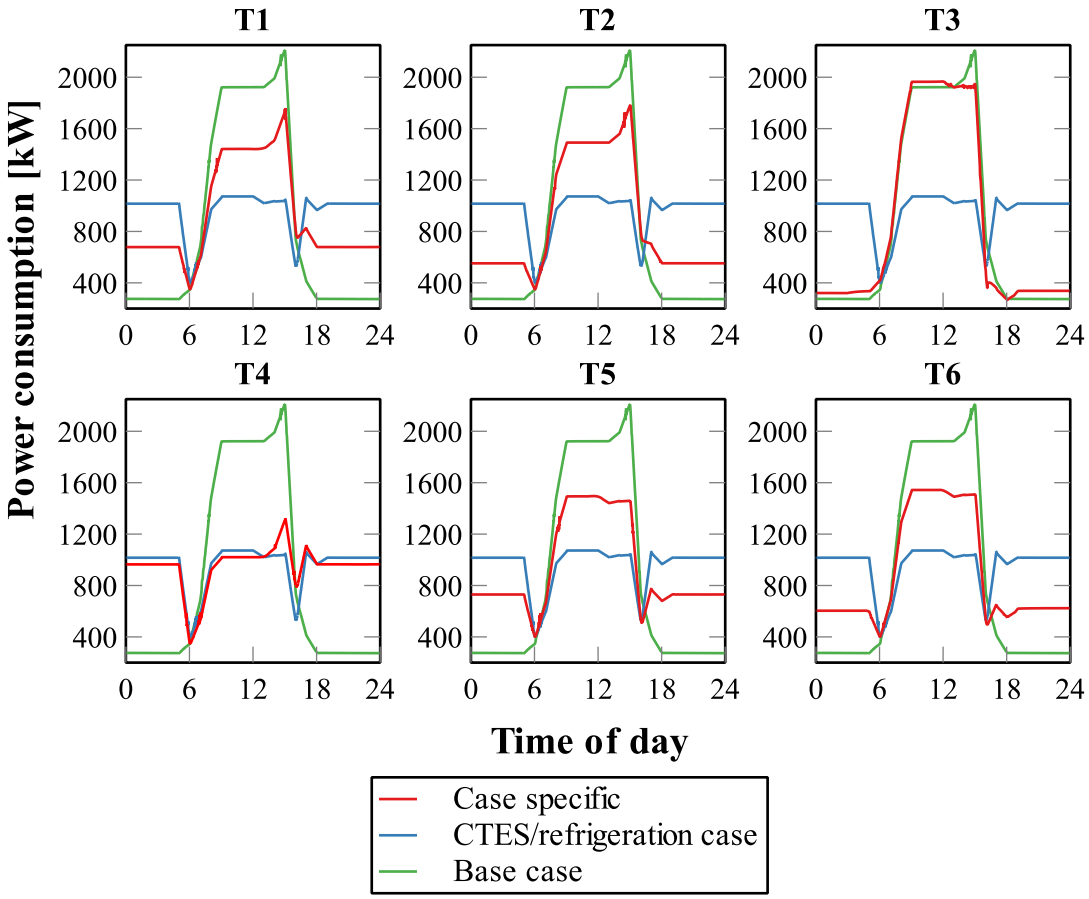

Figure 43: *Power curves for all case studies showing total compressor power consumption throughout the period*

The graphs above show the power consumption throughout the 24-hour period for the different cases, including results from the previous cases for comparison. Common for all cases is the reduction of peak load compared to the base case, and elevated consumption outside production hours due to charging of storages. The degree of these two effects are however very dependent on which storages are integrated. As the graphs reveal, least impact is observed for the case T3, where only the peak during dehumidification is transferred to low-demand hours. Case T4 shows quite similar performance as with the combined CTES/refrigeration concept, where exclusion of the AC storage results in a peak consumption during dehumidifying.

It is interesting to note the similarities between case T1 and T2, which have approximately the same power consumption profile during production hours, but differs at low-demand hours due to the work associated with charging the different-sized storages. This can be understood by how the concept design works; both charger circuits in the bottom cycle generates condensation

heat which is lifted to the upper cycle, and further lifted by the MT compressor group. The difference in work associated with charging the LT and MT storages is reflected in the difference in power consumption during low-demand hours. During discharge, the savings for each circuit differs, but the sum of work of the LT and MT compressors remain more or less equal. This is also valid for the observed similarities between T5 and T6.

6.4 Comparative presentation of results between cases

A presentation over the main results from each case can be found in the table below. The graphs show the relative change in percent between the base case and CTES cases, where negative values mean reduction and positive values mean an increase.

Parameter		BC	Comb	T1	T2	T3	T4	T5	T6
Peak load	*[MW]*	2,21	1,07	1,76	1,78	1,97	1,32	1,50	1,54
Energy consumption	*[MWh]*	20,8	22,8	22,3	21,1	21,0	22,8	22,6	21,5
Heat recovered, DSH	*[MWh]*	5,2	8,5	8,0	7,6	8,2	8,2	8,3	8,4
Heat recovery ratio	*%*	51 %	78 %	76 %	73 %	72 %	78 %	77 %	75 %
Water production 70 °C	*[k liter]*	74,5	120,6	113,8	107,2	115,7	116,8	118,1	119,6
Heat recovered, MC	*[MWh]*	4,6	4,6	4,5	4,4	4,4	4,6	4,6	4,4
Water production 50 °C	*[k liter]*	95,6	95,9	94,0	90,9	91,0	95,3	94,6	91,7
EER_{ref}	-	3,09	2,82	2,88	3,04	3,06	2,82	2,85	2,99
EER_{comb}	-	3,57	3,39	3,45	3,61	3,65	3,38	3,42	3,59

Table 14: *Summarized results for all cases. BC and COMB refers to base case and combined CTES/refrigeration system.*

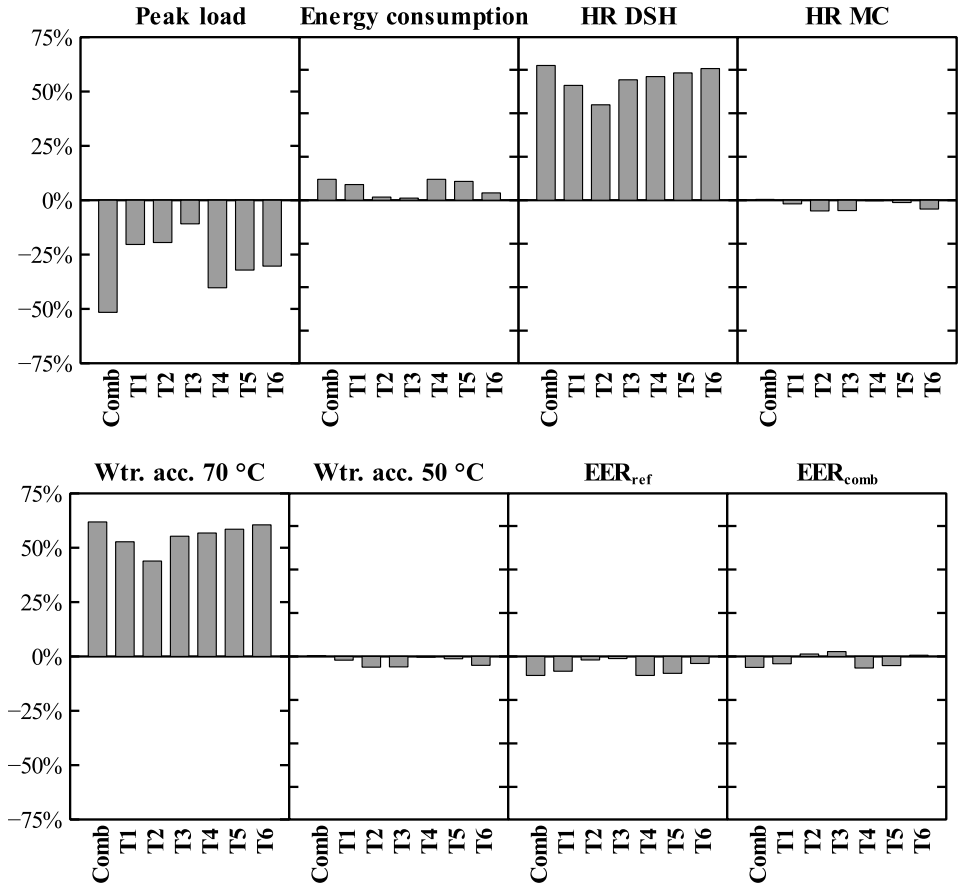

Figure 44: *Relative difference between results from base case and CTES cases*

7 Discussion

This chapter will start with an assessment on the validity of simulation results and a discussion about the simulation models. Discussion of results were partially made in the previous chapter, but main findings for each case will be highlighted and further discussed, before this chapter ends with a comparison between the cases.

7.1 Validity of results and simulation models

Due to limited information regarding thermal demand pattern of the poultry process plant in question, a thermal demand profile was constructed based on typical characteristics for such plants. All simulations were performed with the profile as input, thus the results presented in the previous chapter must be viewed in that context. In essence this means that results might not be representative for the plant, but they serve their role as vehicles for comparing the system with and without CTES integration. Furthermore, the results also indicate how the system performs with respect to inputted thermal demands; adjusting these demands will only change the magnitude of the reported values.

A larger consequence of a constructed thermal demand profile is that the design concept for integration of CTES is partially based on it. The presented concept assumes that there is a non-stop demand at all levels. This assumption can be held true given that the plant employs cold storages at low and medium temperature levels, but dismissing this assumption for the AC demand could lead to different design wherein the same circuit serves both charging and cooling. Furthermore, dimensioning of storage capacities was also based on cooling energy needed during production hours, which is explicitly related to the thermal demand pattern. However, as an investigation into energetic effects of including CTES on all circuits, the presented concept has fulfilled its purpose and generated results which can be valuable to further investigations.

Accuracy of the results is dependent on simplifications made in the simulation model, and some simplifications are necessary for simulation performance reasons. This was described in Chapter 5, and one mentioned simplification was the constant compressor efficiencies. If the model accounted for reduced efficiencies during part load operation, energy consumption of the system would most likely increase. Then again, this effect can be countered to a degree by implementing a more authentic controller configuration which prevents simultaneous part-load operation occurring within the compressor groups. Thus, the combined effect of omitting both

a part load-dependent efficiency curve and authentic controller configuration can argue in favour of the validity for the presented power consumptions. However, for the combined CTES/refrigeration system, not accounting for reduced efficiencies of the redistributed compressors due to the increased pressure ratio, exaggerates their energy efficiency to a degree. As the models stand, this simplification in addition with constant heat transfer properties in the various heat exchangers and storages are the most potent sources for erroneous results.

7.2 Refrigeration system

The refrigeration system has shown through the presented results that it performs well during periods of both high and low demands. Energy efficiency indicators were calculated to 3,09 and 3,57, but the results also reveal that there is some potential to increase the energy efficiency.

One of these potentials is heat recovery, which is not utilized other than hot water pre-heating. The results from the base case shows that almost 10 MWh of heat is recovered for this purpose, while 76 MWh is rejected to sea water through the condensers. Albeit not detailed in this thesis, additional coverage of internal hot demands could be realised through elevating this heat with proven heat pump technology. Considering the already planned utilities, there is also potential for better utilization of heat recovery both in terms of quality and capacity. Results from the simulation showed that the de-superheater only recovered 50% of available superheat. As discussed in Chapter 6.1, increasing size of the de-superheater would increase this ratio, and thus would result in larger volumes of accumulated pre-heated water.

Another option is to elevate the quality, at the cost of reduced water accumulation, by routing the water outlet from the motor cooler circuit and use it as water inlet for the de-superheater.

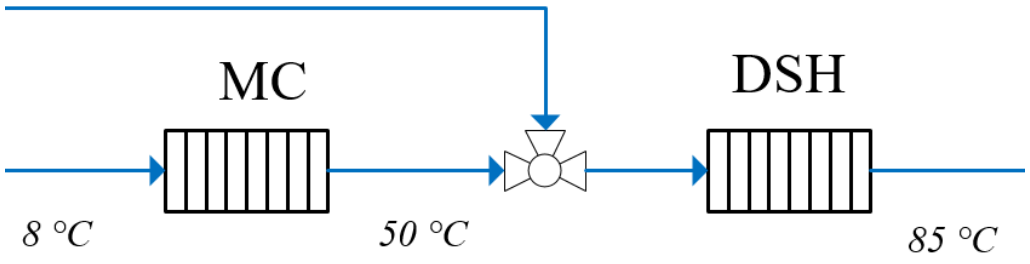

Figure 45: *Hot water pre-heating in series*

If water flow from the MC circuit should not be sufficient, this stream can be mixed with fresh inlet water at 8 °C. This setup was tested for the base case with unaltered heat exchanger

dimensions, and resulted in accumulation of approximately 100 000 liter water at 85 °C. Optimisation of the setup would most likely allow for even larger hot water, as the test also showed that DSH was too small to handle the full discharge water stream from the MC heat exchanger. It should be noted that high water temperature could result in scaling problems in the DSH which would have to be handled.

Condensation pressure for the upper cycle was configured to maintain a constant level, controlled by the expansion valve downstream of the condensers. An alternative solution is to regulate the high pressure accordingly to rate of heat condensation. The condensers are dimensioned for a combined capacity of 8500 kW, but during low demand hours the condensation rate is as low as 1200 kW. Utilizing the extra heat exchange area during these periods allows for a closer temperature pinch, which means reduced work for the upper cycle compressors. Considering that the system operates at low capacity for majority of the time, this would most likely have a significant positive effect on energy consumption.

7.3 CTES concept

The presented concept for integration of CTES with the refrigeration system is designed to allow for control over the heat transfer rate while discharging by regulating refrigerant flow rate. Doing so in a simulation environment is trivial, as the instantaneous heat transfer rate can be measured directly from the storage and used as input to mass flow controllers. For real world operation, determination of heat transfer is typically done by measuring flow rate and temperatures at storage inlet and outlet for the heat transfer medium. This is not straightforward when utilizing two-phase refrigerant as heat transfer medium, and other methods would most likely need to be investigated in order to maintain control over discharge power. As discussed in Chapter 5.3.2, having this control is desired in order to distribute the storage cooling capacity over a scheduled discharge time window. For the studies conducted, the feasibility of having this control was assumed.

Operation of the storages were limited to two modes, charging and discharging, and desired charge and discharge power were determined by dividing the storage capacity over the time available for charging/discharging. This resulted in a quite flat power consumption profile for the CTES concept, as can be seen in Figure 40. According to the integration goal of reducing peak power consumption, this approach proved successful. The two dips in the power consumption curve, which can be seen before and after production, is due to the shift between charging and discharging, which occurs gradually. These dips can be avoided by optimizing the

programmed charge and discharge period, shortening the transition between charging completion and discharging initiation. As the results from the additional CTES studies reveal, the power consumption profile can take many different shapes as consequence of installed storage capacity as well.

Design of the energy storages and choice of PCM has an impact on system performance, and has not been investigated in depth. It should be reiterated that the PCM selected for the LT storage has a manipulated phase change temperature. The best matches the author was able to find, with regards to phase change temperature, was -37 and -50 °C, and an assumption was made that a suitable PCM is available in between this range. Should this assumption not hold true, then the -50 °C material should be selected. In this case, energy consumption would increase because of lower evaporation pressure in the charger circuit, and reduced cooling capacity of the compressor. Furthermore, the storages were oversized to perform with desired discharge power towards end of discharge period. Nominal capacities were in the range of 8-14% larger than rated capacities, and as an indication of how large space is needed to accommodate such a system, storage volumes as they were dimensioned in the simulation model are listed below.

Storage	Total volume [m^3]
LT CTES	184
MT CTES	200
AC CTES	78

Table 15: *Volume of storages, including internal tubes*

For comparison, a standard 20 feet container has a volume of 39 m^3, which makes the total storage volume equivalent to approximately 12 such containers.

7.4 Comparison between systems

The main findings were presented in Chapter 6.4 and clearly indicates that integration of CTES has a positive effect in terms of energy use. Perhaps the most significant effect is the reduction of peak power consumption, which in all cases is reduced. Largest reduction was observed for the proposed concept, with a reduction value of over 1,1 MW. This was expected as this was the case with largest installed CTES capacity. The additional studies also show that installing storages on the LT and MT circuit has the largest impact on peak reduction, while the AC circuit

has less influence. Furthermore, not much deviation was observed if storages were only to be integrated on either the LT or MT circuit. This is however a bit coincidental due to selected storage size and compressor efficiencies and must not be taken as a general truth.

What was further observed was the increased heat recovery in the de-superheater. This is due to the elevated power consumption during off-production hours, and thus more heat for the de-superheater to recover. In contrast with the base case, where an argument was made that the DSH was undersized, the size now has a much better fit with respect to the available heat and for a longer duration of the 24 hr period. This is reflected in the heat recovery ratio, which increases from 51% to 78% between original and combined system. Heat recovery in the motor cooling circuit decreases in most CTES cases, but with very small amounts. The reduction of hot water production of 50 °C is insignificant compared to the gain observed in 70 °C hot water production.

Total energy consumption increases when CTES is integrated into the system, which is reflected in the energy efficiency indicators. The largest deviation compared to the original system is observed for the proposed concept, which consumes approximately 2000 kWh more electrical energy for the 24 hr period. The reason for this is understood by the fact that, even considering ideal storages with no heat gain or efficiency losses, charging the storages with 1 kWh costs more than directly serving the refrigeration demand with 1 kWh, due to the reduced evaporation temperature. As such, this small reduction in energy efficiency might be considered the cost of integrating CTES. However, this is a rather small cost compared to the significant reduction in power consumption. Furthermore, what is not reflected in the energy efficiency indicators is at what times energy is consumed. A large proportion of the energy consumption during production hours have been transferred to outside production hours, and the difference in energy consumption due to charging is also occurring outside production hours. Assuming that there is a price differentiation between day and night on the electrical energy rates, the economic consequence of the increased energy consumption can be diminished. Even so, a larger economic benefit is expected to be realised in the reduction of electrical demand charges, which typically are based on the highest measured peak-hour in a month.

Further economical savings could be argued due to less work input to the sea water pumps, increased production of hot water, prolonged longevity of refrigeration equipment due to more stable operating conditions etc., but quantifying these effects has not been conducted. For future investigation of this concept, it is recommended that an economical evaluation is conducted to

better capture these effects. Such an evaluation would also be necessary to determine capital cost of the concept, and could thus indicate in which direction further work of the concept should take.

8 Conclusion

An energy analysis of the refrigeration system for an upcoming poultry process plant has been conducted, with focus on energy consumption, peak power requirement, heat recovery and potential for cold thermal energy storages. To do so, a simulation model of the refrigeration system was built in the simulation software Dymola, and a concept for integration of cold thermal energy storages has been developed. This concept was also modelled, and simulations were carried out for both systems using a thermal demand profile with duration of 24 hours. Due to limited information regarding thermal demands of the plant, the input profile was constructed with basis in typical characteristics of food-processing plants. This means that the face value of the results might not be representative for the poultry plant in question, but they are representative of system performance, and serves as benchmarking values to assess the energetic effects of thermal energy storage integration.

The following discoveries were made with respect to the original refrigeration system:

- The de-superheater is only able to recover 51% of available heat, which is partly due to low availability during low-demand periods. During high-demand periods however, size of the de-superheater is the limiting factor, and more heat could be recovered with a larger de-superheater. This would improve overall energy efficiency of the system.
- Energy efficiency could be improved by regulating condensation pressure in the upper cycle as a function of condensation rate. Capacity of the condensers are rated for 8500 kW, but condensation rate is much lower most of the time. Lowering the condensation pressure would mean less electrical work input to the upper cycle compressors.
- A proposal was made to connect the two heat recovery heat exchangers in series, a design which could elevate the water quality beyond 70 °C. If implemented, the effects could increase energy efficiency of the plant by reducing the energy consumption for auxiliary heating equipment. This could also lead to a reduction in greenhouse gas emissions, given that the energy source for said equipment is oil or gas.

The following discoveries was made when comparing the refrigeration system and CTES concept:

- Peak power reduction was achieved for all CTES cases within the range of 11%-52%.
- The proposed concept achieved a peak power reduction of over 1,1 MW. This case used storages on all three temperature levels with a combined nominal storage capacity of approximately 22 000 kWh.
- Heat recovery ratio in the de-superheater increased due to elevated availability of heat during periods outside production. Heat recovery for this unit increased from 5,2 MWh to 8,5 MWh.
- Heat recovery from the motor cooling circuit was reduced for most CTES cases, but is concluded as insignificant compared to the increase in high quality water production.
- Total energy consumption was increased for all CTES cases due to more work associated with charging of storages. In energetic terms, this can be considered the cost to reduce peak power consumption. In economic terms, an argument could be made that this increase would be insignificant when accounting for reduction in electrical demand charges and shifting energy consumption from high-rate to low-rate hours.

An overall conclusion based on the findings of this study is that integration of cold thermal energy storages provides both energetic and economic benefits, especially suitable for the food processing industry which is characterized by large daily variations in refrigeration demand, and efforts should be put into developing concepts which can realise these benefits.

9 Further work

Integrating cold thermal energy storages with the refrigeration system can be done in many different ways, and the proposed concept is only one of many alternatives. Thus should an evaluation of not only the proposed concept be conducted, but also compared to other possible configurations. Designing the concept was also based on some constraints and assumptions which needs to be tested. In particular, further investigation into finding suitable phase change materials for freezing applications must be conducted, and feasibility of a discharge/charge rate control system must be evaluated.

Acquiring information of thermal demands would be helpful to generate results which better reflect energy flow of the plant. Further accuracy could be achieved by eliminating the assumptions and simplifications made when modelling the systems. In that regard two recommendations stand out; implementing efficiency curves for the compressors in combination with a more authentic controller configuration, and direct incorporation of the thermal energy storages within the model.

While this thesis has thoroughly described the benefits which CTES brings in energetic terms, economic benefits should be quantified through a cost analysis. This should be carried out as a comparative analysis between the systems, evaluating the difference in operational expenses when accounting for all aspects brought to light in this report. In combination with estimation of investment cost of CTES equipment and construction, payback period can be calculated which can serve as advice to investment decision makers. Optimization of CTES concept can also be conducted on the basis of such an analysis, given that operation and size of storages is partially dependent on electrical rating structure.

Bibliography

[1] SSB, "Produksjon og forbruk av energi, energibalanse," 2018. [Online]. Available: https://www.ssb.no/energi-og-industri/statistikker/energibalanse/aar-endelige.

[2] SSB, "Utslipp av klimagasser," 2018. [Online]. Available: https://www.ssb.no/natur-og-miljo/statistikker/klimagassn/aar-forelopige.

[3] E. Rosenberg, T. M. Risberg, H. J. Mydske, and H. E. Helgerud, "Energy potential in the food industry; Store energipotensialer i naeringsmiddelindustrien," 2007.

[4] T. M. Eikevik, *TEP4255 Compendium*. 2018.

[5] I. Dinçer, "Thermal energy storage : systems and applications," *Thermal Energy Storage - Systems and Applications2e*. Wiley, Hoboken, N.J., 2010.

[6] İ. Dinçer and M. Kanoğlu, *Refrigeration Systems and Applications*. Chichester, UK: Chichester, UK: John Wiley & Sons, Ltd, 2010.

[7] Britannica Academica, "Montreal Protocol," *Britannica Academica*, 2018. [Online]. Available: https://www.britannica.com/event/Montreal-Protocol.

[8] A. Mota-Babiloni, J. Navarro-Esbrí, Á. Barragán-Cervera, F. Molés, and B. Peris, "Analysis based on EU Regulation No 517/2014 of new HFC/HFO mixtures as alternatives of high GWP refrigerants in refrigeration and HVAC systems," *Int. J. Refrig.*, vol. 52, pp. 21–31, 2015.

[9] J. Kazil *et al.*, "Deposition and rainwater concentrations of trifluoroacetic acid in the United States from the use of HFO-1234yf," *J. Geophys. Res. Atmos.*, vol. 119, no. 24, pp. 14–59, 2014.

[10] B. J. Cardoso, F. B. Lamas, A. R. Gaspar, and J. B. Ribeiro, "Refrigerants used in the Portuguese food industry: Current status," *Int. J. Refrig.*, vol. 83, pp. 60–74, 2017.

[11] C. Arpagaus, F. Bless, M. Uhlmann, J. Schiffmann, and S. S. Bertsch, "High temperature heat pumps: Market overview, state of the art, research status, refrigerants, and application potentials," *Energy*, 2018.

[12] P. Gullo, K. Tsamos, A. Hafner, Y. Ge, and S. A. Tassou, "State-of-the-art technologies for transcritical R744 refrigeration systems–a theoretical assessment of energy advantages for European food retail industry," *Energy Procedia*, vol. 123, pp. 46–53, 2017.

[13] W. F. Stoecker, *Industrial refrigeration handbook*. New York: McGraw-Hill, 1998.

[14] A. Messineo, "R744-R717 cascade refrigeration system: performance evaluation compared with a HFC two-stage system," *Energy Procedia*, vol. 14, pp. 56–65, 2012.

[15] H. Mehling and L. F. Cabeza, *Heat and cold storage with PCM*, vol. 308. Springer, 2008.

[16] L. G. Socaciu, "Seasonal thermal energy storage concepts," *ACTA Tech. NAPOCENSIS-Series Appl. Math. Mech. Eng.*, vol. 55, no. 4, 2012.

[17] K. S. Lee, "Underground thermal energy storage," in *Underground Thermal Energy Storage*, Springer, 2013, pp. 15–26.

[18] S. Barbut, *The Science of Poultry and Meat Processing*. 2015.

[19] ASHRAE, *ASHRAE Handbook - Refrigeration*. 2014.

[20] P. J. Fellows, *Food processing technology: Principles and practice: Third edition*. 2009.

[21] C. D. Carroll and C. Z. Alvarado, "Comparison of Air and Immersion Chilling on Meat Quality and Shelf Life of Marinated Broiler Breast Fillets," *Poult. Sci.*, vol. 87, no. 2, pp. 368–372, Feb. 2008.

[22] C. James, C. Vincent, T. I. de Andrade Lima, and S. J. James, "The primary chilling of poultry carcasses - a review," *Int. J. Refrig.*, 2005.

[23] C. (Alfa L. A. Stenhedel, "A Technical Reference Manual for Plate Heat Exchangers in Refrigeration & Air conditioning Applications." 2008.

[24] PCMProducts, "PlusICE E2 - Technical data sheet," 2018. [Online]. Available: http://www.pcmproducts.net/files/E range-2018.pdf.

[25] PureTemp, "PureTemp -37 Technical Data Sheet," *2019*. [Online]. Available: https://www.puretemp.com/stories/puretemp-minus-37-tds.

[26] University of California, "Modelica Buildings Library - User Guide." [Online]. Available: https://simulationresearch.lbl.gov/modelica/userGuide/bestPractice.html. [Accessed: 01-May-2019].

Appendix A: Preliminary work

A.1: Calculation of compressor efficiencies

Volumetric efficiency, given data for indicated cooling capacity $\dot{Q}_{ci}$ and stroke volume $\dot{V}_s$, with specific volume at suction v_s and specific enthalpy difference Δh_{ref} evaluated for relevant refrigerant at relevant state points with REFPROP v9.0, is calculated as:

$$\eta_v = \frac{\dot{Q}_{ci} \cdot v_s}{\dot{V}_s \cdot \Delta h_{ref}}$$

Isentropic efficiency, given data for indicated power consumption $\dot{P}_i$, with specific enthalpy and entropy at suction (h_s, s_s) evaluated for relevant refrigerant at relevant state points with REFPROP v9.0, is calculated as:

$$\eta_{is} = \frac{\left(\frac{\dot{V}_s \cdot \eta_v}{v_s} \cdot (h_{ds} - h_s)\right)}{\dot{P}_i}$$

Where specific discharge enthalpy given isentropic compression is calculated as:

$$h_{ds} = f(T_c, s_s)$$

Effective isentropic efficiency, based on the assumption that respectively 10% and 30% of the power input can be regarded as heat losses for piston and screw compressors, is calculated as:

$$\eta_e = 0{,}9 \cdot \eta_{is} \;\&\; \eta_e = 0{,}7 \cdot \eta_{is}$$

LT Compressor group

The LT compressor group operates between an evaporation and condensation temperature at -40 & -5 °C and uses CO_2 as working fluid. Due to the IHX between compressor suction and discharge line, suction properties are evaluated with 5K superheat. This superheat is not accounted for in Δh_{ref}, which is evaluated as the difference between specific saturated vapor enthalpy at evaporation temperature and specific saturated liquid enthalpy at condensation temperature. The following compressor data was given:

Compressor	$\dot{V}_s$ [m^3 hr^{-1}]	$\dot{Q}_{ci}$ [kW]	$\dot{P}_i$ [kW]
LT1 (Piston)	452	667	167
LT2 (Piston)	222	337	82
LT3 (Piston)	222	337	82

MT Compressor group

This group of two screw compressors and one piston compressor operates between an evaporation and condensation temperature of -10 & 35 °C and employs ammonia as working fluid. The group draws saturated vapor out of the MT separator, thus the suction properties are evaluated as such at evaporation temperature. Specific refrigeration capacity is then evaluated as specific suction enthalpy and specific saturated liquid enthalpy at condensation temperature. The following compressor data vas given:

Compressor	$\dot{V}_s$ [m3 hr-1]	$\dot{Q}_{ci}$ [kW]	$\dot{P}_i$ [kW]
MT1 (Screw)	3370	2440	563
MT2 (Screw)	2676	1940	448
MT3 (Piston)	679	362	86

AC Compressor group

The AC compressor group operates between an evaporation and condensation temperature of 4 & 35 °C and uses ammonia as working fluid. As for the MT group, no suction superheat, thus suction properties are evaluated as saturated vapor at evaporation temperature. Specific refrigeration capacity is evaluated as the difference between saturated vapor and liquid enthalpy at evaporation and condensation temperature, respectively. The following compressor data was given:

Compressor	$\dot{V}_s$ [m^3 hr^{-1}]	$\dot{Q}_{ci}$ [kW]	$\dot{P}_i$ [kW]
AC1 (Piston)	1018	1110	190
AC2 (Piston)	1357	1480	252

Calculated efficiencies

Based on the listed equations and statepoint values evaluated as they are described for each compressor group, efficiencies have been calculated in a spreadsheet. The results can be viewed in the next table. Take note of the unrealistic high value for volumetric efficiency for both screw compressors; however, this does not impact the results of the energy analysis.

				Suction			Discharge			Δh_{ref}	Efficiencies		
Compressor	P_e	P_c	$\frac{P_c}{P_e}$	h_s	v_s	s_s	h_{ds}	h_d	T_d		η_v	η_{is}	η_e
Units	*bar*	*bar*	-	*kJ/kg*	*m^3/kg*	*kJ/kgK*	*kJ/kg*	*kJ/kg*	*°C*	*kJ/kg*	-	-	-
LT1	10,0	30,5	3,03	440	0,0396	2,070	490	502	50	247	0,850	0,807	0,727
LT2	10,0	30,5	3,03	440	0,0396	2,070	490	501	49	247	0,874	0,831	0,748
LT3	10,0	30,5	3,03	440	0,0396	2,070	490	501	49	247	0,874	0,831	0,748
MT1	2,9	13,5	4,65	1594	0,4183	6,228	1817	1848	113	1085	0,990	0,879	0,615
MT2	2,9	13,5	4,65	1594	0,4183	6,228	1817	1849	113	1085	0,990	0,877	0,614
MT3	2,9	13,5	4,65	1594	0,4183	6,228	1817	1852	114	1085	0,740	0,866	0,780
AC1	5,0	13,5	2,72	1610	0,2515	6,041	1750	1798	93	1100	0,897	0,743	0,669
AC2	5,0	13,5	2,72	1610	0,2515	6,041	1750	1797	93	1100	0,898	0,747	0,672

A.2: Calculation of cooling capacity for CTES integrated with the refrigeration system

Compressor cooling capacity after rearrangement of compressors have been calculated for the now so-called charging compressors, with the assumption that all efficiencies are unchanged. Cooling capacity can be calculated as:

$$\dot{Q}_c = \frac{\dot{V}_s \cdot \eta_v}{v_s} \cdot \Delta h_{ref}$$

Suction properties are evaluated at pressure level in the charging circuit and superheat value of 5 K. This superheat is considered useful, leading to Δh_{ref} to be calculated as the difference between specific suction enthalpy and specific enthalpy at CTES inlet. The latter property is equal to the specific saturated liquid enthalpy of the relevant separator refrigerant is throttled from, that is $h_{in} = h_{satliq}(P_{sep})$.

Based on these conditions the following statepoint values are retrieved from REFPROP.

Circuit	Refrigerant	P_e (bar)	h_s	h_{in}	v_s
CTES LT	CO_2	6,82	437	113	0,058
CTES MT	CO_2	19,7	443	188	0,020
CTES AC	NH_3	3,41	1611	362	0,368

Compressor arrangement in the combined CTES/refrigeration system is as follows:

Compressor	Old label	$\dot{V}_s$	η_v
LT	LT 1	452	0,850
LT-C 1	LT 2	222	0,874
LT-C 2	LT 3	222	0,874
MT 1	MT 1	3370	0,990
MT 2	MT 3	679	0,740
MT-C	New, equal LT 1	452	0,850
AC	AC 1	1018	0,897
AC-C	AC 2	1357	0,898

Thus the new (combined) cooling capacity for each circuit in the combined CTES/refrigeration system can the calculated. Operating conditions for the LT, MT and AC circuits are as before.

Circuit	$\dot{Q}_c$
LT	667
LT-C	608
MT	2802
MT-C	1352
AC	1110
AC-C	1148

Appendix B: Additional results

B.1: Results from standalone CTES simulations

These simulations were carried out to produce input values for the top-level model of the combined CTES/refrigeration system. This section presents the results for charging and discharging power for each energy storage, accompanied with parameterization input for each case.

CTES LT

Data	Value	Unit
Height	2	m
Width	2	m
Length	46	m
Tube, inner diameter	10	mm
Tube, wall thickness	1	mm
Number of tubes	85 x 85	-
Volume, storage	184	m^3
Volume, PCM	146	m^3
Heat transfer area, external	12 529	m^2
Heat transfer area, internal	10 441	m^2
Energy capacity PCM (latent)	5720	kWh

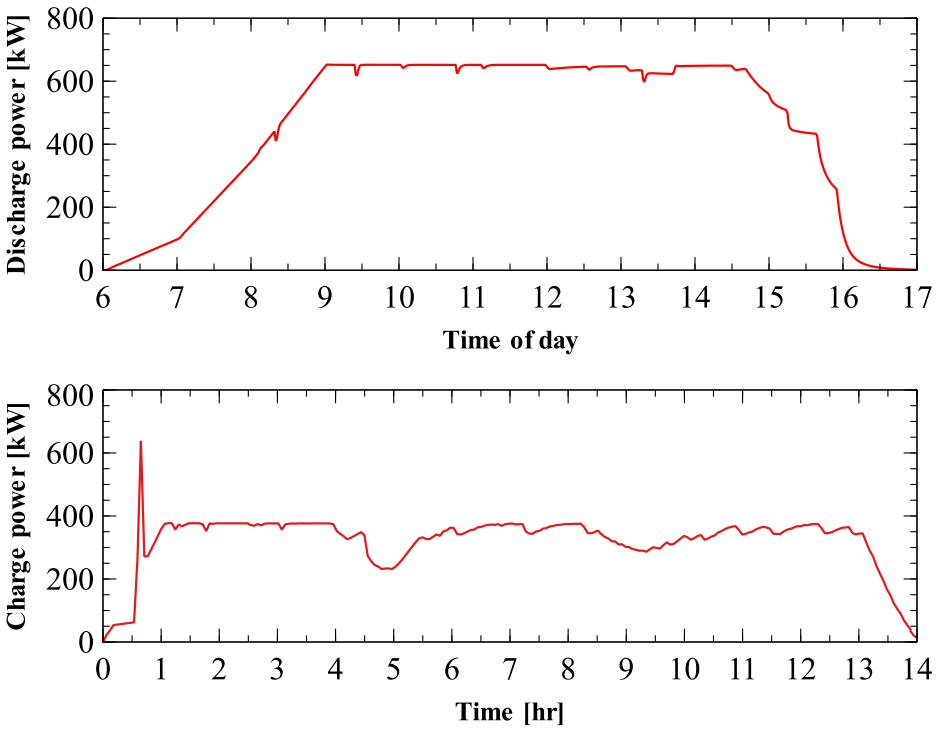

Figure 1: Results from simulation of CTES LT

CTES AC

Data	Value	Unit
Height	1,4	m
Width	1,3	m
Length	43	m
Tube, inner diameter	10	mm
Tube, wall thickness	1	mm
Number of tubes	85 x 85	-
Volume, storage	78	m^3
Volume, PCM	43	m^3
Heat transfer area, external	11 713	m^2
Heat transfer area, internal	9760	m^2
Energy capacity PCM (latent)	4166	kWh

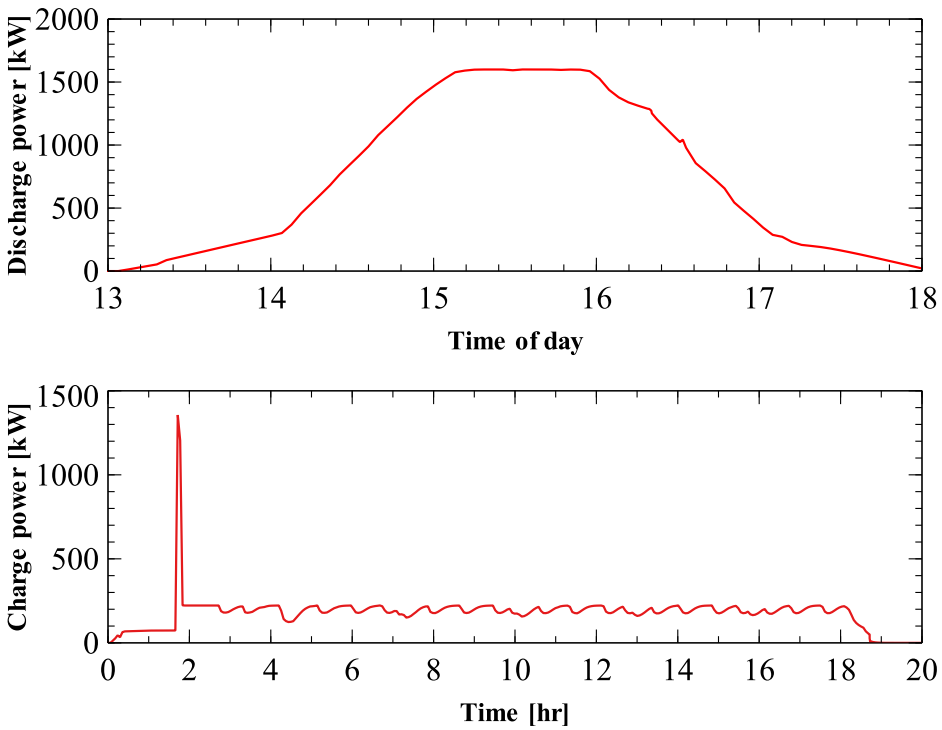

Figure 2: Results from simulation of CTES AC

CTES MT

Data	Value	Unit
Height	2	m
Width	2	m
Length	50	m
Tube, inner diameter	10	mm
Tube, wall thickness	1	mm
Number of tubes	85 x 85	-
Volume, storage	200	m^3
Volume, PCM	159	m^3
Heat transfer area, external	13 619	m^2
Heat transfer area, internal	11 349	m^2
Energy capacity PCM (latent)	13 824	kWh

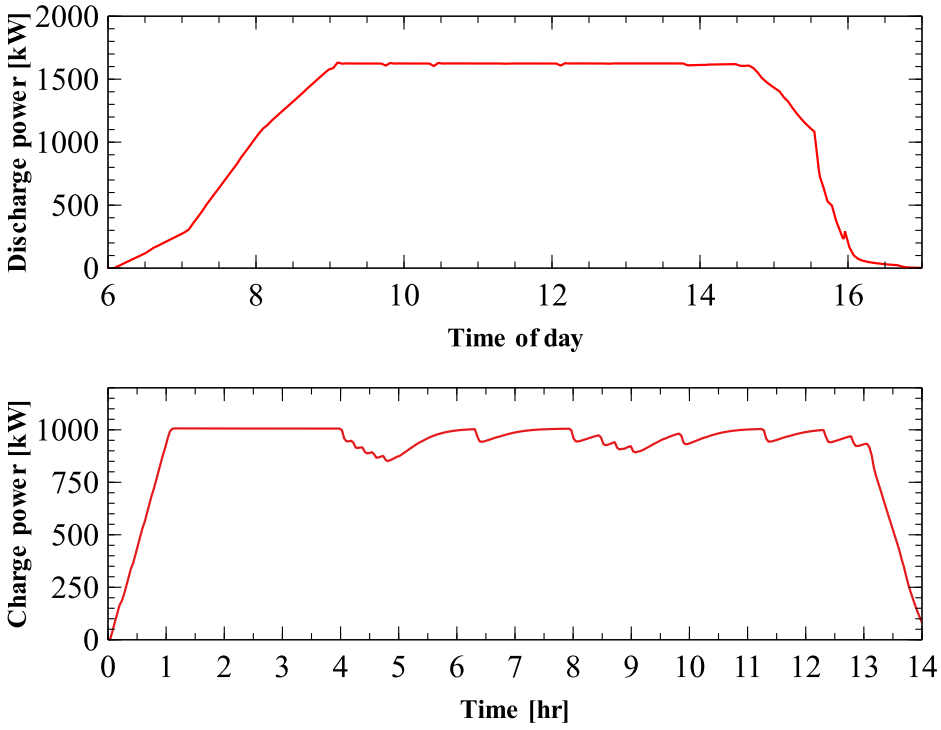

Figure 3: Results from simulation of CTES MT

Appendix C: Draft for scientific paper

Energy flow analysis of a poultry process plant

Eirik Starheim Svendsen[(a)], Armin Hafner[(a)], Håkon Selvnes[(a)]

[(a)]Norwegian University of Science and Technology (NTNU), Department of Energy and Process Engineering, N-7491 Trondheim, Norway, eirikssv@stud.ntnu.no

ABSTRACT

Improving industrial processes in terms of energy efficiency is a key measure in the face of global warming, and different solutions for different sub-sectors must be researched. Thermal demands for industrial food-processing plants can be characterized as irregular throughout a 24-hr period and dependent on production rate, and such plants must employ complex energy systems to handle these demands. This report aims to evaluate the energy system of a poultry processing plant with focus on energy consumption, peak power requirement and heat recovery. A concept for integration of cold thermal energy storage (CTES) is included, and a comparison between the systems is made by building simulation models and carrying out simulations with a timeline of 24 hours. Main findings from the comparison shows that the CTES concept is able to reduce peak power consumption with 52%, with the cost of energy consumption increasing with 10%.

Keywords: Industrial refrigeration, Food processing, Energy analysis, Cold thermal energy storage, Simulation

1. INTRODUCTION

Global warming is perhaps the largest threat to mankind and solutions must be researched to counter the effects of the threat. The industrial sector, being a large consumer of primary energy and a large contributor of greenhouse gas emissions, is one of many sectors where appropriate measures should be taken. The shares held by this sector in Norway with respect to primary energy consumption and greenhouse gas emission, was 30% and 20% of total consumption/emission in 2016 [1][2]. Developing and implementing solutions which can increase energy efficiency in this sector could decrease both primary energy use and greenhouse gas emission, but due to the variety of different industrial processes it is necessary to investigate and research such solutions apt for the different sub-sectors.

The food-processing industry is such a sub-sector, and a study published by Enova [3] estimated that energy consumption in this sector could be reduced with 30%, which amounts to 1,3 TWh/year. Half of the potential is held by thermal energy sources, which if were realized would contribute towards reducing emissions by approximately 50 000 ton CO_2-equivalents per year. Many of the measures recommended in the report is attributed to utilize waste heat from different processes.

Norsk Kylling AS is currently in the process of building a large-scale poultry processing plant, and has ambitions of setting a new standard for efficient use of energy and sustainability. The plant will employ a cascade NH_3/CO_2 refrigeration system, covering refrigeration demands by chiller and freezing process equipment, cold storages, air-cooling and cooling of production areas. In addition, some heat recovery utilities are planned to be used for hot water pre-heating.

In line with their ambition, they are considering integration of cold thermal energy storages in order to reduce peak power consumption. A proposed design for CTES integration has been made and is included in this paper, and will be evaluated and compared to the ordinary refrigeration system with respect to energetic effects

2. REFRIGERATION SYSTEMS AND SIMULATION MODELS

2.1. Tools

In order to conduct the energy analysis, models have been built in the simulation software *Dymola* used in conjunction with refrigerant and component libraries from *TLK-Thermo GmbH*. This software is based on the Modelica language, and provides the user an environment to model advanced energy systems and run transient simulations. The add-on libraries, *TIL 3.5.0, TIL-Media* and *TIL-SLEHX* provides many common pre-modelled components and refrigerants used in refrigeration systems.

2.2. Original refrigeration system

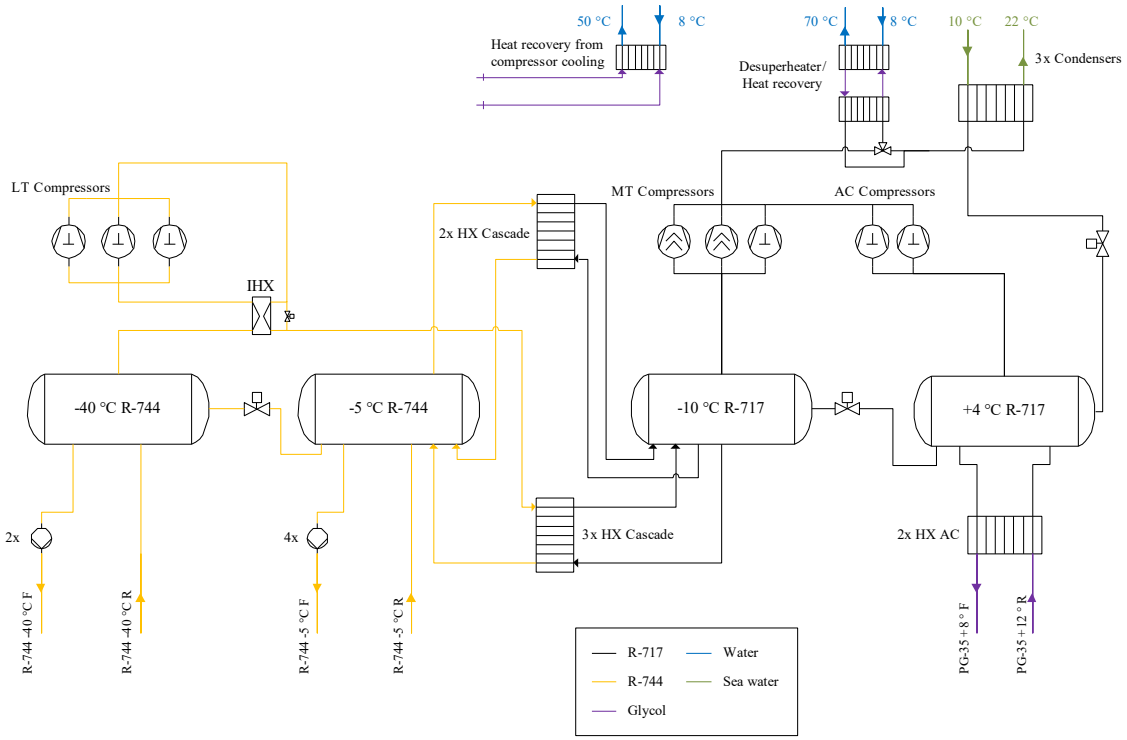

Figure 1: Simplified process and instrumentation diagram for the refrigeration system

The poultry processing plant will employ a cascade NH_3 / CO_2 refrigeration system which covers refrigeration demands at -40 °C, -5 °C and +4 °C. In addition, two heat recovery utilities are featured for hot water pre-heating, extracting superheat from the top cycle prior to condensers and extracting heat from a compressor cooling circuit. Description of each of these circuits, from now on labelled low temperature (LT), medium temperature (MT), air-cooling (AC), heat recovery de-superheater (DSH) and heat recovery glycol cooling circuit (MC), including capacities is listed in Table 1.

The bottom circuit utilizes CO_2 as working fluid and serves the refrigeration demands at LT and MT level. Refrigerant pumps are connected to each separator and pumps liquid CO_2 to the different consumers within the plant. The pumps overfeed the consumers so that the return line

is a mix of vapour and liquid. The vapour which returns from the LT consumers is separated, and drawn by a group of three piston compressors which elevates pressure to condensation level.

Circuit	Capacity (kW)	Refrigeration demand
LT (-40 °C)	1250	Freezing process equipment and storages
MT (-5 °C)	3250	Chilling process equipment, storages and production areas
AC (+4 °C)	2600	Air-cooling with different demands according to production, washdown and dehumidifying
DSH	430	Pre-heats water from 8 to 70 °C
MC	625	Pre-heats water from 8 to 50 °C

Table 1: Description of energy circuits in the refrigeration system

Discharge stream from the LT compressors are condensed in a group of three cascade plate heat exchangers against NH_3 from the upper circuit, before returning to the MT separator.

Return stream from MT consumers is separated in the MT separator, and vapour from this tank is led through another group of cascade plate heat exchangers by natural convection. The vapour condenses against NH_3 and is returned to the MT separator. An expansion valve between the separators ensures that enough liquid is present in both tanks.

The upper circuit utilizes NH_3 as working fluid and covers refrigeration demand for the AC circuit, has a DSH for heat recovery and further elevates the condensation heat from the bottom circuit to the condensers. Two compressor groups are used in this circuit, with the MT group consisting of two screw compressors to cover base load and a piston compressor for capacity control, and an AC compressor group which prevents unnecessary expansion and re-compression of vapour generated in the AC circuit. To cover the AC demands, liquid NH_3 is fed to a group of two plate heat exchangers where glycol is employed as a secondary fluid for further transportation. These exchangers, and the cascade heat exchangers, are of the gravity flooded type, meaning NH_3 is fed to the exchangers by gravity.

Further heat recovery from the system is accomplished by extracting heat from a glycol cooling circuit, which purpose is to cool the heads of all piston compressors, and the oil for the screw compressors.

2.3. Concept for CTES integration

A concept for CTES integration is presented, which aims to reduce peak power consumption of the refrigeration system. The motivation for this goal is to realise savings in the electrical demand and energy rates, assuming the rating structure differentiates between high- and low-cost hours (day/night), and that demand charges are based on highest measured peak-hour in a month. The concept is designed trying to utilize the already installed compressor capacity, and integration on all three refrigeration circuits will be done in order to fully explore the possibilities offered by CTES. Storages are sized to cover approximately 50% of the refrigeration energy needed during discharge period, and suitable phase change materials (PCM) are selected from the commercial market.

Figure 2 shows how integration of the energy storage is proposed for the LT circuit, but the same method is used on all circuits. Control of the system is accomplished by a number of three-way valves. To charge the storage an expansion valve is opened and adjusts feeding to the storage as if it was a DX evaporator.

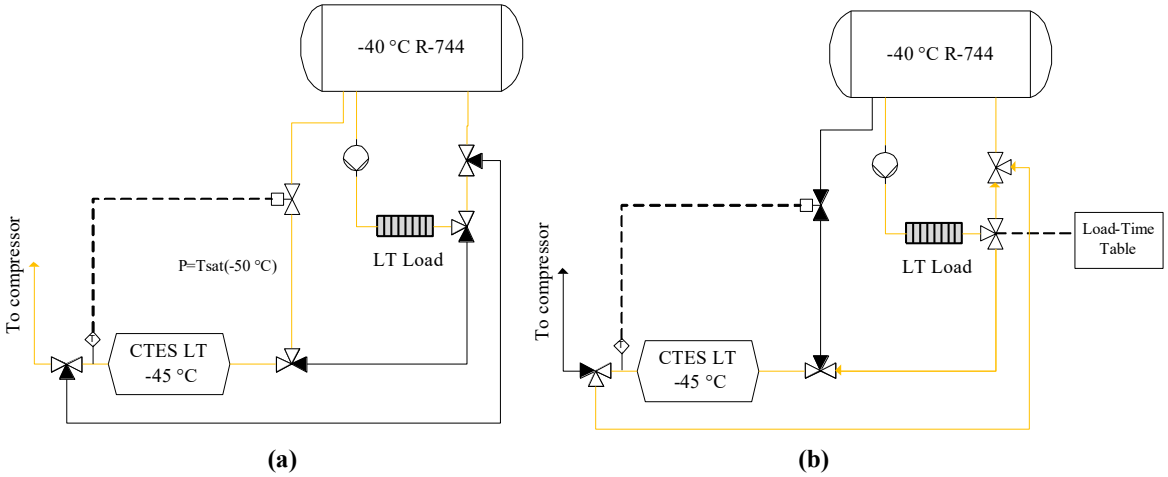

Figure 2: Integration of CTES storage on the LT circuit. (a) Charging (b) Discharging

The evaporation level in this "charger circuit" is set to be 5 K below that of the phase change temperature of the storage to ensure proper heat transfer. The superheated vapour leaving the storage is drawn to a now-relocated compressor. The charging circuit is shut off when discharging occurs. When the storages are in discharge mode, the stream returning from refrigeration consumers are first met by a three-way valve where the stream is distributed between a direct return to the separator, or through the charged storage. The three-way valve adjusts flow rate to the storage in order to have control over the discharge rate. The storage will condense the two-phase stream before it returns to the separator. In effect, the degree of vapour returning from the consumers are now reduced because of the storages, which means less work for the compressors in the refrigeration system.

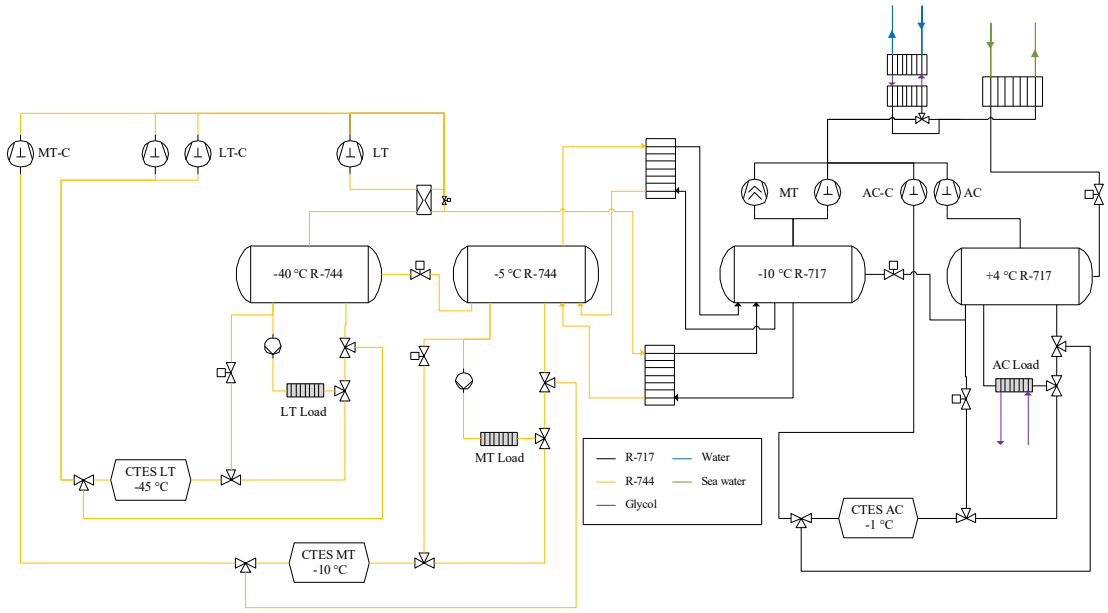

Figure 3: Simplified process and instrumentation diagram for the CTES concept

2.4. Simulation scenario

To perform a comparative analysis between both systems, they were both subjected to equal boundary parameters. Due to limited information regarding the thermal demands of the plant, a thermal demand profile had to be constructed with basis in typical patterns characterizing for food processing plants.

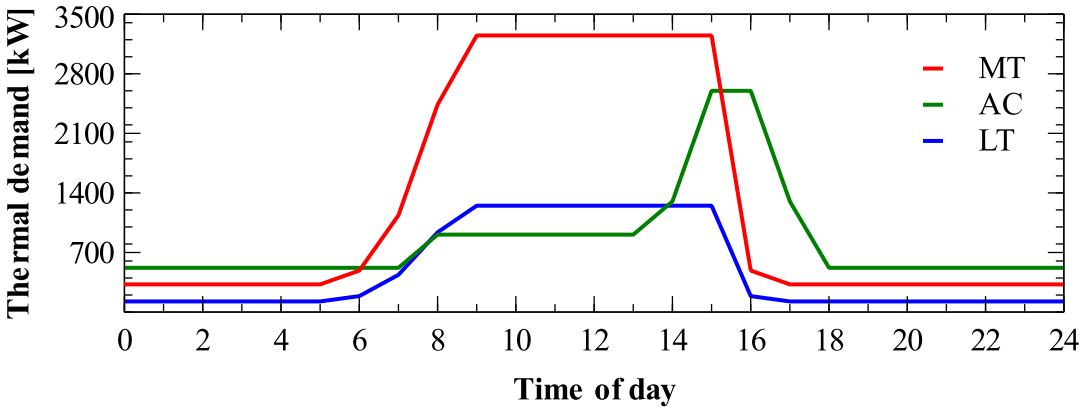

Figure 4: Thermal demand profile used for simulations

Outside production hours all demands are relatively low and associated with maintaining room temperature in cold storages. When production initiates and process equipment is switched on, the demand increases significantly. Near the end of production hours, washdown is initiated which increases the AC demand, which is further elevated towards max capacity of the system due to dehumidifying of production areas.

Operation and dimensioning of CTES storages are influenced by the thermal demand pattern, and descriptions for each storage is listed below.

Data	Unit	CTES AC	CTES MT	CTES LT
PCM	-	PlusICE E-2 [4]	Wtr-salt sol. [5]	Puretemp -37 [6]
Δh_{pc}	kJ/kg	325	283	145
T_{pc}	$°C$	-2	-10,7	-45
E_{st}	kWh	3800	12 775	5000
V_{pcm}	m^3	40	147	128
$\dot{Q}_{dis,cap}$	kW	1600	1625	650

Table 2: Storage properties for simulation of CTES case. Δh_{pc}= phase change enthalpy, T_{pc}=phase change temperature, E_{st}=rated capacity, V_{pcm}=volume of PCM, $\dot{Q}_{dis,cap}$=capped discharge rate

The storages have two modes of operation, charging and discharging. For the MT and LT storages, discharging occurs between 06 and 16, while for the AC discharging occurs between 13 and 18. Charging occurs rest of the available time.

2.5. Results and discussion

Simulations results from the original system, hereby referred to as base case, showed that the system had an energy consumption of 20,8 MWh for a 24 hr period, with a peak power of 2,21 MW.

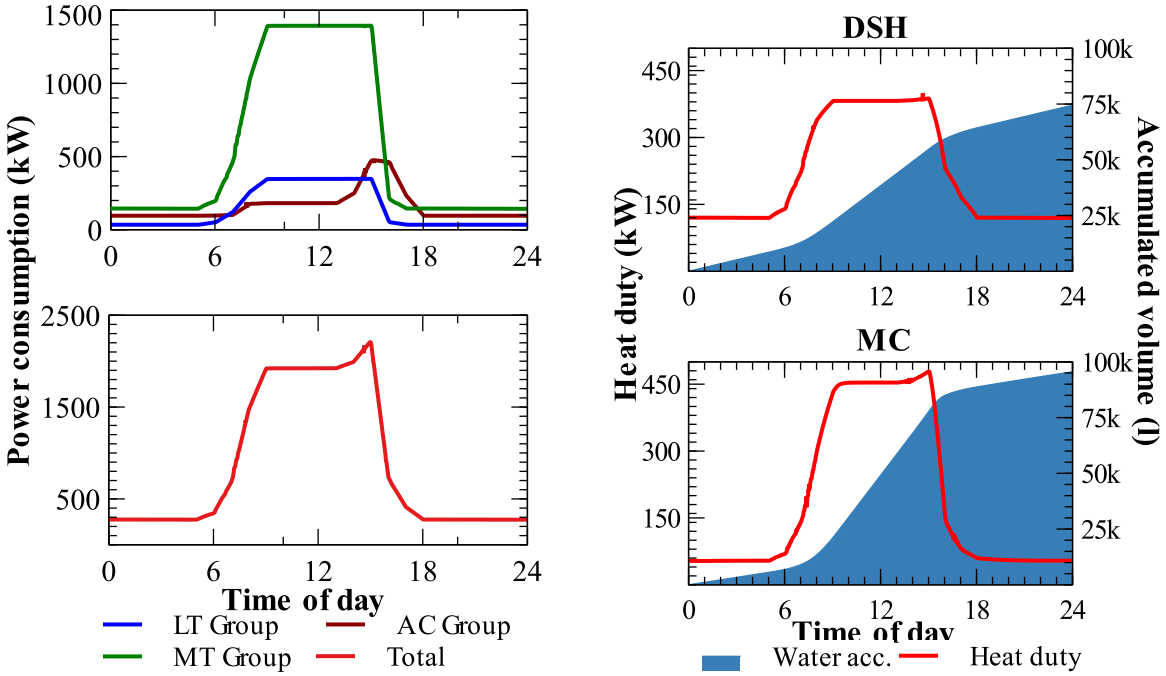

Figure 5: Graphs showing results from base case simulation

The total power consumption profile shows a strong dependency between required electrical input and refrigeration demands for the factory. Furthermore it can be seen that the MT compressor group is the compressor group which holds the largest share of consumption, and also the largest capacity operation range. The same dependency with refrigeration demands can be observed for the hot water production. Total water production ability of the system is 74 500 and 95 600 l water at 70 and 50 °C.

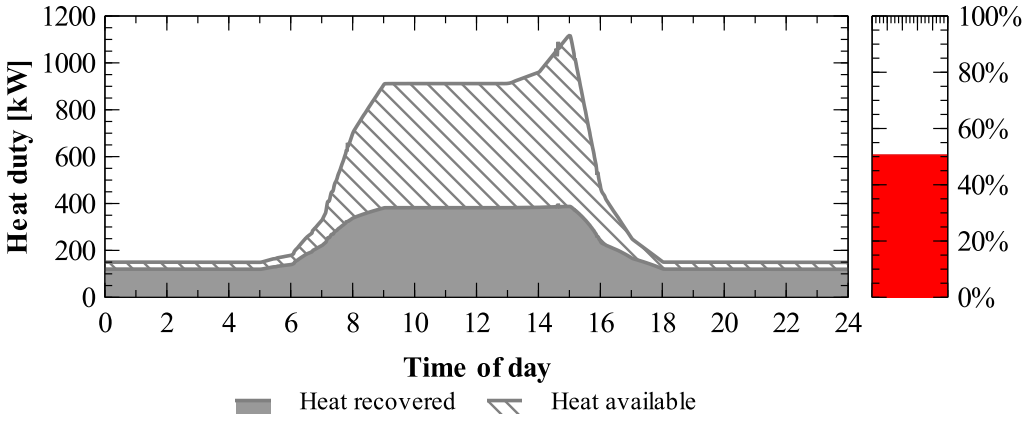

Figure 6: Heat recovery in the DSH for base case

By assuming that the size of the DSH were dimensioned so it could ensure that the NH_3 were cooled down do 40 °C (5 K above condensation temperature), it can be observed that the ratio of recovered heat over available heat is around 50%. During periods with low demand this is

limited by small availability, but during high-demand periods size of the DSH is the limiting factor, as can be seen in Figure 6. Thus, by adding more plates to the heat exchanger, a larger portion of heat could be recovered.

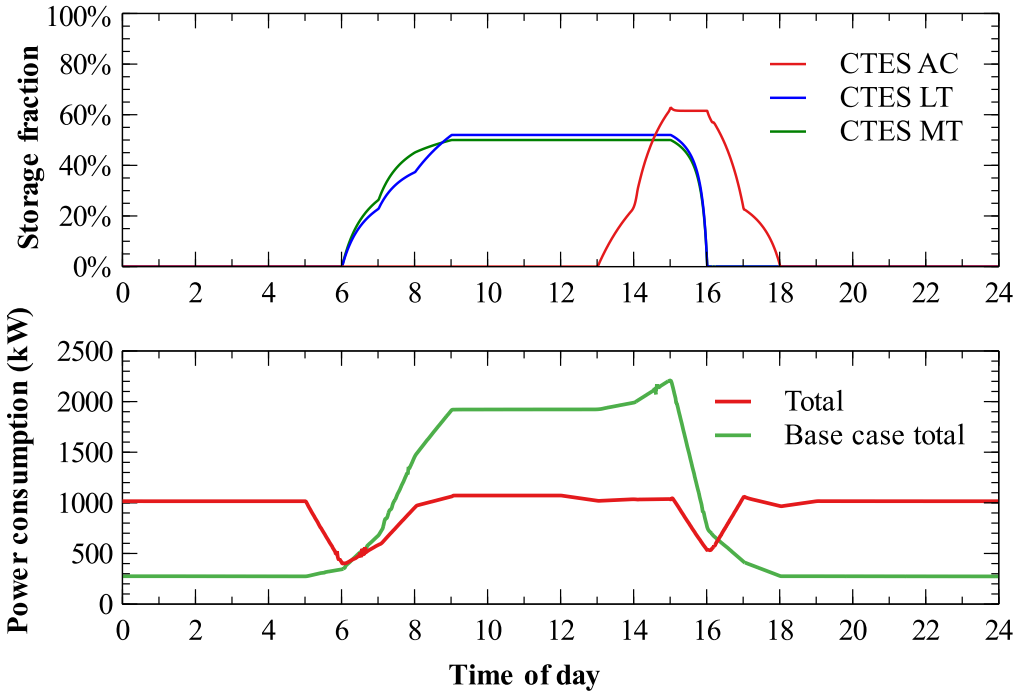

Figure 7: Top: Share of refrigeration demand covered by storage. Bottom: Total power consumption curves for both cases

The upper graph in Figure 7 shows when the different storages kick in, and how the intended control allows for a smooth transition towards capped maximum discharge rates. The percentages indicate how much of the refrigeration demand of the relevant circuit is covered by its storage. Effect of the storages can be seen in the lower graph. What can be observed is that the concept system is able to reduce peak power consumption with over 52%, or a reduction of over 1,1 MW. Furthermore, the power consumption is more stable throughout the period, due to extra work during off-production hours associated with charging storages. With regards to energy consumption, this has increased with approximately 2000 kWh. However, a large proportion of energy consumption has been shifted from high-cost to lost-cost hours, and the extra work occurs during low-cost hours. This combined with the generated savings on the demand charges, diminishes the economic consequence of increased energy consumption.

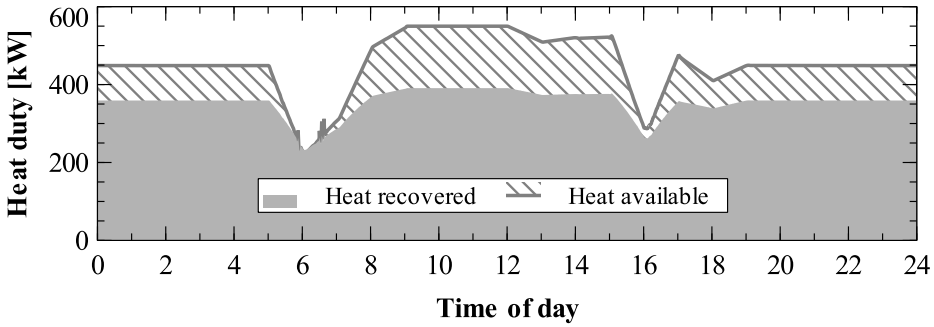

Figure 8: Heat recovery in DSH for CTES concept

With regards to heat recovery the same performance was observed for the MC heat exchanger, but a significant positive increase was observed for the DSH. Due to the more stable power consumption, size of the DSH now has a much better match with available heat, which results in a water production of 120 600 l at 70 °C.

3. CONCLUSIONS

An energy analysis of the refrigeration system for an upcoming poultry processing plant has been conducted. The potential for integration of cold thermal energy storages has been assessed, a design concept has been proposed, and a comparative analysis of the two systems has been presented. Results from the base case simulation showed some potential regarding heat recovery, where the utilization of available heat for the de-superheater could be increased if sized larger. Comparing results from both cases it was found that the CTES concept was able to reduce peak power consumption with 52% at the cost of 10% increased energy consumption. It is concluded that this is a small cost, which economic consequence would be most likely diminished when compared to the economic gain of reduced demand charges. For future work it is recommended that an economic evaluation is conducted in order to quantify the economic consequences, accounting for both investment cost and operational expenses, but also to point out the direction in terms of optimizing the CTES concept.

REFERENCES

[1] SSB, "Produksjon og forbruk av energi, energibalanse," 2018. [Online]. Available: https://www.ssb.no/energi-og-industri/statistikker/energibalanse/aar-endelige. [Accessed: 09-Oct-2018].

[2] SSB, "Utslipp av klimagasser," 2018. [Online]. Available: https://www.ssb.no/natur-og-miljo/statistikker/klimagassn/aar-forelopige. [Accessed: 09-Oct-2018].

[3] E. Rosenberg, T. M. Risberg, H. J. Mydske, and H. E. Helgerud, "Energy potential in the food industry; Store energipotensialer i naeringsmiddelindustrien," 2007.

[4] PCMProducts, "PlusICE E2 - Technical data sheet," 2018. [Online]. Available: http://www.pcmproducts.net/files/E range-2018.pdf.

[5] H. Mehling and L. F. Cabeza, *Heat and cold storage with PCM*, vol. 308. Springer, 2008.

[6] PureTemp, "PureTemp -37 Technical Data Sheet," *2019*. [Online]. Available: https://www.puretemp.com/stories/puretemp-minus-37-tds.

Eirik Starheim Svendsen

Energy flow analysis of a poultry process plant

NTNU
Kunnskap for en bedre verden